Project No. 12-69 **COPY NO.**

___

GUIDELINES FOR DESIGN AND CONSTRUCTION OF DECKED PRECAST, PRESTRESSED CONCRETE GIRDER BRIDGES

FINAL REPORT

Prepared for
National Cooperative Highway Research Program
Transportation Research Board
National Research Council

R.G. Oesterle and A.F. Elremaily
Construction Technology Laboratories, Inc.
5400 Old Orchard Road, Skokie, IL 60077

In Association with:
Roy Eriksson, Eriksson Technologies, Inc.
Chuck Prussack, Central Pre-Mix Prestress Co.
Z. John Ma, University of Tennessee, Knoxville

July 30, 2009

Project No. 12-69

GUIDELINES FOR DESIGN AND CONSTRUCTION OF DECKED PRECAST, PRESTRESSED CONCRETE GIRDER BRIDGES

FINAL REPORT

Prepared for
National Cooperative Highway Research Program
Transportation Research Board
National Research Council

R.G. Oesterle and A.F. Elremaily
Construction Technology Laboratories, Inc.
5400 Old Orchard Road, Skokie, IL 60077

In Association with:
Roy Eriksson, Eriksson Technologies, Inc.
Chuck Prussack, Central Pre-Mix Prestress Co.
Z. John Ma, University of Tennessee, Knoxville

July 30, 2009

ACKNOWLEDGMENT OF SPONSORSHIP

This work was sponsored by the American Association of State Highway and Transportation Officials, in cooperation with the Federal Highway Administration, and was conducted in the National Cooperative Highway Research Program, which is administered by the Transportation Research Board of the National Research Council.

TABLE OF CONTENTS

TABLE OF CONTENTS (continued)

TABLE OF CONTENTS (continued)

LIST OF FIGURES

LIST OF FIGURES (continued)

AUTHOR ACKNOWLEDGEMENTS

The research reported herein was performed under NCHRP Project 12-69 by Construction Technology Laboratories, Inc (CTLGroup). Dr. Ralph G. Oesterle, Senior Principal Structural Engineer at CTLGroup was Principal Investigator. The Co-Investigator primarily responsible for development of this report was Roy Eriksson, President and CEO, Eriksson Technologies, Inc. with assistance from Chuck Prussack, President, Central Pre-Mix Prestress Co. The other Co-Investigator are Dr. Ahmed Elremaily, Senior Structural Engineer, CTLGroup, Dr. Z. John Ma, Associate Professor, University of Tennessee (UTK), and Lungui Li, Ph.D. Candidate at UTK.

The research team acknowledges the following individuals for their insightful comments and contribution to the content of this report: David Shearer, Shearer Design; Monte Smith, Sargent Engineers; Jerome Nicholls, Nicholls Engineering; Keith Kaufman, Knife River; and Steve Seguirant, Concrete Technology Corporation.

ABSTRACT

This report documents part of the results of a study of decked, precast, prestressed, concrete bridge girders. This type of bridge provides benefits of rapid construction, and improved structural performance. The research was performed to develop guidelines for design and construction and to address issues that significantly influence performance. The first goal was accomplished by development of guidelines for design, construction, and geometry control based on successful methodology currently being used.

Construction and geometry control were identified in the project as key issues for further work. There are certain issues involved in erection/construction that are relatively unique to this type of bridge. Current non-users have little experience with these issues and need guidelines as to how to handle these issues. In particular, construction geometry control for differential camber, skewness, and cross-slope needed to be addressed. Therefore, the project included a major task to document best practices for existing systems based on successful methodology currently being used.

Data was collected using interviews with designers, and precasters, with significant experience with this type of bridge. The practicality of the existing practices was assessed based on results of interviews and on the knowledge and experience of the research team. Written descriptions of selected practices were developed to address previously defined issues. The collected information is presented within this Design and Construction Guidelines for Decked Precast Prestressed Concrete Girder Bridges document provided as a separate report for this project. Step-by-step design example that illustrate all significant steps in the design process are provided in appendices to these guidelines.

The second goal of the project was to develop an improved longitudinal joint system. The performance of longitudinal joints between the flanges of adjacent decked girders was defined as a major issue inhibiting the general use decked girders. Results of analytical and experimental studies: to develop an optimized family of girder section with consideration for future re-decking, to define live load and camber leveling load demand on the flange-to-flange joint, to define trial alternate joints, to test trial joints to identify an improved alternate joint, and to test full-scale panel tests of the selected alternate joint to investigate the performance under static and fatigue flexural and flexure-shear loading are reported in a separate document.

EXECUTIVE SUMMARY

A "decked" concrete girder is a precast, prestressed concrete I-beam, bulb-tee, or multi-stemmed girder with an integral deck that is cast monolithically and prestressed with the girder. These girders are manufactured in precast concrete plants under closely controlled and monitored conditions, transported to the construction site, and placed side by side in the bridge. Load transfer between adjacent units is accomplished using specially designed connections along with a grouted shear key. Sections that are not too long or too heavy for transportation by truck can be used to construct long-span girder bridges. This type of bridge construction provides the benefits of rapid construction, improved safety for construction personnel and the public, and improved structural performance and durability.

In spite of their benefits, the use of decked precast, prestressed concrete girders has been limited because of concerns about certain design and construction issues that are perceived to influence the structural integrity of the bridge system. These issues include connections between adjacent units, longitudinal joints, longitudinal camber, cross slope, live load distribution, continuity for live load, lateral load resistance, skew effects, maintenance, replaceability and other factors that influence constructability and performance.

The primary objective of NCHRP Project 12-69 is to develop guidelines for design and construction for long-span decked precast, prestressed concrete bulb tee girder bridges. These guidelines will provide highway agencies with the information necessary for considering a bridge construction method that is expected to reduce the total construction time, improve public acceptance, reduce accident risk, and yield economic and environmental benefits.

In developing these guidelines, the NCHRP Project 12-69 had two goals: document existing practices and improve upon them. This first goal was to provide guidelines for design, construction, and geometry control based on successful methodology currently being used. To date, use of long-span decked precast, prestressed concrete girder bridges has mostly been limited to the northwest region of the United States where this type of bridge has been used very successfully. This goal has been accomplished by conducting interviews with knowledgeable designers and

precasters, by collecting and reviewing existing design and construction practices, and presenting the collected information within this document.

Currently, the most widely used longitudinal connection between precast concrete members is a combination of a continuously grouted shear key and welded transverse ties spaced at intervals from 4 ft to 8 ft on-center. This type of connection is intended to transfer shear and prevent relative vertical displacements across the longitudinal joints. Implications from a survey of issues performed as part of the NCHRP Project12-69 indicated that, if this type of joint is properly designed and constructed, the performance can be good to excellent. This type of connection is addressed in the methodologies currently being used. However, there is also a perception of cracking and leakage with this joint, indicating that an improvement was necessary.

The second goal, therefore, focused on improving the longitudinal joint system and providing guidelines for its use. This goal was accomplished by developing a joint that includes headed reinforcement bars lap spliced and grouted within a narrow joint preformed into the longitudinal edges of the precast deck portion of the precast girders. This type of joint transfers both moment and shear between the precast elements. Guidelines for construction and geometry control specific to the improved longitudinal joint system are also included within this document

Work in the NCHRP Project 12-69 has been limited to the decked bulb tee (DBT) because of the structural efficiency of this section and because this is the section that is most common in current use among pre-decked systems. Most of the procedures in use for designing and fabricating DBT girders are the same as or similar to those used for other types of precast, prestressed bridge girders, such as conventional bulb tees. This document presents design and detailing guidelines for DBT girders with emphasis on those areas that are specific to DBTs.

CHAPTER 1

PRELIMINARY ASSESSMENT

1.1 DESIGN CRITERIA

1.1.1 Design Specifications

Most jurisdictions in the U.S. have adopted the AASHTO LRFD Bridge Design Specifications, including any interim revisions. These guidelines are based on the LRFD Specifications (1) unless otherwise noted.

1.1.2 Loads

1.1.2.1 Dead Load

Dead loads include member weight (Figure 1-1) and any appurtenances on the bridge. Loads anticipated to be placed in the future, such as a wearing course must be established.

1.1.2.2 Live Load

Design live load should be established for the project as well as identifying any vehicles for which the bridge must be load rated. It is becoming more common to require that a bridge be rated at the time of design. If the bridge serves a special use, those vehicles that are anticipated to use the bridge must be identified as well.

1.1.3 Roadway Geometry

Since there is no cast deck on DBT girder bridges, the ability to conform to complex roadway geometries is more limited. It is therefore desirable to keep roadway geometry on the bridge as simple and straightforward as possible. Ideally, the horizontal alignment on the bridge should be a tangent. Skews should be limited to 30 degrees if possible.

Vertical alignments should be adapted to fit the profile of a cambered girder to the extent possible. Methods to adjust the vertical profile of the girder are discussed in

Section 2.8.1 of these guidelines. However, these methods add complexity and cost to the fabrication process.

1.2 SITE ASSESSMENT

1.2.1 Accessibility of Site

Accessibility to the project site can impact the type, configuration, and geometry of the bridge. Distance from the fabrication plant to the project site, road condition, and the type and load rating of intermediate bridges are important factors. For remotely located sites, it is prudent for the designer to “drive the route” to identify any issues or factors that may impact design, fabrication, construction, transportation, or erection. Indeed, DBTs provide an advantage over bridge types which require field-cast concrete.

1.2.2 Vertical Clearance Requirements

Vertical clearance requirements must be clearly and unambiguously established at the start of the project. It must be recognized that the camber inherent in prestressed girder systems is subject to deviation from predicted values. Realistic estimates of girder camber should be made with an allowance for deviation beyond what is predicted. Girder camber is an estimate at best, and with greater use of high-strength concrete, high levels of prestress, and longer more slender girder usage, a reasonable level of variability should be assumed.

Improved methods of predicting camber have been adopted by AASHTO. Even so, it must be understood that any camber prediction procedure is an estimate at best. Many parameters, each with inherent variability, can compound total prediction error and lead to higher or lower than anticipated girder camber (2). Recognition of this, combined with proper planning and tolerant detailing practice, can help to minimize the impact of camber variability.

1.2.3 Water Crossing Issues (hydraulics, shoreline, etc.)

Appropriate flood levels should be established for the site. If possible, waterway channels should be kept as natural as possible. By not narrowing the waterway no change in stream velocity occurs and potential scour problems are then minimized. The use of DBTs may provide an advantage because of the long-span capabilities.

1.2.4 Permitting and Environmental Issues

As with other types of bridges, good coordination with permitting and environmental agencies is essential to a smooth running project. Span lengths, pier locations, and location of temporary bents are issues which may be impacted by jurisdictional regulations.

1.3 COORDINATION WITH LOCAL PRECAST PRODUCERS AND CONTRACTORS

1.3.1 Availability of Product Types

The specific dimensions of DBTs vary from region to region and even from fabricator to fabricator within each region. State departments of transportation often have girder standards developed for use within their states for which fabricators have the appropriate forms. Generally it is advisable to check with the precast fabricators located within a reasonable distance of the proposed project site to establish the specific girder types that are available. Fabricators can typically provide a catalog of available girder types, along with detailed dimensions and beam properties.

1.3.2 Material Properties

1.3.2.1 Concrete Properties

Prior to commencing design, the range of feasible concrete strengths should be established. While there is a trend towards higher design strengths of concrete nationwide, the typical 28-day concrete strength used on a project is largely dictated by current practice in a region, which is heavily influenced by factors such as available aggregate types.

1.3.2.1.1 Air Entrainment For durability and to ensure that the top surface of the girder can be screeded and finished properly, the top portion of the girder is commonly cast with air-entrained concrete where freeze-thaw may be an issue. Typically, air entrainment of 4 to 8% is used. The depth of the air-entrained layer can range from just the top 2 in. to the entire top flange of the girder. The top air-entrained layer is placed soon after the bottom portion so as to avoid forming a cold joint between the two layers. The compressive strength and thus the modulus of elasticity of the air-entrained layer is typically lower than that of the concrete in the bottom of the girder.

When the entire top flange is air-entrained concrete, the impact on section properties must be recognized and factored into the design calculations. However, for shallow upper layers, the impact on section properties is often minimal and is frequently ignored.

1.3.3 Prestressing Systems and Conventions

The primary load-carrying reinforcement in DBTs is pretensioned strand. These can be arranged as a straight pattern, as a draped pattern, or a combination of the two. Draped pattern details can vary widely.

Depending upon the governing agency, how details of a strand pattern are conveyed in a set of contract drawings can vary. Some agencies show actual, detailed strand layouts while others show only the total prestress force and its centroid at critical locations. Still others show only the required moment capacity and stress limits for design, or the design load and leave the design up to the fabricator.

1.3.4 Design Conventions

Design conventions can vary significantly from agency to agency. The governing agency with respect to design should be established up front in a project. Any standard drawings, details, and special design requirements should be identified early for potential use in the design phase of the project.

1.3.5 Trucking Capabilities, Shipping Distance

Girder weight and length are potentially critical issues in preliminary design selection. Local fabricators should be consulted early in a project to identify girder hauling and erection capabilities (Figure 1-2).

1.3.6 Crane Availability and Rates

Identification of cranes type availability is an important preliminary planning issue (Figure 1-3). Requiring a large crane from out of the area for a project may result in unexpectedly high erection costs. However, overall project benefits might be such that the requirement of a large crane is compensated for in other ways, such as elimination of one or more spans of the bridge, expedited construction schedule, etc. Cost and

availability of cranes should, therefore, be established in the early stages of the project to enable their cost to be accurately accounted for in the cost analysis of the project.

1.3.7 Preliminary Cost Estimates

Published load tables (3) can provide valuable assistance in estimating girder depths and span lengths. Local fabricators can then assist with preparing reasonable preliminary cost estimates.

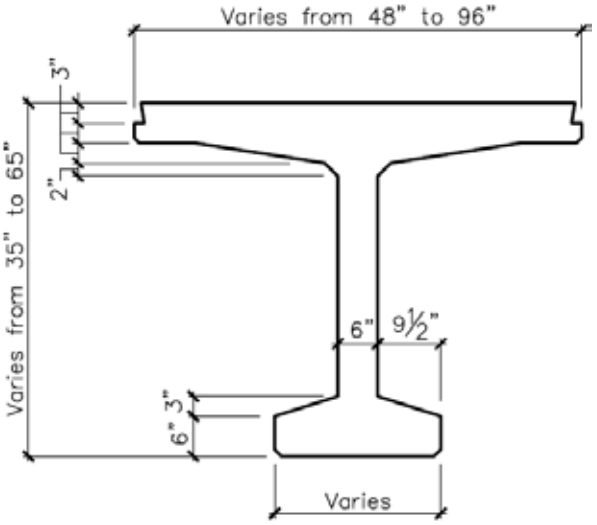

Figure 1-1. Typical decked bulb tee (DBT) cross section.

Figure 1-2. Typical hauling rig.

Figure 1-3. Crane picking girder from truck.

CHAPTER 2

SYSTEM CONFIGURATION

2.1 STRUCTURAL SYSTEM

2.1.1 Continuity

2.1.1.1 Simple-Span

DBT bridges are typically configured as simple-span bridges. These can be single-span bridges or multi-span bridges with each span acting independently as a simple-span. The primary advantage to this type of system is its ease of constructability.

2.1.1.2 Continuous

The most common DBT bridges currently in service are single-span bridges. In addition, for multi-span bridges, the large majority of DBT bridges currently in service are designed and built as a series of simple-spans. However, there has been some experience with DBT bridges made continuous for live load, and there is reason to expand this practice. Making a precast girder bridge continuous improves the structural efficiency of the system. Compared with simple-span bridges, continuous span (jointless) precast, prestressed concrete bridges are used to improve durability, increase seismic resistance, and increase span capacity. Continuity also can reduce the lateral resistance demand on piers, definitely improve riding quality, and, most importantly, reduce maintenance needs by eliminating joints.

Many states make conventional precast, prestressed girder bridges continuous using a cast-in-place connection between girders over the piers, e.g., using negative moment reinforcement within the cast-in-place deck slab. The girders are designed as simple-span for dead load but continuous for superimposed dead load and live load. For DBT bridges, the negative moment continuity connection is not as simple but can be accomplished. Section 3.4.1 of these guidelines provides examples of establishing continuity by extending bars from the top flanges of the girders, coupling them, and possibly stressing them.

In simple-span non-composite bridges, time-dependent deformations result in little or no change in the distribution of forces and moments within the structure. However, multiple-span composite bridges, made continuous for superimposed dead loads and live loads, become statically indeterminate. As a result, any inelastic deformations that occur after the connection has been made will generally induce statically indeterminate forces and restraining moments in the girders. Sources of inelastic deformation include concrete creep and shrinkage, and temperature gradients. Design criteria that include the potential effects of creep, shrinkage, and temperature gradients are discussed in Section 4.3.3.2 of these guidelines.

2.1.1.3 Integral abutments

DBT girders are commonly connected integrally to the end walls of the abutments (4). Section 4.13.7 of these guidelines provides examples of transverse joints at the abutment. Expansion joints at abutments can be eliminated from the bridge by incorporating integral abutments into the bridge. Effectively, the expansion joints are shifted away from the bridge itself (Figures 2-1 and 2-2) to locations where maintenance of the joint is easier and any leakage that does occur in the joint is inconsequential with respect to the structural elements of the bridge.

2.1.2 Girder Splicing

Generally, longer spans and wider girder spacing improve the economics of a bridge. However, since DBTs include an integral top deck, the weight per unit length of the girder becomes very high with longer spans. This condition can cause girders to become too long or too heavy to ship or to handle. A technique to solve this problem is to segment the girder into two or more pieces and splice the segments together at the jobsite. This technique has been used successfully on numerous bridges, enabling span lengths to extend to 200 feet and beyond (5).

2.1.2.1 Single-Span vs. Multi-Span Post-Tensioning

Single-span post-tensioning consists of segmenting the girder into pieces. Each segment is cast separately and pretensioned or conventionally reinforced for handling and construction loads. At the job site, the pieces are arranged into their final locations with respect to the overall finished girder, the joints are cast, and the entire girder is then

post-tensioned to cause the girder to act as a single, integral piece. The girder then becomes equivalent to a single-element girder (i.e., one with pretensioning only, and no post-tensioning). It can be erected and detailed into the bridge as usual.

Multi-stage post-tensioning can also be employed. The first stage of post-tensioning would consist of connecting the girder segments together to form complete girders. Once the individual girders are erected, tendons are then installed along the full length of the bridge and tensioned. This introduces continuity to the bridge and enhances the structural performance. However, the tradeoff for this is increased complexity of fabrication and construction and increased cost.

2.1.2.2 Girder Segmentation and Splice Locations

Typically, girders are segmented into two or three elements. A three-element scheme is the most common, the advantage of which is that there is no joint at the midspan region, which is the location of maximum flexure. The locations of the other joints can be selected to minimize other structural issues.

2.1.3 Provisions for Future Redecking

Where traffic or environmental conditions may lead to the requirement of deck replacement, LRFD Article 2.5.2.3 requires that provisions be made for a protective overlay, future deck replacement, or supplemental structural resistance. For DBT bridges, these requirements can be satisfactorily addressed utilizing the following options:

1. Inclusion of a Sacrificial Layer – This can take the form of added thickness of the deck and/or improvement of the quality of the deck material, such as using air-entrained concrete for the top several inches of concrete.

2. Replacement of DBTs – Because of the characteristic of accelerated bridge construction using DBTs, full deck replacement, when needed, may be most feasible by simply removing and replacing all the DBTs of the bridge.

3. Deck replacement – For situations where Option 1 & 2 are not viable, details exist for creating a system in which just the top deck can be removed from the DBT. The new deck can consist of a full-depth precast, prestressed concrete

deck. Alternatively, the new deck can be installed as a conventional cast-in-place deck.

Provisions for redecking are further discussed in Sections 3.5 and 4.16 of these guidelines.

2.2 GIRDER SIZE AND SPACING

Typical DBT girder depth ranges from 35 in. to 65 in. Overall girder width varies between four and eight feet. Formwork is adjusted to meet the desired depth and width of the unit.

The shape of the bottom bulb of the girder can also be varied depending upon the number of strands that are desired in the bulb (Figure 2-3). In general, wider bulbs are more structurally efficient than narrower ones. That is, shapes which encompass rows with more strand locations, which cause the centroid of the strand group to be placed further from the centroid of the girder cross section, are more efficient than configurations which disperse the strand pattern vertically.

2.2.1 Selection of Girder Depth and Depth Limitations

Generally, using fewer, deeper beams at a wide spacing results in the most economical superstructure. Due to shipping and handling constraints, however, the maximum girder spacing for DBTs is usually about 8.00 ft. Clearance limitations or preexisting conditions may also cap the maximum depth of girder that can be used. Preliminary design charts are often available from regional precast suppliers for their specific girder cross-sectional shapes that can help determine an economical girder type and bridge layout. It is best to consult these charts rather than generic ones as fabricator-supplied design charts will be based on the materials and design conventions of their region.

2.2.2 Weight Limitations

Maximum haul weight of an individual precast girder by truck typically varies between 50 and 220 kips. Several factors can influence this, including weight restrictions imposed by state and local jurisdictions and equipment limitations. Weight limitations by

rail are in the range of 120 to 200 kips. Barged product can be much heavier, typically limited by the ratings of the barge and loading equipment.

2.2.3 Length Limitations

Girder length may be constrained by method of transportation. When shipped by truck, roadway geometry can limit girder length. Rail shipments tend to be the most restrictive. Barge transportation is typically the least restrictive with respect to girder length. Length limitation concerns should be thoroughly discussed with local precast manufacturers in the planning and design stages.

2.3 DIAPHRAGMS

The need for and use of intermediate diaphragms has long been somewhat controversial. When the deck is cast-in-place, diaphragms can often be omitted since the slab is effective in transferring loads to adjacent beams and effect of diaphragms in load distribution is marginal. This has been addressed by several investigations (6, 7, 8, 9). When a full-thickness integral deck is precast as part of the beam, diaphragms are considered necessary except for shorter spans, certain girder types, or where other means exist for connecting the girder stems (10).

Absence of a monolithic deck structure and presence of joints are parameters that have raised questions on the live load distribution and continuity of DBT bridges. The live load distribution equations for DBTs in the current AASHTO Specifications are either based on the assumption that longitudinal joints and intermediate diaphragms do not transfer any transverse moment between girders (i.e., “not sufficiently connected”), or to consider the moment transfer (i.e., “sufficiently connected”) requires calculation of parameters not defined properly for DBTs. Based on limited field tests performed in Alaska (11, 12), there is a need to reexamine the impact of this assumption. Using the calibrated 3D FE models, parametric studies were performed to study the effect of intermediate diaphragms (13). It has been found that that intermediate diaphragms reduce the maximum horizontal shear force in connectors. However, current AASHTO Specifications for live-load distribution do not consider the effect of intermediate diaphragms.

2.3.1 Concrete Diaphragms

2.3.1.1 End diaphragms

End diaphragms are necessary to support and transfer edge loads at the end of the girder to the substructure and serve to tie to the girders together to better enable the bridge cross section to function as unit, which also aids in load transfer. They also can act as a means of holding the approach fill back. Typical details for concrete end diaphragms are given in Figures 2-4 to 2-6.

2.3.1.2. Intermediate diaphragms

Intermediate concrete diaphragms can be precast or cast-in-place (Figures 2-7 to 2-10). Precast diaphragms are usually cast as a secondary pour in the precast yard. Less typically, they can be poured with the initial casting of the girder. If intermediate diaphragms are to be field-cast, access holes must be created to enable the concrete to be pumped into the diaphragm as well as for venting (Figure 2-7). If shipping weight is a concern, field-casting may be the better alternative.

2.3.2 Steel Diaphragms

Steel diaphragms (Figure 2-11) have the advantage of being lightweight. A variety of configurations are possible, but K-shaped diaphragms are the most popular due to their simplicity, flexibility, and structural efficiency.

2.4 JOINTS

2.4.1 Longitudinal

Conventionally, DBT girders are connected longitudinally using a system of welded plates and grouted longitudinal keyways. Mechanical connections are embedded in the flanges and spaced four to eight feet apart along the length of the girders. Field-welded plates are used to make the connections. The longitudinal joints are then grouted their full lengths. The mechanical connections provide transverse tensile capacity to the joint to ensure that the joint stays together, while the grouted shear key provides the primary vertical load-carrying mechanism for the joint. Structurally, this longitudinal joint

system is modeled as a hinge, that is, it transfers shear between units, but not moment. Section 3.4.2 describes the design procedure of the longitudinal joints in detail.

2.4.2 Transverse

Transverse joints, that is, joints at the member ends, are similar to transverse joints in conventional I-girder bridges. A variety of conventional expansion joints have been used successfully, such as strip seals and compression seals. Alternatively, a transverse joint can be sealed with grout or by using a closure pour.

2.5 BEARINGS

Elastomeric bearing pads (Figure 2-12) have proven to be a practical and cost-effective solution for bearings of DBT bridges. In addition to their ability to carry the normal loads associated with this type of bridge, their lateral flexibility help to minimize the effects of shrinkage and negative temperature changes in the transverse direction of the bridge (14). Elastomeric pads can be reinforced or non-reinforced, many of which are non-shimmed.

2.6 BARRIER AND RAILING SYSTEMS

This section of the Guidelines contains some figures that include specific details. These details are provided for concept only and should not be considered as final designs.

Both parapet and post and rail barrier systems are commonly used in DBT bridges. Figures 2-13 through 2-18 show typical details for these systems. Note, however, that flange thicknesses and typical flange reinforcement historically used in DBTs may be inadequate for LRFD design criteria. To resist the substantially higher barrier design loads, the thicknesses of the overhang may need to be significantly increased, the length of the overhang shortened, or both. Additional transverse deck reinforcement is likely required as well. As an alternative to designing a system, a crash-tested system can be used (15).

2.6.1 Parapets

Integral concrete parapets are commonly used to form the barrier system on DBT bridges. Bent reinforcing bars are typically embedded into the flange of the exterior girders during fabrication and protrude from the top of the girder during shipment and erection (Figure 2-13). Once all the girders have been erected and the longitudinal joints have been completed, the parapets are cast.

2.6.2 Post and Rails Barriers

Post and rail barriers have the advantage of requiring no field-cast concrete. Typically plates and other hardware are embedded in the exterior portion of the flanges of the exterior girders, and any required holes are formed during casting (Figure 2-15). A short curb may also be cast. The remainder of the barrier system is field-bolted when erection and connection of the girders have been completed.

2.7 PROVISIONS FOR BRIDGE WIDENING

Provisions for future widening of a DBT can be incorporated into the exterior girders by:

- Casting embedments for future welded shear connectors (and casting a protective layer of concrete over the plates) into the overhang of the girder for future use or
- Omitting the shear key and embedded plates and cutting back the flange as necessary to attach connection details when the actual widening operation takes place.
- Moving the exterior girder and adding new interior girders.

2.8 BRIDGE AND GIRDER GEOMETRY CONTROL

2.8.1 Girder Camber

In conventional pretensioned girder bridges with cast-in-place deck slabs, the impact of girder camber on bridge geometry is minimal. The use of proper details of the girder and slab permits the designer to easily accommodate any reasonable deviations

in camber from predicted values. Final grade of the bridge is set strictly by setting screed elevations to whatever values are necessary. Any variation in elevation of the top of the girder itself is usually then of little consequence in overall roadway geometry. However, with DBT bridges, the top flange of the girder often serves as the actual riding surface. Therefore, fabrication and detailing techniques must be utilized to ensure the girders integrate well with the desired overall geometry of the bridge.

Estimates of girder camber should be made with the recognition that girder camber is inherently variable due to the many parameters that influence it. Allowances should therefore be made in tolerances in the project to permit a reasonable level of deviation of actual camber from predicted values.

2.8.1.1 Controlling Girder Profile with Formwork

The profile of the top of DBT girders is typically controlled in two ways: varying the thickness of the top flange of the girder or altering the shape of the bottom of the formwork. Both techniques have been successfully used, with the former being the more common technique.

2.8.1.1.1 Articulation of Prestressing Form. Altering the bottom of the form involves special formwork. Normally, the bottom pan of a prestressing form is flat and level. However, the bottom form can be articulated using a series of straight segments of equal length. This permits the profile of the bottom of the girder to approximate a desired vertical curve with several straight segments. Aesthetically, the girder appears to have a continuous curvature (Figures 2-19 and 2-20).

2.8.1.1.2 Screeding Top Flange of Girder. A simpler method of controlling the vertical profile of a girder is by varying the thickness of the top flange of the girder. This permits small variations in profile to be easily and inexpensively made. Large changes, however, become problematic as additional concrete is required, which increases materials cost and weight of the units.

2.8.1.2 Adapting Roadway Profile to Girder Profile

In addition to directly controlling the shape of the profile of the girder, judicious selection of pier elevations can mitigate the adverse affects of girder camber (16). For a

two-span bridge, raising the center pier elevation by a distance of 4C, where C is net girder camber, eliminates the rollercoaster effect that would otherwise occur with collinear bearing seats (Figure 2-21). Similarly, for a three-span bridge, the two interior piers can be raised by a distance 8C to allow the individual girder profiles to better follow the roadway profile (Figure 2-22).

2.8.2 Bridge Skew

Skews cause special problems with DBT girders that are not present in cast-in-place bulb tee systems. Camber of the girder causes upward bowing of the overall girder (Figure 2-23). Therefore, the top surface of the girder increases in elevation as you move away from the bearings towards midspan. When the ends of the girders are skewed, the corners of the deck will have different elevations because one corner is farther “up” the camber curve than the other corner. Consequently, for a skewed girder, the top elevation of the deck at the obtuse corner is higher than at the acute corner. If girders are placed on a flat pier, the adjacent girder corners will not match because of this difference. This causes a saw tooth effect of the deck surface at the ends of the girders, which can become quite pronounced for highly cambered girders with high skews. A method to eliminate the saw tooth effect is to increase the bearing elevation of each adjacent girder as you move from the acute corner of the deck to the obtuse corner.

2.8.3 Bridge Cross Slope

Bridge cross slopes can be accommodated by either varying the thickness of the top flange of the girder, by tilting the girders with respect to plumb, or by a combination of the two. Experience has shown that, due to the high lateral resistance of DBTs, girders may be tilted up to 4 degrees from plumb to accommodate changes in bridge cross slope. However, lateral stability should be checked and temporary bracing should be provided.

For crowned roadways, bridges with an odd number of girders require that the top surface of the center girder be altered to meet the profile of the crown (Figure 2-25).

2.8.4 Girder Asymmetry

Exterior girders require special treatment of the overhang side. No longitudinal joint is present and details must be included to accommodate the railing system. Girder asymmetry can influence handling stability.

2.9 OVERLAYS

2.9.1 Water-Proofing Membrane

Although high quality concrete is used in the fabrication of DBTs, water-proofing membranes are often applied to provide umbrella protection against corrosion from de-icing salts to the girders, connections, and substructure. A membrane is applied directly to the top surface of the bridge (Figure 2-26) and two to three inches of asphalt are then laid down (Figure 2-27). The asphalt overlay provides the added benefit of improving ride-ability of the bridge surface.

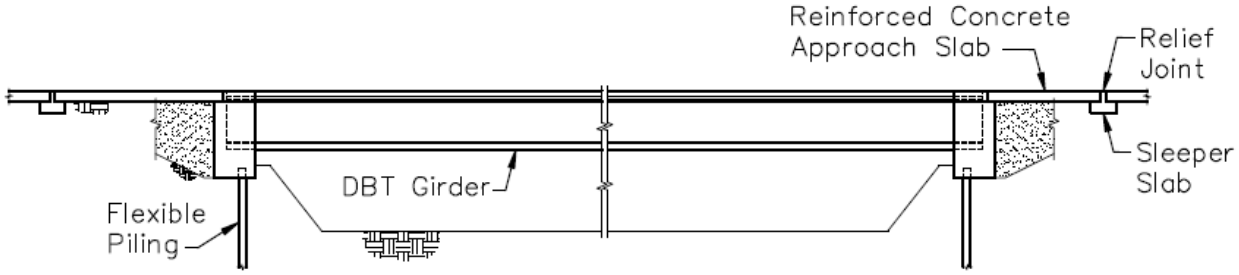

Figure 2-1. Integral abutments on a single-span bridge.

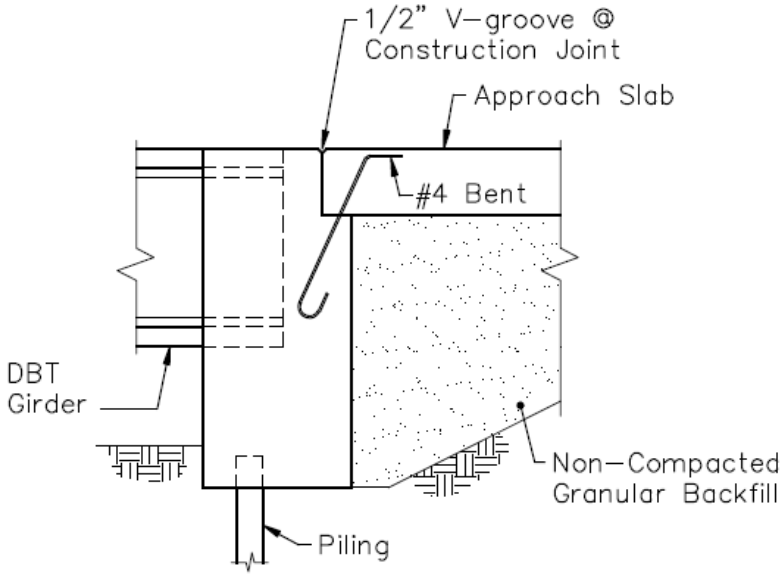

Figure 2-2. Integral abutment detail.

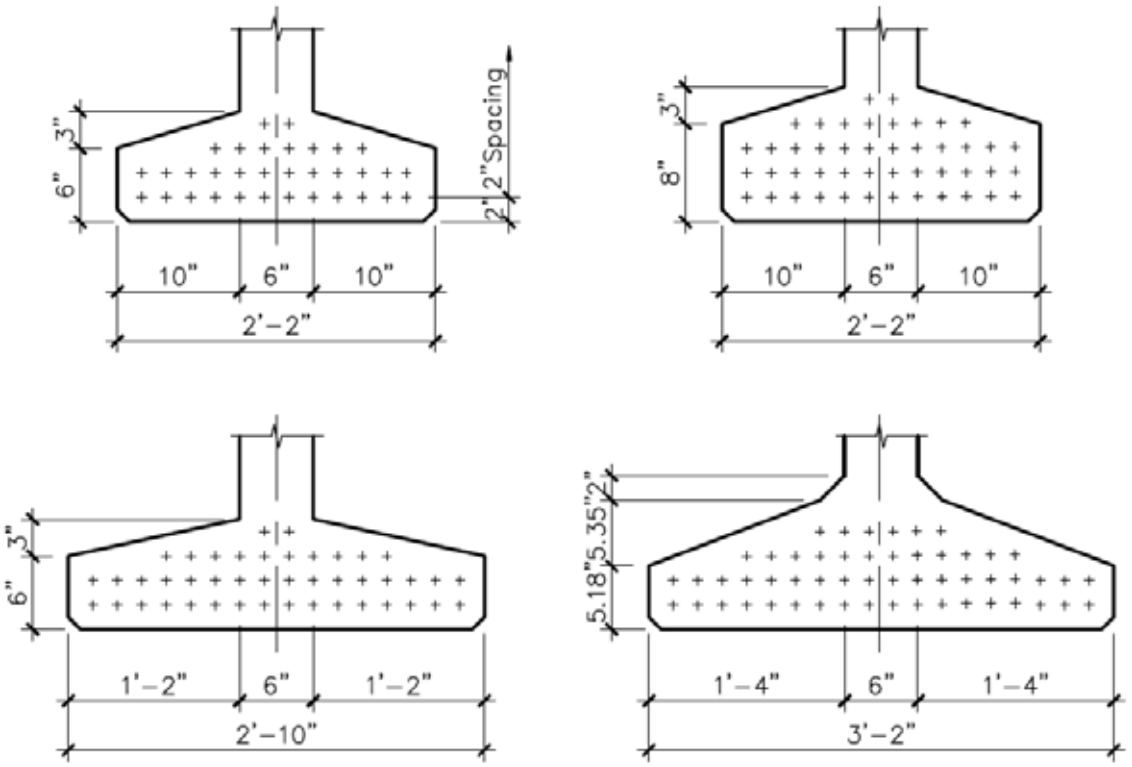

Figure 2-3. Typical DBT cross section with limits of variability.

Figure 2-4. End diaphragm details.

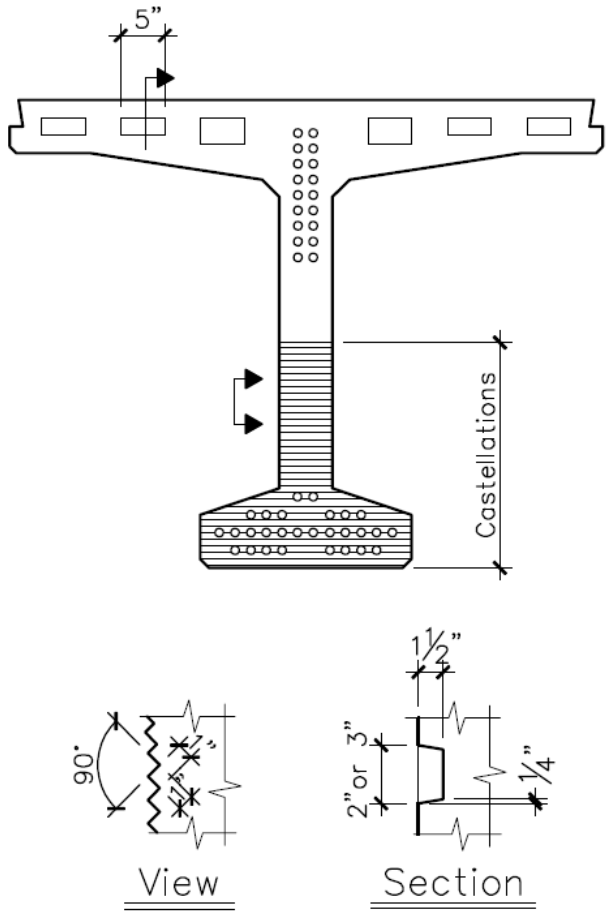

Figure 2-5. End diaphragm details.

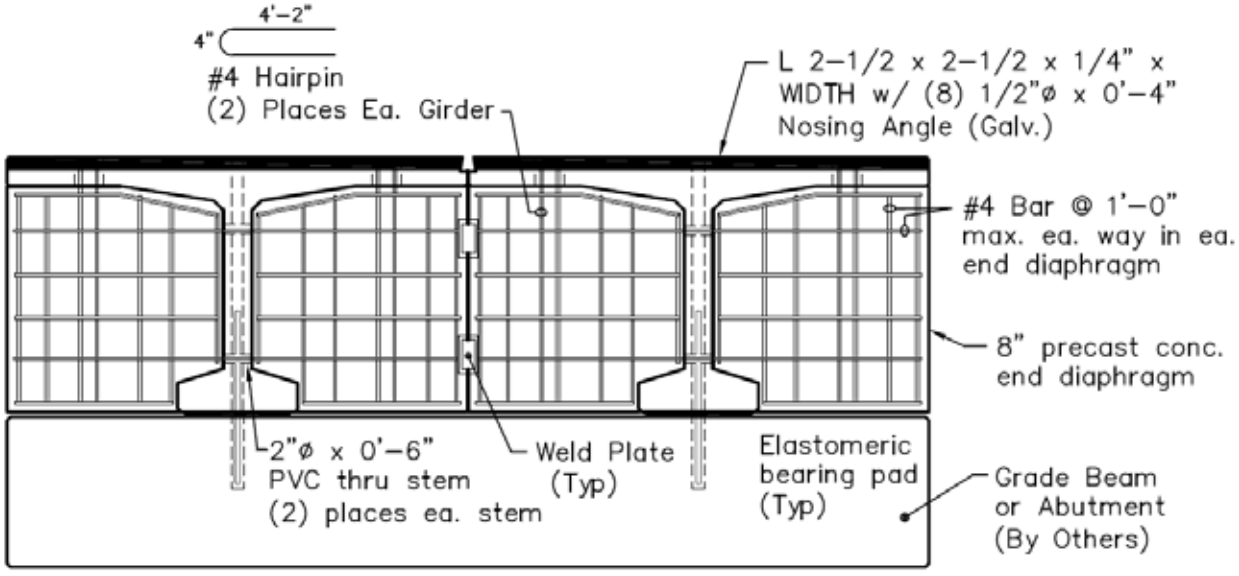

Figure 2-6. End diaphragm details.

Figure 2-7. Access holes in deck to cast intermediate diaphragm.

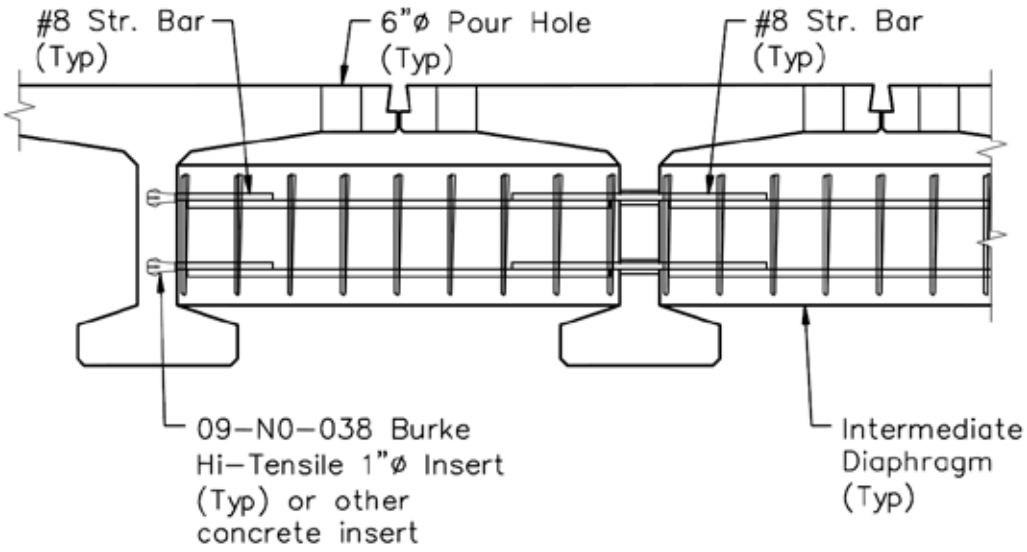

Figure 2-8. Intermediate diaphragm details.

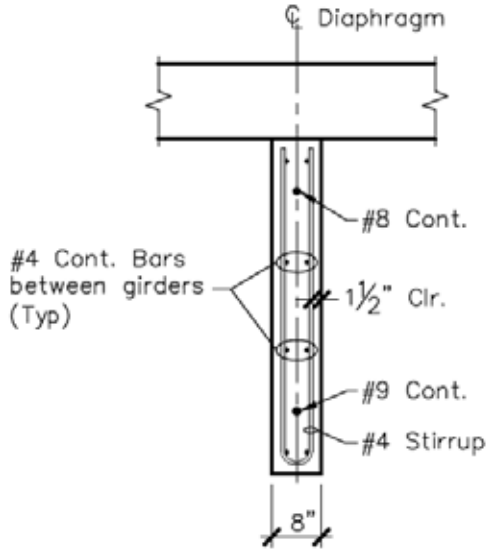

Figure 2-9. Section through intermediate diaphragm.

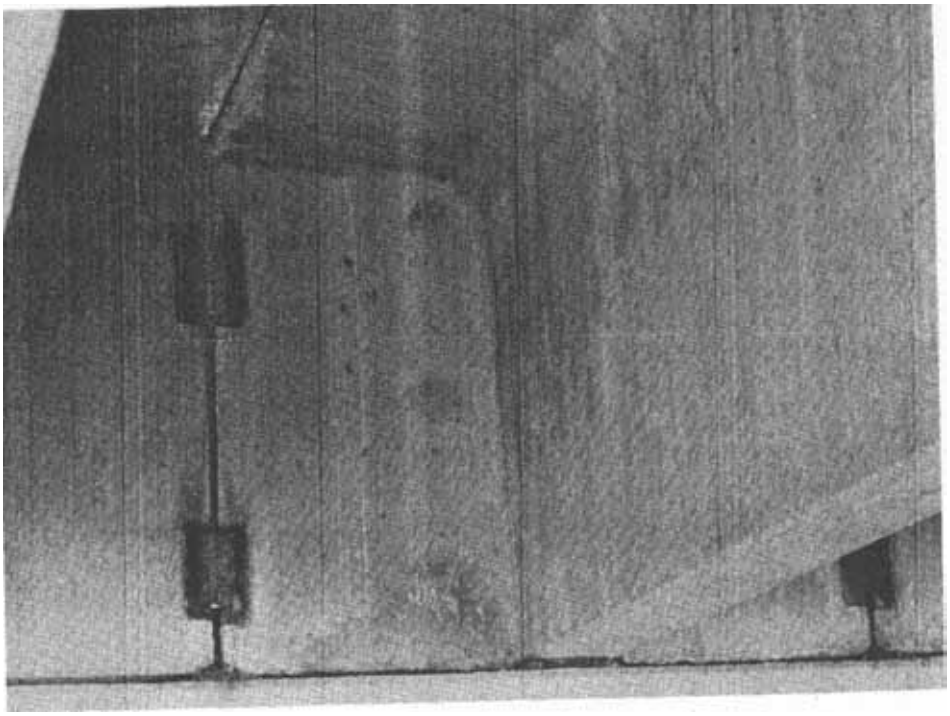

Figure 2-10. Plant-cast diaphragm with field-welded connections.

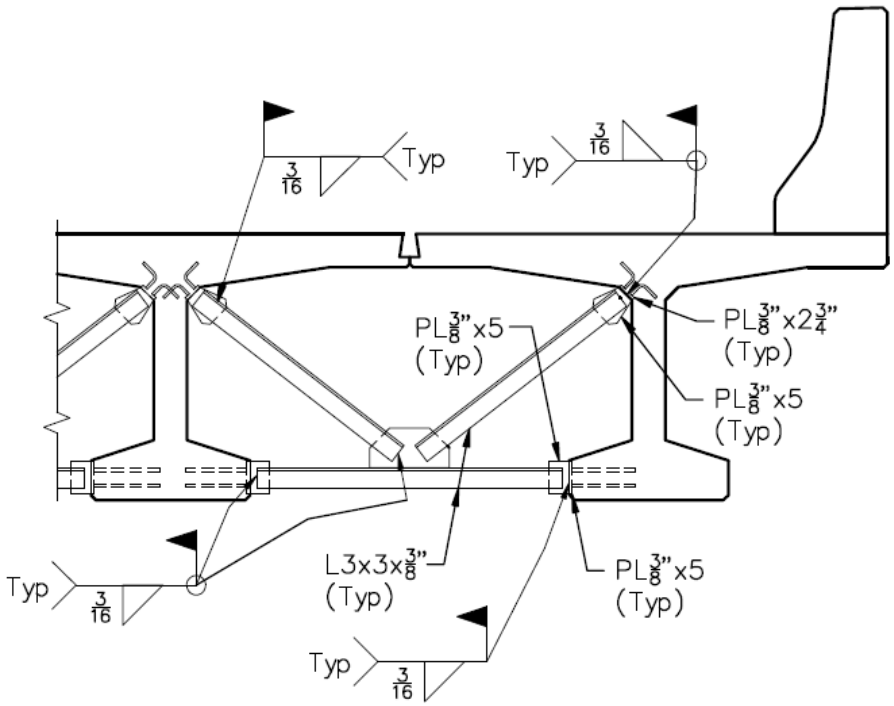

Figure 2-11. Steel K-brace intermediate diaphragms.

Figure 2-12. Bearing detail.

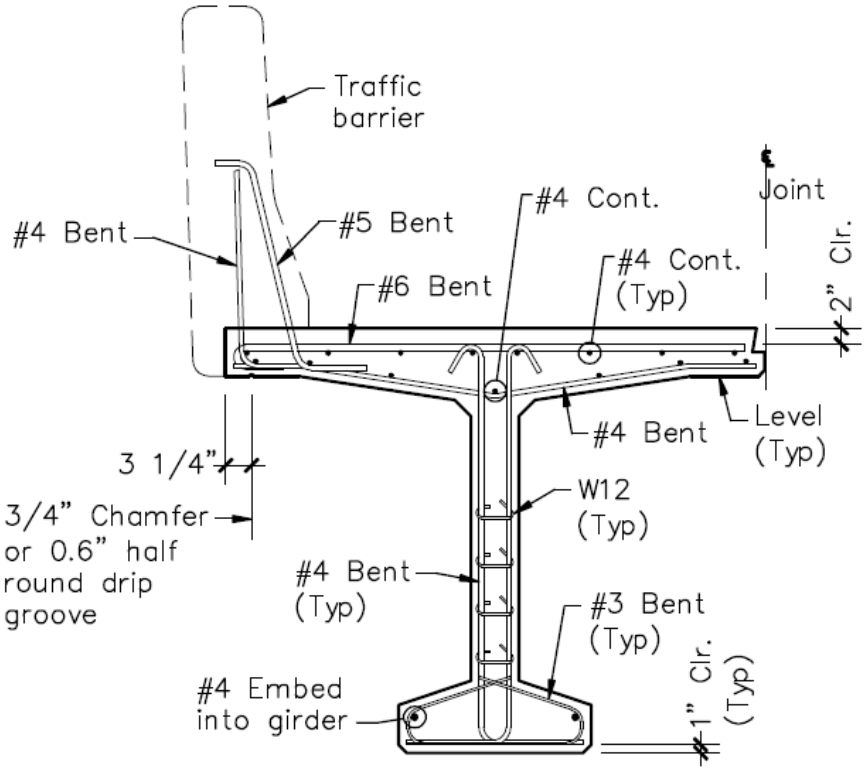

Figure 2-13. Concrete parapet detail.

Figure 2-14. Post and rail barrier.

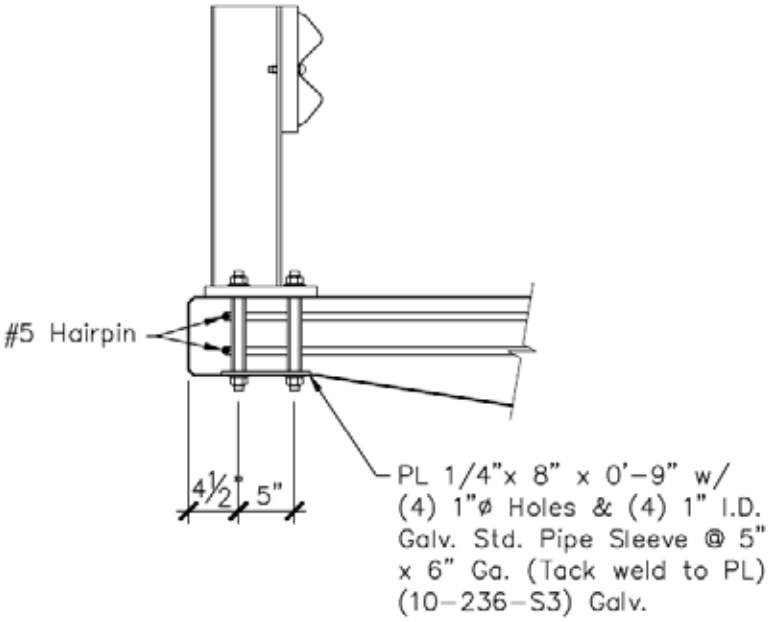

Figure 2-15. Railing connection detail.

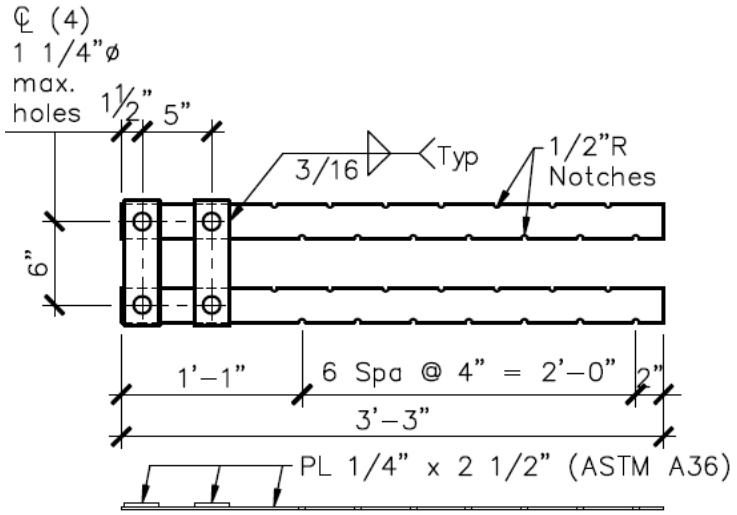

Figure 2-16. Embedded rail post anchorage plate details.

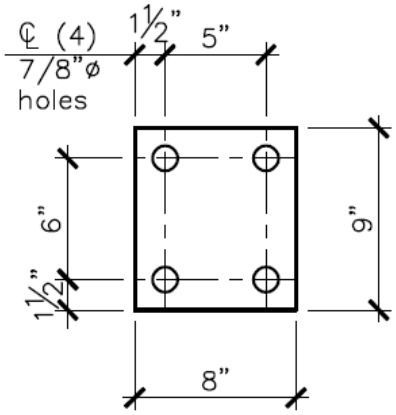

Figure 2-17. Rail post anchorage plate details.

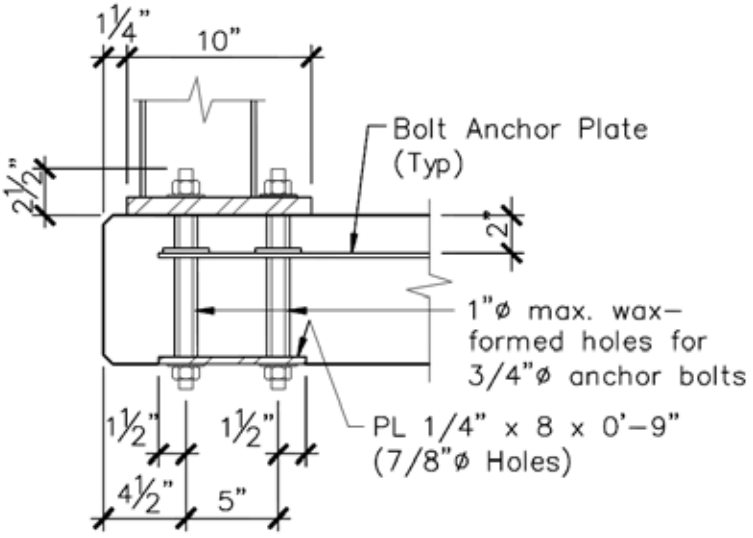

Figure 2-18. Rail post anchorage.

Figure 2-19. Girder camber can be increased using formwork.

Figure 2-20. Substantially higher curvatures can be achieved using formwork

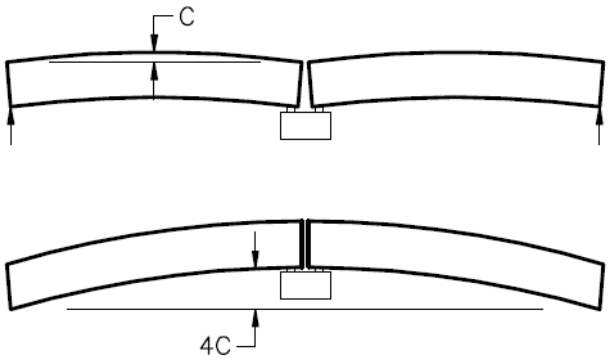

Figure 2-21. Pier elevation adjustment for a two-span bridge.

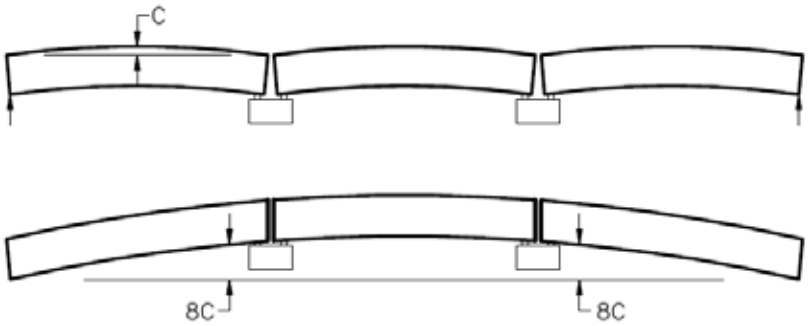

Figure 2-22. Pier elevation adjustment for a three-span bridge.

Figure 2-23. Upward camber of girder due to prestress.

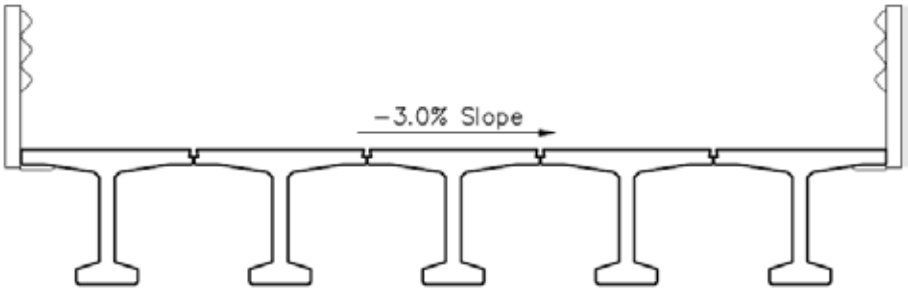

Figure 2-24. Roadway crowns can be accommodated.

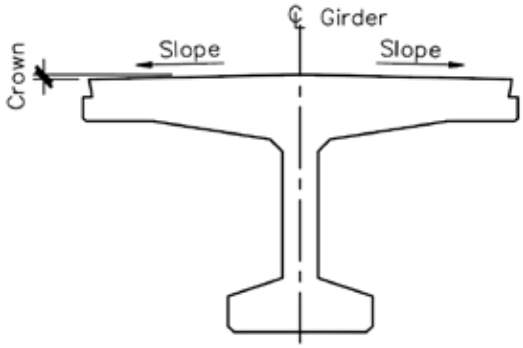

Figure 2-25. Center girder with top flange screeded to match desired roadway crown.

Figure 2-26. Installation of a water-proofing membrane

Figure 2-27 Installation of an asphalt overlay

CHAPTER 3

FABRICATION AND CONSTRUCTION

3.1 GIRDER FABRICATION

DBT girders are generally fabricated using the same methods as those used for the fabrication of conventional I-girders and bulb tee girders, which fall under the general category of precast pretensioned concrete girders. Over a period of more than fifty years, fabrication techniques have undergone continuous refinement. Most girders are fabricated in metal forms in PCI-certified plants by experienced personnel under carefully monitored conditions. As a result, significant flexibility in design variations is possible, and a high degree of quality is typical.

3.1.1 Forming

3.1.1.1 Conventional Single-Stage

DBTs are typically formed in the same manner as conventional precast, pretensioned concrete I-girders. In-depth discussion of the fabrication process is provided in the PCI Bridge Design Manual (3).

3*.1.1.2 Two-Stage Re-Deckable*

Two-stage re-deckable involves a second concrete placement for the top flange after allowing the first placement to set. This re-deckable system is further described in Section 3.5 of these guidelines. It is recommended that the second placement be made prior to pulling the side forms and detensioning. Therefore, the top flange becomes part of the prestressed section in the initial girder. This not only improves the efficiency of the initial girder, it is necessary for efficient construction. In order to detension, the side forms have to be pulled. If detensioning occurs after the Stage 1 girder is cured, but prior to casting the top flange, forming for the top flange becomes a second and more complicated operation. The more efficient approach is to keep the side forms in place for both castings. The casting cycle time will be increased. However, the benefit is increased efficiency and decreased cost of the future re-decking. Also, it is recommended that this re-deckable system only be used in those applications where provisions for full depth re-decking is required and where full girder replacement with

new decked girders is not a viable option. It should be noted that the changes in the stress in the girder during future removal and after re-decking need to be considered in the original design.

3.1.2 Prestressing

Prestressing of DBTs is essentially identical to that of conventional precast, prestressed I-girders. Complete details on all aspects of prestressing, including both pretensioning and post-tensioning, can be obtained in the PCI Bridge Design Manual (3). Figure 3-1 shows prestressed strand and reinforcement for a girder bottom bulb and stem.

3.1.3 Embedded Hardware

Unlike conventional I-girders, a significant element of DBTs is their embedded hardware. Care must be taken to ensure that embedded plates are carefully laid out and secured against movement during casting to ensure proper matching and fit-up to the connections in adjacent members.

3.1.4 Concrete Placement

3.1.4.1 One-Stage vs. Two-Stage

For current practice, DBT girders are cast in a similar fashion to that of conventional precast, pretensioned concrete girders. Typically, they are cast in a precast fabrication plant in fixed beds several hundred feet in length. A fixed metal bottom pallet is used with removable metal side forms.

A common practice where freeze-thaw is an issue and air-entrainment in the upper region of the girder is desired is to cast the girders in two stages. The portion up to the top of the stem is cast using high-strength concrete. The remaining portion—the fillet and top flange or perhaps only the top few inches—is cast with an air-entrained concrete mix that is of lower strength. The advantage of this is a more workable top surface that facilitates surface finishing, but which provides higher durability.

The second stage may be the “monolithic” top flange of a conventional DBT or it may be the debonded top flange of the re-deckable system. For the “monolithic” top

flange of a conventional DBT, the top layer is placed soon after the bottom portion so as to avoid forming a cold joint between the two layers. Two- stage casting for future re-decking is further discussed in Section 3.5.1.2.

3.2 TRANSPORTATION

3.2.1 Girder Stability

Girder stability must be assured at all stages of fabrication, handling, transportation, erection, and construction. Girders can become unstable for a variety of reasons and conditions, including not being secured properly, improper handling, and lifting or being supported at incorrect locations.

Lateral bending stiffness is the most important parameter that determines lateral stability (17, 18). DBT girders have an advantage in this respect due to their large, stiff top flanges. As a result lateral stability is typically not a major concern for single-element girders. However, when girder spans are extended using splicing techniques or when the top flange is narrowed for weight considerations, lateral stability of the girder during both handling and transportation should be investigated.

3.3 ERECTION SCHEMES

Figures 3-2 and 3-3 demonstrate erection schemes. Girder cross sections need not necessarily be symmetric. For example, to accommodate a roadway crown, the profile of the top flange of the girder may be altered in which one side of the flange is thicker relative to the other. Such a situation results in an asymmetric girder cross section where the center of gravity of girder mass is not centered over the midpoint of the top flange. To assist in keeping asymmetric girders level during erection operations, an additional crane line can be attached to the top flange using an insert as indicated in Figure 3-4.

3.4 GIRDER INSTALLATION

3.4.1 Girder Continuity Connections

As discussed in Section 2.1.1.2, making a multi-span precast girder bridge continuous improves the structural efficiency of the system. For typical I-girder bridges

continuity is established using mild reinforcing placed in the cast-in-place deck over the piers. For DBT bridges, which typically do not have a cast deck, continuity can be established by extending bars (19) or top strands from the top flanges of the girders into the end diaphragm region (Figure 3-5). Bars can be connected by the use of laps, hooks, welding, grouted sleeves, or mechanical connections. Extended top strands can be developed by passively extending them into the diaphragm (20). It is also possible to stress top strands by coupling them and applying a jacking force.

3.4.2 Conventional Weld Plate Joints

3.4.2.1 Camber Leveling

Differential camber in DBTs is a common occurrence. Several steps can be taken during the fabrication and storage stages of the girder to minimize the potential for differential camber in girders that will be placed adjacent to each other in the bridge. In general, all aspects of the fabrication process should be as uniform as possible for each girder. Mix design and concrete batch quality should be carefully monitored. Cure time should not vary, which may inadvertently occur if only some of the girders are permitted an extended curing period. Location of temporary supports for girders in fabrication yard should be uniform. Exposure to sunlight should also be uniform.

Three methods typically employed to level girders are:

- Jacking – A cross beam and portable hydraulic jack are used to apply counteracting forces to the tops of girders to adjust the elevations of the girder surfaces to a level condition (Figure 3-6).

- Surcharging – Heavy weights are loaded onto the tops of girders to reduce differential camber (Figure 3-7). Surcharging will likely only work for minor differential camber in that differential camber leveling forces can be significant. Section 4.3.2.1 of these guidelines provides estimates of camber leveling forces.

- Crane-Assisted Leveling – A crane is used to lift one end of the girder to bring the connectors near the middle of the girder into vertical alignment with the adjacent girder's connectors. Welds are made or clamps are

installed and the crane incrementally lowers the lifted end to progressively bring further connectors along the longitudinal joint into vertical alignment. When all the ties are welded or clamps installed, the girder is released from the crane.

Leveling procedures using the jacking method include:

1. Erect all girders before leveling.

2. Screw coil threaded rod into girder with least camber (low girder), making sure that the rod is screwed a minimum of 1 ¼" into insert in the girder (Figure 3-6 and 3-8).

3. Install leveling beam as shown on the leveling diagram, placing hydraulic jack on the side on one side of the leveling keyway and wood cribbing on the other.

4. Use hydraulic jack to level girders align girders. When cambers between adjacent girders are matched to the highest degree practical, weld the number of ties that are required to resist the jacking force along each girder keyway before releasing hydraulic jack.

5. Move to next diaphragm or keyway and repeat procedure until entire bridge is leveled and weld ties are welded. A straight edge placed perpendicular to centerline of bridge should not show greater than 3/8" deviation in 10 feet.

3.4.2.2 Weld Plate Installation

Weld plates as shown in Figure 3-9 may be designed to resist the camber leveling forces until the grout is placed and cured. Alternately, temporary clamps as shown in Figure 3-10 may be used to resist the camber leveling forces until the welds are made and joints are grouted.

3.4.2.3 Joint Grouting

3.4.2.3.1 Joint Preparation Figure 3-11 shows a typical grouted shear key detail. Figure 3-12 shows a longitudinal joint prior to grouting. The joint should be

thoroughly cleaned prior to grouting. Typically, this is accomplished in the fabrication plant by sand blasting the joint prior to hauling.

3.4.2.3.2 Grouting Figure 3-13 shows grouting of shear keys in progress and Figure 3-14 shows a completed grouted key. Grout key materials include: sand-cement grouts; non-shrink grouts; and epoxy grouts. Most grouts used in shear keys connecting bridge elements are a mixture of Portland cement, sand, and water. Prepackaged high-strength, non-shrink grouts are recommended for DBT shear keys. Proportions are usually one part cement to 2.5 to 3 parts sand, with enough water to make the grout easily flowable and completely fill the keyway. When such grouts are used, the water-cement ratio is usually about 0.50. This is a relatively high value, resulting in low strength and high shrinkage. These mortars also exhibit a tendency for the solids to settle, leaving a layer of water on the top. Special ingredients or treatments can improve these characteristics, but add to the cost. There are several proprietary products designed to expand sufficiently during initial hardening and curing to offset subsequent shrinkage of the grout. These mortars are prepared mixtures of cement, fine aggregate and an expansive ingredient. This ingredient may provide expansion by liberating gas, oxidation of metals, and formation of gypsum or using expansive cement. It should be kept in mind that the shear key constitutes a very low percentage of the total width of the bridge deck. Thus, while the unit shrinkage of sand-cement grout is much greater than that of the precast units, the total shrinkage of the deck members may actually contribute more to the separation at the joints than the shrinkage of the grout itself. Several railroads (box beam bridges) place a well graded aggregate in the keyway, then pour in a low viscosity epoxy resin. The railroads require that the keyways be sand-blasted in the casting yard prior to shipment. The pre-placed aggregate method allows the work to be accomplished more quickly than the mixed mortar method.

3.4.3 Headed Bar Joints

3.4.3.1 Background

Currently, the most widely used longitudinal connection between precast concrete members is a combination of a continuously grouted shear key and welded transverse ties described in Section 3.4.2. This type of connection is intended to transfer shear and prevent relative vertical displacements across the longitudinal joints.

Implications from a survey of issues performed as part of the NCHRP Project12-69 indicated that, if this type of joint is properly designed and constructed, the performance can be good to excellent. However, there is also a perception of cracking and leakage with this joint, indicating that an improvement is needed. Therefore, a major goal of the NCHRP Project12-69 was development of an improved longitudinal joint system. It was anticipated that behavior of DBT bridges can be improved by providing transverse moment continuity in addition to shear transfer in the longitudinal joints.

As described fully in the main final report for NCHRP Project 12-69, this goal was accomplished by carrying out analytical studies to define service load demands on the flange-to- flange connections due to live load forces and camber leveling forces, and by carrying out laboratory testing on trial alternate joint systems to investigate the performance of selected alternate joint systems under static and fatigue loading.

The result of these studies was the development of a joint that includes headed reinforcement bars lap spliced and grouted within a narrow joint preformed into the longitudinal edges of the precast deck portion of the precast girders. The geometry and the reinforcement for the alternate joint are shown in Figures 3-15 and 3-16.

This type of joint transfers both moment and shear between the precast elements. Laboratory testing indicated that this longitudinal joint detail has sufficient strength, fatigue characteristics, and crack control for the maximum loads determined from the analytical studies for all combinations of span length, girder spacing, girder depth, and bridge skew used in the analytical studies. Therefore, it was concluded that this longitudinal joint detail is a viable alternate connection system to transfer the forces between adjacent DBT girders. Guidelines for construction and geometry control specific to this alternate longitudinal joint system are included in the following sections.

3.4.3.2. Camber Leveling

Analyses carried out in NCHRP Project 12-69 for non-skewed bridges indicated that camber leveling forces induce a maximum transverse shear in the longitudinal joint of 0.87 kip/ft. The effect of the skew is such that the leveling shear is increased near one end of the longitudinal joint and reduced near the other end. This effect is more pronounced with the increase of the skew angle. The maximum calculated joint shear

was 1.01 kip/ft for 15^{o} skew angle, 1.18 kip/ft for 30^{o} skew angle, and 1.45 kip/ft for 45^{o} skew angle. The background for the analyses is discussed more fully in Section 4.3.1 of this document.

The upper bound calculated camber leveling shear force of 1.45 kip/ft for a bridge with a skew angle of 45^{o} results in an initial nominal shear stress of 20 psi on the 6 in. thick deck section. It is anticipated that the camber leveling will typically be accomplished using the jacking method discussed above with temporary clamps similar to the clamps shown in Figure 3-10. An example design for temporary clamps, using 1.5 k/ft. as the maximum camber leveling shear force, is included in Appendix A of this document.

As discussed above when using the weld plates joints, the plates may be designed to resist the camber leveling forces until the grout is placed and cured. With the headed bar joints, however, the temporary clamps as shown in Figure 3-10 are needed to resist the camber leveling forces until the joints are grouted and sufficiently cured. Tests of the joint grout material discussed below indicate that properly mixed and place grout material should attain a compressive strength of approximately 6000 psi in one day which should be sufficiently strong to resist the calculated maximum initial nominal shear stress of 20 psi on the 6 in. thick deck section.

3.4.3.3 Reinforcement

Figure 3.16 displays the reinforcement layout used in the slab specimen. There are five layers of reinforcement in each panel along the specimen depth direction with a 2 in. cover at the top and 1 in. cover at the bottom. The top two layers and bottom two layers of reinforcement simulate deck reinforcement in the top flange of DBT girders. The middle layer of the reinforcement consists of epoxy coated headed bars which project out of the panel to splice with the headed bars in the adjacent panel in the longitudinal joint. All the epoxy coated reinforcement has a nominal yield stress of 60 ksi. The spacing of the headed bar is 6 in. and the splice length (inside head to inside head) is also 6 in. One longitudinal headed bar was placed along the center line of the joint both above and below the spliced headed reinforcement. The headed reinforcement is No. 5 bar with a standard 2 in. diameter circular friction welded head. The head thickness is 0.5 in.

3.4.3.4 Joint Grouting

3.4.3.4.1 Joint Preparation The surfaces of the shear key should be thoroughly cleaned to remove all contaminants that can interfere with adhesion and to develop a surface roughness to promote a mechanical bond between the grout and base concrete. After the removal of the surface concrete, proper preparation should provide a dry, clean and sound surface offering a sufficient profile to achieve adequate adhesion. Methods of surface preparation include chemical cleaning or sand blasting. Sandblasting using Black Beauty 2050 sand was chosen for sandblasting to prepare the surfaces of the test specimens in the NCHRP Project 12-69 laboratory test studies. The profiles of the surface before and after sandblasting are shown in Figure 3.17. Typically, sand blasting the joint surfaces would be accomplished in the fabrication plant prior to hauling.

3.4.3.4.2 Grouting Figure 3-18 shows a full scale panel test specimen before and after grouting. Because of the width of the joint, formwork is required to support the joint grout.

The longitudinal joint, which is filled with closure-pour materials connecting the top flange of the adjacent DBT girders, is considered to be the structural element of the bridge deck. Therefore, it is important for the selected closure-pour material to reach its design compressive strength in a relatively short time for the purpose of accelerated bridge construction. As described in Section 3.2.5 of Appendix F of the main report for NCHRP Project 12-69, two grout materials, SET 45 HW (SET) and EUCO-SPEED MP (EUCO), were used for trial testing. Both of these materials are magnesium phosphate-based materials and were used with a 60% extension of pea gravel. A thoroughly washed and dried uniform-sized sound 0.25 in. - 0.5 in. round pea gravel was used to extend the grouts. The pea gravel was tested with 10% HCL to confirm that it was not calcareous.

The compressive strengths of the grout SET and EUCO, tested with 60% extension, reached at least 5670 psi compressive strength within one day. For grout SET, the initial setting time and final setting time were 15-20 minutes and 45-60 minutes, respectively. For grout EUCO, the initial setting time and final setting time were 6-10

minutes and 15-20 minutes, respectively. Based on the results of the comparative study, the grout SET was selected for use in the test specimens. The selection was based primarily on the longer setting time of the grout SET.

3.5 FUTURE RE-DECKING

3.5.1 Deck Removal

Full deck replacement of deck bulb tee girder bridges is an issue that has been raised as a possible impediment to their use. Therefore, a feature that is necessary is the ability to re-deck the system at a future date. This can take the form of casting a sacrificial layer on top of the top flange to serve as a wearing course. With this approach, the girder is fabricated with a one-stage casting as further discussed below in Section 3.5.1.1

Alternatively, the system can be designed and built such that the full depth of the top flange can be removed and recast at a later date as part of a rehabilitation process for the bridge.

One potential method of full depth removal could involve fabricating the girders and incorporating them into a bridge in the conventional manner. This would involve a one-stage casting of the girder. In the future, when the deck has deteriorated to the point where replacement is deemed necessary, the top flange of the girder can be removed using accepted demolition procedures and a new deck installed, either by casting a new deck in the field or installing a full-depth precast deck.

A parametric study was conducted as part of NCHRP Project 12-69 to investigate the engineering feasibility of re-decking a conventional deck bulb tee girder bridge by removing and replacing the entire top flanges of all the girders. The study indicated that, with this method of deck replacement, the prestressed girder can safely endure the stress changes resulting from the large top flange of the girder being removed. However, when the new deck is cast, the resulting stresses cause both the maximum net compressive and tensile stresses to exceed their allowable levels by substantial amounts. Further, deflection of the system is unacceptably large. For this approach to be feasible, shoring would have to be installed under the girders until the new deck is

installed. This may or may not be feasible at the bridge site. Additionally, temporary diaphragms would likely have to be installed as well to stabilize the girders.

An alternative approach to the shoring is to design the girder with the anticipation of future deck replacement. For the girder to be able to accommodate the stresses induced by the weight of the new deck until composite action is developed requires that part of the flange not to be removed with the deck in addition to an increase in the required prestressing force. The interface between the flange and the deck will need to be detailed to allow for easy deck removal while providing adequate horizontal shear capacity. This approach involves a two-stage casting as further discussed in Section 3.5.1.2.

3.5.1.1 One-Stage Casting

A one-stage casting would be used to construct a system in which a wearing course is included in the section. The entire system would be prestressed. An allowance would be made in the top flange such that a certain amount of the thickness would be assumed to be worn away. The structural properties would need to reflect this assumption.

Benefits to this approach include ease of fabrication and resistance to transverse cracking. This system would provide maximum durability since it would be completely precast and pretensioned. Future re-decking would consist of grinding down or truing of the surface. A new sacrificial layer would then be recast in the field and ground to true the surface.

3.5.1.2 Two-Stage Casting

The two stage approach would permit essentially the entire top flange to be removed and recast at a later date. Tadros and Baishya (21) and Tadros et al (22) explored connections between the girder and cast-in-place portion to facilitate re-decking. An innovative shear key interface with a minimal amount of transverse reinforcement crossing the interface was used. Full horizontal shear was able to be developed. However, since much of the horizontal shear was taken by the shear keys, little protruding steel was present, which permitted much easier removal of the deck. For DBT systems, two-stage casting with a cold joint allows for easy deck removal.

After deck removal and replacement, the girder section is converted from a fully prestressed system to a composite system as illustrated in Figure 3-19. Overall dimensions of each system are identical. However, in the first case, the entire system is prestressed, whereas in the second case, only the lower portion is prestressed. This significantly reduces the efficiency of the system after re-decking. Issues associated with the design and construction of this system includes the following:

- Camber Leveling – Camber leveling procedures would be similar to the one-stage system. However, since the prestress profile would differ, cambers will differ. A different camber prediction procedure than the one in current use will likely need to be developed.

- Release Stresses – Because of the two stages of casting, the stress history in the girder is more complex than that of the one-stage system. Stresses will need to be checked at the application of each load and when section properties change, such as when the CIP section is cast. Higher stresses are expected in the lower portion since there is less area over which the prestressing force is applied.

- Horizontal Shear at Interface – Since there is a cold joint between the two systems, horizontal shear capacity needs to be ascertained.

- Detailing – Detailing of both the strand pattern, shear steel, and other reinforcement will need significant attention.

3.5.2 System Stability

Long, slender girders can become unstable during handling and transportation and also possibly during re-decking. Fortunately, due to the high lateral stiffness of DBTs, lateral stability is not typically a concern. However, during the re-decking process, the top flange may be removed as well as potentially some or all of any sub-flange that might exist, thereby drastically reducing lateral stiffness of the system and potentially rendering it structurally unstable. In such situations, it is critical that the strength and serviceability of the system, as well as the system stability, be maintained at all times. Service stresses under construction loads must be kept within allowable limits. The

strength of the system must also be assessed and ensured that it is adequate to resist required factored loads.

Temporary cross-bracing should be installed prior to removal of or alteration of any structural elements of the system and should remain in place until work is complete and the overall system has been restored to its safe, in-service condition. Mast (17, 18) gives procedures for assessing stability of girders.

3.5.3 Placement of New Deck

Replacement decks can consist of precast prestressed full-depth deck panels or can be conventionally formed and cast in place.

3.5.3.1 Precast, Prestressed Full-Depth Deck Panels

Precast full-depth decks provide several advantages over CIP decks:

- Higher concrete strength
- Better workmanship
- Prestressing for better durability and strength
- Rapid construction

3.5.3.2 CIP Deck

As a system CIP decks provide the advantage of high flexibility with regard to geometry. Desired final grades are easily achieved and rideability of the finished surface is high. There is also the added advantage of being a system that is familiar to most bridge builders.

Figure 3-1. Harped strand configuration.

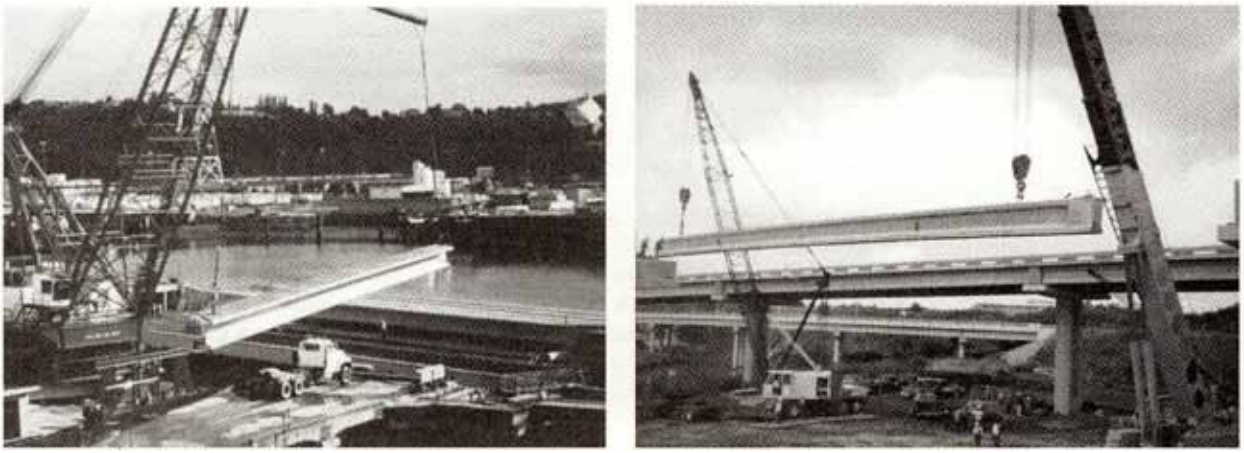

Figure 3-2. One-crane and two-crane erection schemes.

Figure 3-3. Erection using a launching truss.

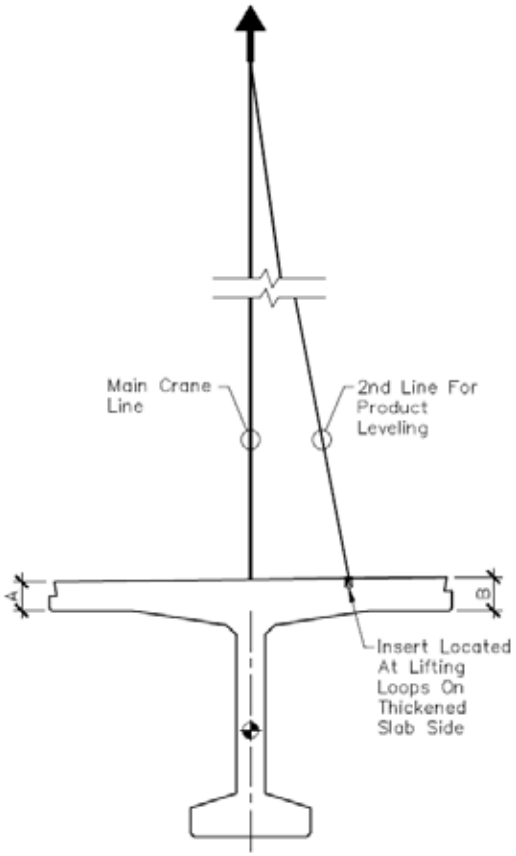

Figure 3-4. Erection of asymmetric girder.

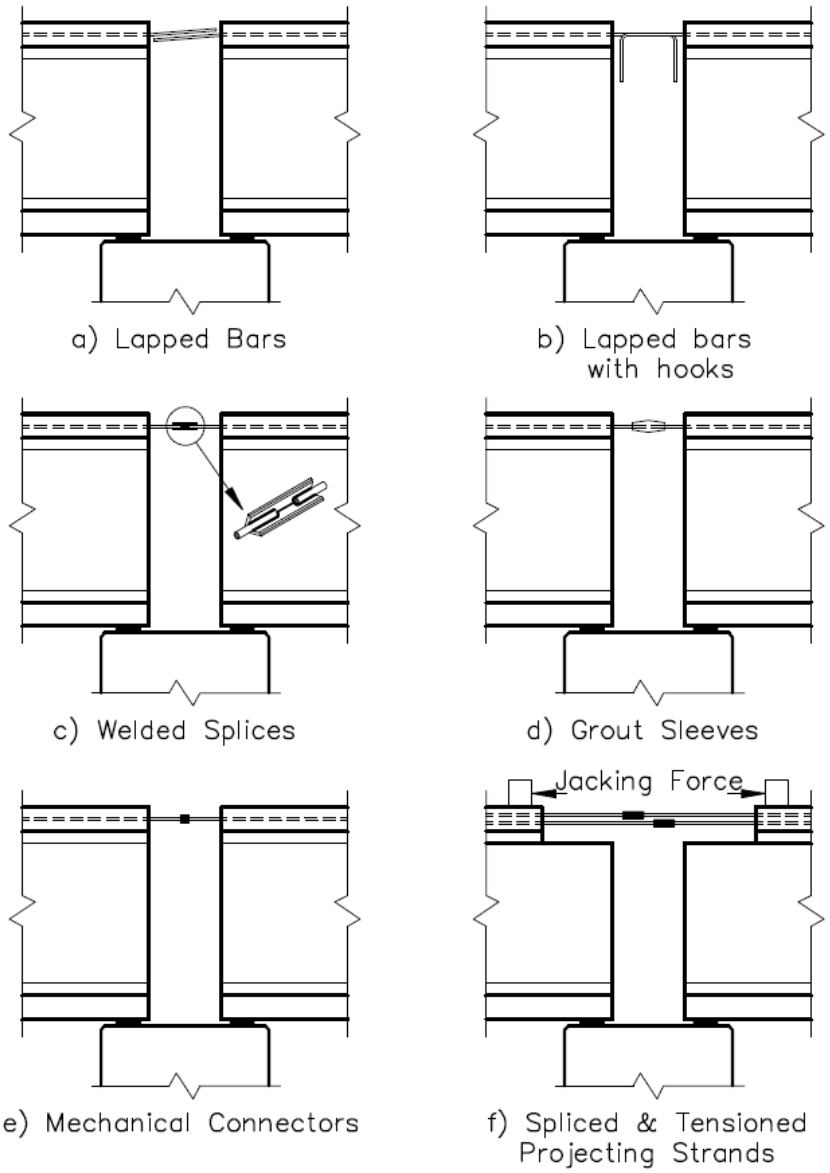

Figure 3-5. Establishing continuity in non-composite systems.

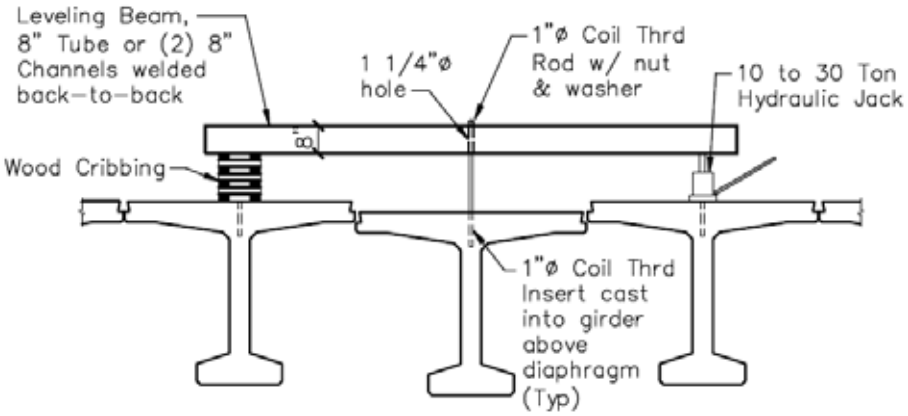

Figure 3-6. Camber leveling diagram.

Figure 3-7. Heavy weights can be applied to the tops of girders with excessive camber to level them prior to connecting flange weld plates.

Figure 3-8. Coil insert cast into girder top to assist with camber leveling operation.

Figure 3-9. Weld plate installed and welded.

Figure 3-10. Temporary clamps may be used to resist leveling forces.

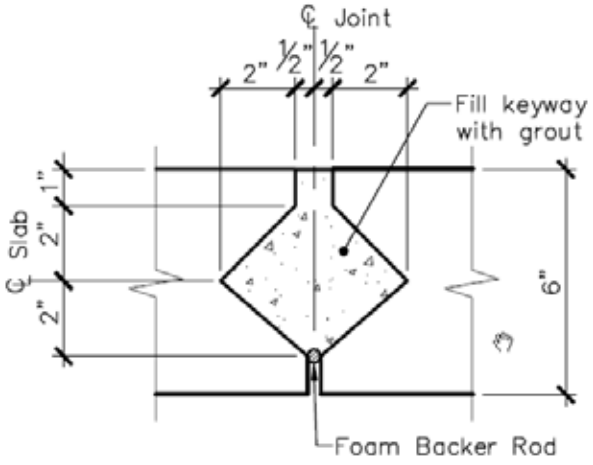

Figure 3-11. Grouted shear key detail.

Figure 3-12. Longitudinal joint prior to grouting.

Figure 3-13. Grouting of shear key.

Figure 3-14. Grouted shear key.

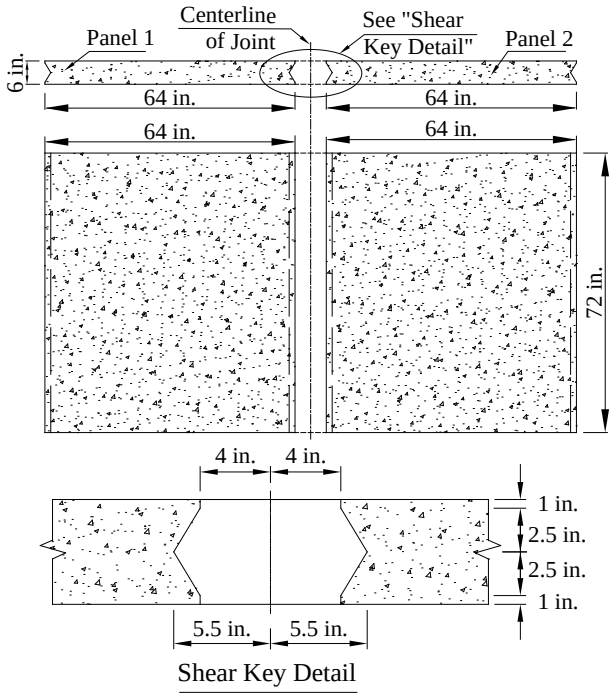

Figure 3.15. Dimensions of Full-Sale Panel Test Specimen

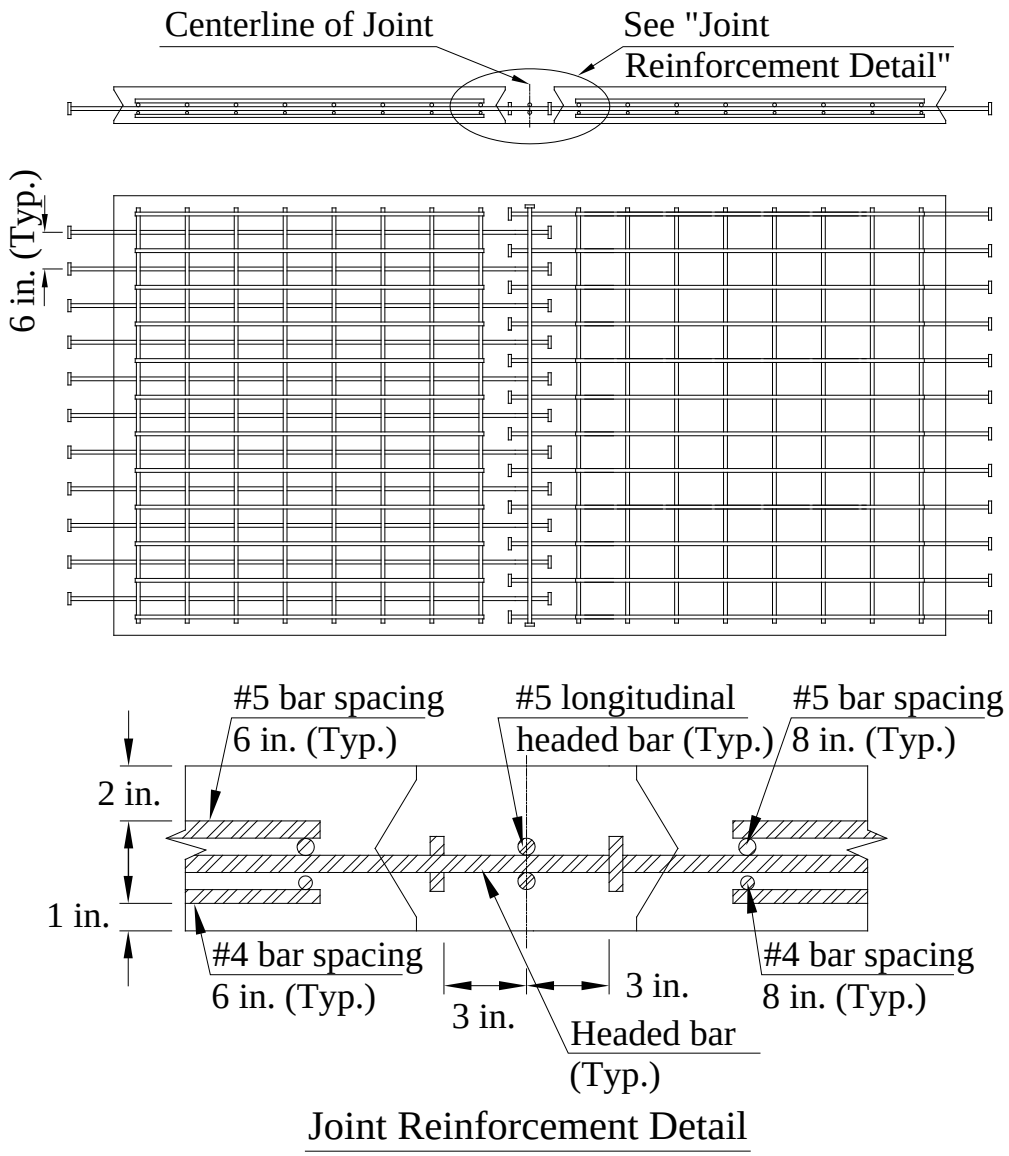

Figure 3.16. Reinforcement for Full-Sale Panel Test Specimens

(a): Before Sandblasting *(b): After Sandblasting*

Figure 3.17. Profile of Joint Surface

(a): Before Grouting *(b): After Grouting*

Figure 3.18. Panel Specimen

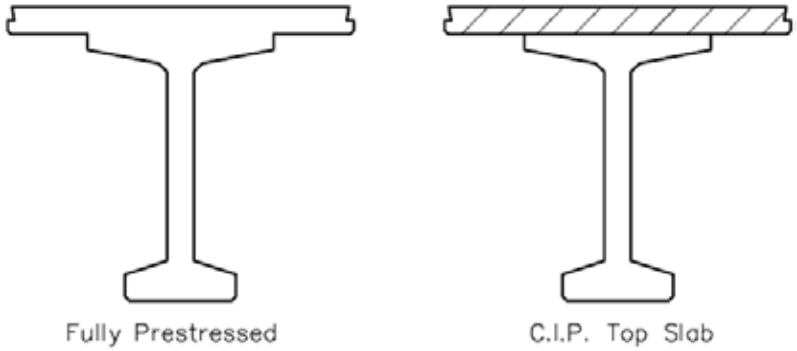

Figure 3-19. Re-deckable system with initial fabrication and after re-decking.

CHAPTER 4

DESIGN THEORY AND PROCEDURES

A step by step design example is provided in Appendix A

4.1 MATERIAL PROPERTIES

4.1.1 Concrete

4.1.1.1 Basic Properties

4.1.1.1.1 Normal-Weight Concrete. The moduli of elasticity of the beam and deck concrete are typically computed using the following equation:

$E_c = 33{,}000\ w_c^{1.5}\ \sqrt{f'_c}$ (ksi) (LRFD 5.4.2.4-1)

Where: w_c = unit weight of concrete (kcf)

f'_c

= Specified compressive strength of concrete (ksi)

4.1.1.1.2 Light-Weight Concrete. Concrete type can be normal weight, sand lightweight, or all lightweight. The LRFD Specs define lightweight concrete as having an air-dry density not exceeding 0.120 kcf. In addition to weight calculations, designating a concrete type as lightweight will influence three other areas of the calculations:

- Modulus of rupture (LRFD 5.4.2.6)
- Resistance factor for shear (LRFD 5.5.4.2)
- Tensile and shear capacity of concrete (LRFD 5.8.2.2)

4.2 SECTION PROPERTIES

The top portion of a DBT is often cast with air-entrained concrete for durability purposes. This region can vary in depth between just couple of inches to a zone encompassing the entire top flange of the girder. When the depth of the top layer is relatively shallow, the change in section properties is typically low, and its impact on design is often ignored. However, when the entire top flange is cast with a different

material, such as in Figure 4-1, section properties of the girder must be recomputed to reflect the impact.

The modular ratio, n, is used to adjust the section properties of the gross cross section to reflect the variation in modulus of elasticity of the two strengths of materials. Typically, the bottom portion of the girder has the higher strength. The width of the top portion is therefore linearly reduced by the modular ratio, and the section properties are recalculated. Note that computed stresses in the upper portion must be subsequently reduced by factoring their values by n to compensate for a lower modulus of elasticity of the top concrete.

Strength design is also impacted with variation in concrete strengths. For flexural design, typically the lower strength concrete (i.e., the strength of the upper layer) is assumed for the entire girder cross section for simplicity since the compression block under positive flexure is typically confined to within the top few inches of the girder. For shear design, however, the higher strength concrete is typically assumed for the entire cross section since shear acts over the shear depth, which is typically most of the depth of the girder.

4.3 LOADS

4.3.1 Temporary Construction Loads

A type of construction load not typically present with other types of prestressed girders but which may need to be considered in the design of DBTs is camber leveling load. Camber leveling is accomplished by jacking or surcharging as discussed in Section 3.4.2.1. During construction, individual welded connectors or temporary clamps are used to hold adjacent members in alignment while the keyway between the members is grouted. If the welded connectors are used for this purpose, they should be designed for the temporary transfer vertical shear across the joints. After the grout is sufficiently cured, the grout resists the vertical shear forces across the joints and the welded connectors become tension ties.

A study of camber leveling forces was carried out in NCHRP Project 12-69. The objective of this study is to determine the shear forces transferred across the joint due to

leveling of differential camber. Following is a summary of the methodology and findings of this study.

The first task was to determine the potential magnitude of differential camber to consider. Alaska DOT (23) specifies a camber tolerance of ± 1/8 in. per 10 ft of length with maximum of 1 in. from approved camber. Alaska DOT also specifies that the camber of any girder shall not differ from that of any other girder by more than 1 in. PCI Design Handbook (24) reports a typical differential camber tolerance of 1/4 in. per 10 ft with a maximum of 3/4 in. Washington State DOT (25) specifies a differential camber tolerance of 1/8 in. per 10 ft of beam length. Based on consultation with experts from the precast-prestressed concrete industry, there seems to be a consensus that with the current industry standards the maximum limits on differential camber are hard to achieve for longer spans. Due to this variation between different specifications, camber measurement data was reviewed (26, 27) to define the practical limits on differential camber between girders in a span. Based on the data presented above, the research team recommends using a differential camber tolerance of 1/8 in. per 10 ft with no upper limit.

Using this differential camber criterion, a parametric study was conducted using finite element analyses to determine the range of expected camber leveling shear for different girder depth, girder spacing, and skew angle. Three different overall girder depths are investigated: 41 in., 53 in., and 65 in. For each girder depth, 4 ft and 8 ft spacing are considered. The study included non-skewed bridges as well as bridges with skew angles of 15^o, 30^o, and 45^o. The shortest practical span for each combination of girder depth and spacing was used. For the 4 ft spacing, the bridge consisted of 12 girders, while for the 8 ft spacing the bridge consisted of 6 girders with an overall bridge width of 48 ft. For six girder bridges, one middle girder is leveled against two girders on one side and three girders on the other side. For twelve girder bridges, one middle girder is leveled against five girders on one side and six girders on the other side.

The maximum joint shear for non-skewed bridges was 0.87 kip/ft. The effect of the skew is such that the leveling shear is increased near one end of the longitudinal joint and reduced near the other end. This effect is more pronounced with the increase of the skew angle. The maximum calculated joint shear was 1.01 kip/ft for 15^o skew angle, 1.18 kip/ft for 30^o skew angle, and 1.45 kip/ft for 45^o skew angle.

Although the maximum initial camber leveling shear force will reduce with time, this initial force needs to be considered in design of the camber leveling procedures. As discussed in Section 3.4.2.1 and 3.4.3.2, for camber leveling procedures, weld plates or temporary clamps may be used to resist the camber leveling forces until the joints are grouted. The maximum calculated levels of temporary joint shear force described above, dependent on whether the bridge is a non-skewed or skewed bridge, can be used to determine the design shear force for the welded connectors. An example design for temporary clamps, using 1.5 k/ft. as the maximum camber leveling shear force, is included in Appendix B

In addition to joint shear forces, the maximum flexural stresses resulting in the girders due to camber leveling were calculated. The maximum calculated stress is approximately 890 psi. This is likely a conservatively high calculated stress considering that:

- The differential camber used to verify the 1/8 in. per 10 ft. was the maximum camber difference between any two of the girders in a group, it is unlikely that this maximum differential camber would actually occur between an interior girder and the two adjacent girders as modeled in the analyses for this study;

- The analyses assumed that 100% of the deferential camber was removed during the leveling process;

- Creep is expected to reduce camber leveling stresses to approximately 35% of the initial stresses;

- The effect of camber leveling has not been shown to be a problem in decked girder bridges presently in use;

Although the nominally high tensile stresses were calculated using conservative assumptions and creep is expected to reduce the level of these stresses in a short time, further consideration was given to these nominally high stresses.

Additional analyses were therefore performed to investigate the sensitivity of the calculated stresses to span length. A governing condition for maximum calculated

camber leveling forces in the prior parametric study was a short span. The maximum forces for each girder depth analyzed were calculated using the shortest span length. The additional analyses were therefore carried out to determine if the calculated tensile stresses decreased significantly as the spans were increased. For each combination of girder depth and spacing, the span was varied from the practical shortest span to the longest possible span for that particular section. The analyses did not indicate a significant drop with increased span length. Calculated maximum tensile stresses, ranging from approximately 400 to 500 psi at the longest possible spans, are still nominally high.

One of the reasons given above to support a conclusion that tensile stresses due to camber leveling should not be a problem is that the effects of camber leveling has not been observed to be a problem in decked girder bridges currently in use. However, it should be noted that an allowable of 0 tensile stress is commonly used in the design of decked girders under service load. Based on this observation and the nominally high calculated flexural tensile stresses in this camber leveling study, an allowable of 0 tensile stress is included in these design guidelines. This criterion allows a margin of tensile capacity to help compensate for camber leveling tensile stresses rather than attempting to calculate the effects of camber leveling in the design process.

4.3.2. Live Load

The design vehicular live load under the LRFD Specs is the HL-93 load, which consists of the design truck or design tandem, combined with the design lane load. Other types of vehicles may be applicable as well, such as for rating or for permitting. As discussed in Section 1.1.2.2, any live load to be designed for in additional to HL-93 should be established in the preliminary assessment stage of the project.

4.3.2.1 Live Load Distribution – Overview

As with other types of bridges the apportioning of live load to individual girders in a DBT bridge is handled using the so-called live load distribution technique. The superstructure is modeled as a simple or continuous beam on roller supports. The design live load is then positioned so as to generate the maximum and minimum moments and shears. The results of the entire live load (gross results) are then distributed to individual girders using dimensionless distribution factors. Typically,

separate distribution factors are computed for moment and shear, which are further subdivided into exterior and interior girder cases.

There are two basic approaches to computing the live load distribution factor in accordance with the LRFD Specs: the approximate method and the refined method of analysis.

The approximate method is treated in Article 4.6.2, including specifics on conditions of its use, which is the most typical approach used in engineering practice. DBT bridges are designated as Bridge Type "j" in which the supporting components are precast concrete tee sections with shear keys, with or without transverse post-tensioning, and the deck type is integral concrete. Separate treatments are given for moment and shear, for interior and exterior beams, for single lane loaded and multiple lanes loaded cases, and for "sufficiently connected" or "not sufficiently connected" cases. The conventional DBT construction with welded shear connections is considered "not sufficiently connected". Construction with the proposed alternate longitudinal joint with spliced headed bars is considered "sufficiently connected".

Details on the procedures for the approximate methods as they relate specifically DBTs are discussed in Sections 4.3.2.2 and 4.3.2.3 below. The refined method is discussed in Section 4.3.2.4

4.3.2.2 Live Load Distribution – Not Sufficiently Connected

For most bridge systems, the LRFD specifications give two distinct groups of equations to determine the live load distribution factor of a bridge girder. One set of equations provides the distribution factor under general or multilane loaded conditions. The other set of equations provides the distribution factor when the bridge is subjected to a single-lane loaded condition. However, the equations for the DBT bridge system, in which the girders are connected only enough to prevent relative vertical translation, do not distinguish between the single-lane and multilane loaded condition. Typically, designers use the distribution factor equations for the single-lane loaded condition to rate bridges for permit loads or overload conditions in which the bridge will be subjected to only one truck. Because the LRFD design does not distinguish between the multilane loaded and single-lane loaded condition, there is a load rating penalty for the DBT bridge system. Based on a field testing program (11), a more accurate set of distribution factor

equations that describe the behavior of the DBT bridge system under a single-lane loading condition has been proposed (12).

Moment, Interior Girder, Not Sufficiently Connected (Regardless of Lanes Loaded):

S/D

Where,

C = K(W/L) £ K

$D = 11.5 – N_L + 1.4N_L(1\text{-}0.2C)^2$

When C £ 5:

$D = 11.5 – N_L$

When C > 5:

$$K = \sqrt{\frac{(1+m)I}{J}}$$

For preliminary design, K may be taken as 2.0 for tee beams. For stocky, open sections, such as DBTs, the St. Venant torsional constant, J, can be approximated by:

$$J = \frac{4A^4}{40.0I_p} \qquad \text{(C4.6.2.2.1-2)}$$

Moment, Exterior Girder, Not Sufficiently Connected, Two or More Lanes Loaded: Use lever rule.

Shear, Interior Girder, Not Sufficiently Connected, One Lane Loaded: Use Lever Rule

Shear, Interior Girder, Not Sufficiently Connected, Two or More Lanes Loaded: Use Lever Rule

Shear, Exterior Girder, Not Sufficiently Connected, One Lane Loaded: Use Lever Rule

Shear, Exterior Girder, Not Sufficiently Connected, Two or More Lanes Loaded: Use Lever Rule

4.3.2.3 Live load distribution –Sufficiently connected

Moment, Interior Girder, Sufficiently Connected, One Lane Loaded:

$$g = 0.06 + \left(\frac{S}{14}\right)^{0.4}\left(\frac{S}{L}\right)^{0.3}\left(\frac{K_g}{12.0Lt_S^3}\right)^{0.1} \qquad \text{(Table 4.6.2.2.2b-1)}$$

Where:

g = distribution factor

S = spacing of supporting components (ft)

L = span length (ft)

t_s = depth of concrete slab (in)

$$K_g = n\left(I + Ae_e^2\right) \qquad \text{(4.6.2.2.1-1)}$$

In which:

$$n = \frac{E_B}{E_D} \qquad \text{(4.6.2.2.1-2)}$$

Where:

EB = modulus of elasticity of beam material (ksi)

ED = modulus of elasticity of deck material (ksi)

I = moment of inertia of beam (in4)

e_g = distance between the centers of gravity of the basic beam and deck (in)

Figure 4-2 illustrates e_g for a Decked Bulb Tee.

Moment, Interior Girder, Sufficiently Connected, Two or More Lanes Loaded:

$$g = 0.075 + \left(\frac{S}{9.5}\right)^{0.6}\left(\frac{S}{L}\right)^{0.2}\left(\frac{K_g}{12.0Lt_s^3}\right)^{0.1}$$

Moment, Exterior Girder, Sufficiently Connected, One Lane Loaded:

The Lever Rule is used for this case. This procedure consists of modeling the deck as simple-span planks between girders or as a simple-span beam with a cantilever for exterior beams. Each wheel line of the live load vehicle is placed in order to maximize the reaction under each girder. The total reaction under a girder is the fraction of the vehicle weight borne by that girder or, in other words, the distribution factor.

For exterior beams in which a diaphragm or cross-frame is present, the minimum distribution factor is that which would result if the bridge cross section were assumed to be rigid and translates and rotates as such. In equation form, this would be as follows:

$$R = \frac{N_L}{N_b} + \frac{X_{ext}\sum_{N_L} e}{\sum_{N_b} x^2} \qquad \text{(C4.6.2.2.2d-1)}$$

Where:

R = reaction on exterior beam

N_L = number of lanes loaded under consideration

e = eccentricity of design truck

x = horizontal distance from center of gravity of pattern of girders to each girder

X_{ext} = horizontal distance from center of gravity of pattern of girders to exterior girder

N_b = number of beams

Moment, Exterior Girder, Sufficiently Connected, Two or More Lanes Loaded:

$$g = eg_{interior}$$

In which:

$$e = 0.77 + \frac{d_e}{9.1}$$

Reduction of Distribution Factor for Moment for Skewed Supports:

If units are sufficiently connected to act as a unit, the following reduction factor may be applied.

$$Reduction = 1 - c_1 (\tan \theta)^{1.5} \qquad \text{(Table 4.6.2.2.2e-1)}$$

$$c_1 = 0.25 \left(\frac{K_g}{12.0 L t_s^3} \right)^{0.25} \left(\frac{S}{L} \right)^{0.5}$$

If $\theta < 30^o$ then $c_1 = 0.0$. If $\theta > 60^o$ use $\theta = 60^o$

Shear, Interior Girder, Sufficiently Connected, One Lane Loaded:

$$DF = 0.36 + \frac{S}{25.0}$$

Shear, Interior Girder, Sufficiently Connected, Two or More Lanes Loaded:

$$DF = 0.2 + \frac{S}{12} - \left(\frac{S}{35} \right)^{2.0}$$

Shear, Exterior Girder, Sufficiently Connected, One Lane Loaded: Use Lever Rule

Shear, Exterior Girder, Sufficiently Connected, Two or More Lanes Loaded:

$$g = eg_{interior}$$

In which:

$$e = 0.6 + \frac{d_e}{10}$$

Shear Correction Factor for Skewed Supports

For computing the distribution factor for shear at the supports near the obtuse corner, the following correction factor may be applied:

$$CorrectionFactor = 1.0 + 0.20\left(\frac{12.0Lt_s^3}{K_g}\right)^{0.3} \tan\theta$$

4.3.2.4 Live Load Distribution –Refined Methods

Refined methods discussed in LRFD Article 4.6.3. Section 4.6.3.2.1 for analysis of decks indicates that, for locations of flexural discontinuity through which shear may be transmitted should be modeled as hinges. This is appropriate for the longitudinal joint locations for conventional DBT construction with welded connectors.

For construction with the proposed alternate longitudinal joint with spliced headed bars, the deck is considered continuous for moment and shear. Section 4.5.2.2 of LRFD Article 4.5 for mathematical modeling indicates that the stiffness properties shall be based on cracked and/or uncracked sections consistent with the anticipated behavior. The analytical study carried out in NCHRP Project 12-69 for live load demands on the proposed alternate joint indicated that the joint would be expected to crack under maximum moments calculated using uncracked stiffness in the model. However, the commentary for Section 4.5.2.2 indicated that, for bridges within the elastic range of behavior, the cracking of concrete seems to have little effect of the global behavior. Therefore, for live load distribution, LRFD implies that use of an uncracked section may be adequate.

4.3.3 Structural Systems

4.3.3.1 Simple-Span

The predominant structural system used in DBT bridges is simple-span. Design and detailing conventions for simple-span DBT bridges are identical to those of conventional precast, prestressed I-girder bridges.

4.3.3.2 Continuous for Live Load

4.3.3.2.1 Review of Research. For multi-span bridges, there are advantages in making a precast bridge continuous as discussed in Section 2.1.1.2 of theses guidelines. Section 3.4.1 of these guidelines provides examples of establishing continuity by extending bars from the top flanges of the girders, coupling them, and possibly stressing them. However, multiple-span composite bridges, made continuous for superimposed dead loads and live loads, become statically indeterminate. As a result, inelastic deformations that occur after the connection has been made will generally induce statically indeterminate forces and restraining moments in the girders. Some sources of inelastic deformations in conventional precast concrete girders with cast-in-place decks are not present in DBTs. Therefore, statically indeterminate forces and restraining moments in DBTs will differ from those in conventional precast concrete girders, as discussed below.

a. Conventional Precast Concrete Girders with Cast-in-place Decks

Sources of inelastic deformation in conventional precast concrete girders with cast-in-place decks include creep and shrinkage, and temperature gradients. Creep of the girder concrete under the net effects of prestressing and self-weight will tend to produce additional upward camber with time. When girders are made continuous at a relatively young age, it is possible that positive moments will develop at the supports over time. These positive restraint moments are caused by continual cambering upwards as a result of ongoing creep strains associated with the prestress. In conventional girders with cast-in-place decks, differential shrinkage between the deck concrete and girder concrete results in downward deflection. Also, loss of prestress due to creep, shrinkage and relaxation results in downward deflection. Therefore, differential shrinkage and loss of prestress has a tendency to reduce this positive moment.

In addition to creep and shrinkage of concrete, temperature gradients can play a major role if the girders are made continuous. Solar heating of the top deck will

tend to produce upward camber adding to the positive restraint moment caused by creep. Large restraining positive moment can cause cracking in the bottom flange near the pier locations (28, 29). Heat of hydration in the cast-in-place deck concrete can have a mitigating effect on the development of positive restraint moment. The cast-in-place deck may be heated to temperature that is higher than the supporting girder temperature by heat of hydration during the initial hydration when the concrete is still plastic. Contraction of the deck concrete with subsequent cooling after the concrete has hardened results in a downward deflection thereby reducing the positive restraint moment caused by creep and solar heating.

Oesterle et al. (28-30) presented the results of an experimental and analytical research program, funded by NCHRP, and the Federal Highway Administration, on the behavior of continuous and jointless integral abutment prestressed concrete bridges with cast-in-place deck slab.

Results of the analytical studies showed that the age of the girder when the deck was cast was the most significant factor in determining whether positive or negative restraint moments occurred at the interior transverse joints over the piers due to the interaction of creep and shrinkage. Results also indicated that the live load continuity of the bridge may be reduced significantly with long-term and time dependent loading effects and with thermal effects.

In the experimental part of the jointless bridge research (28, 29), testing of materials, bridge components, and a full scale girder indicated that:

1. Expected shrinkage of the deck concrete did not occur in the concrete in the outdoor environment of Skokie, Illinois. Thus, the effects of deck shrinkage to mitigate the effects of girder creep did not occur.

2. Heat of hydration effects in the cast-in-place deck concrete can have a mitigating effect on the development of positive restraint moment.

3. Daily temperature effects with heating and cooling of the deck with respect to the girder have a significant effect on restraint moments. Solar

heating of the deck causes positive restraint moments of the same order of magnitude as the moments due to girder creep and are additive to the moments caused by creep.

4. Load tests on the full scale girder that was monitored and load tested periodically over an 18 month time frame, demonstrated that cracking due to positive moment at the transverse connection reduced continuity for live-load. When the restraint and dead load moments were added to the live-load moments, effective continuity was negative (i.e., less than 0%). That is, the total midspan positive moment in the tested continuous girder was slightly higher than the anticipated positive moment in a simply supported girder.

5. The positive moment due to combined creep and temperature effects resulted in stresses in the positive moment reinforcement in the connection over the pier that reached or exceeded yield stress.

Results of this research indicated that positive moment reinforcement does not affect the net resultant midspan service level stresses. If positive moment reinforcement is provided and positive restraint moments tend to develop, the need to superimpose the positive restraint moment on the dead and live load moment essentially negates any decrease in service level stresses resulting from the negative moment continuity connection over the piers.

If negative restraint moments develop, positive moment reinforcement is not needed. Therefore, these studies (28-30) indicated that there is no net benefit, in terms of service level stresses in the prestressed girder, by providing positive moment reinforcement in the transverse connections. It is understood, however, that there may be benefit, in terms of structural integrity, for providing the positive moment reinforcement.

The FHWA Jointless bridge project (28, 29) also included a study of the combined effects of live load and sources of secondary moment for the negative moment response prestressed concrete girders made continuous for live load. Results of this study indicate that the negative moment affecting deck

reinforcement stresses can be determined from an elastic, gross section analysis for live load, and the effect of secondary continuity moments can be ignored.

Recently, NCHRP Project 12-53 was completed and results are included in NCHRP Report 519 (31). This project was carried out to further examine the behavior of simple-span precast/prestressed girders made continuous by connections at the transverse joints over the piers. The focus was on the effectiveness of the positive moment connection and on design criteria for this connection. Results of analytical studies were similar to those reported in the previous study (30). That is, if positive restraint moments develop, these restraint moments must be added to the positive moments caused by dead and live load, and that the net positive moment at the midspan is essentially independent of the amount of positive moment reinforcement provided in the transverse connection. In addition, analytical studies indicated that cracking in the transverse joint decreases live-load continuity.

NCHRP Project 12-53 (31) also included experimental studies. Live load testing indicated that, contrary to analyses results, the continuity with application of live load was near 100% until the positive moment crack at the connection became very large. The full scale testing result in the NCHRP 12-53 study, with essentially no live-load continuity lost due to positive moment cracking, differed from the result of full-scale testing in the jointless bridge study (28, 29). However, some results from the NCHRP 12-53 full-scale tests were similar to those observed in the jointless bridge study including:

1. The shrinkage strains in the deck concrete were significantly less than expected.

2. The effects of heat of hydration in the deck concrete were significant.

3. Daily thermal effects were significant.

Based on the analyses and testing, recommendations for the positive moment connection in NCHRP Report 519 included:

1. The positive moment connection should be provided and designed for the calculated moment due to dead, live and restraint moment. However,

minimum reinforcement should be provided for a moment equal to $0.6M_{cr}$ where M_{cr} is the cracking moment of the connection. Also, the design moment should not exceed 1.2 M_{cr} because providing more reinforcement is not effective. If the design moment exceeds 1.2 M_{cr}, design parameters should be changed. The easiest change to reduce the positive moment is to specify a minimum age of the girder at the time of making the continuity connection.

2. If the contract documents specify that the girders are a minimum age of 90 days when continuity is established, the restraint moment does not have to be calculated. This is based on the observation from surveys and analytical work that, if the girders are more than 90 days old when continuity is formed, it is unlikely that time-dependent positive restraint moments will form.

3. The transverse connection can be considered fully effective if, "… the calculated stress at the bottom of the continuity diaphragm for the combination of super imposed permanent loads, settlement, creep, shrinkage, 50% live load and temperature gradient, if applicable, is compressive."

b. Decked Girder Bridges

The major difference between the DBT bridges and the type of bridge studied in the NCHRP and jointless bridge projects described above is that, in the DBT bridges, the deck is part of the precast prestressed section. There is no differential shrinkage or heat of hydration strains to help mitigate the effects of the creep in the prestressed section. For DBT girders made continuous, if the camber under sustained dead load is upward after the continuity connection is made, then positive restraint moments will develop from time-dependent effects. Therefore, the criterion for neglecting restraint moments from time-dependent effects if the girders have a specified minimum age of 90 days is questionable for DBT bridges. In addition, restraint moments due to thermal gradients from solar heating may add significant positive moment.

Considering that DBT bridges essentially do not have any differential contraction between the deck and the girder due to differential shrinkage or heat of hydration effects, positive restraint moment from combined creep and temperature effects may be large. Regardless, however, of all the study and discussion of positive restraint moments and loss of live load continuity in these simple span girders made continuous presented above, this type of bridge girder has generally performed exceptionally well for decades. The only reported serious problems with this type of bridge include a small number of incidences with excessive cracking in the positive moment connection regions near the ends of the girders (24, 25). The distress observed in these girders was likely due to high positive thermal gradients combined with large capacity of positive moment reinforcement in the connections over the piers. However, if the capacity of the positive moment reinforcement is limited to not exceed 1.2 $M_{cr,}$, as recommended in the NCHRP Report 519, and the positive moment reinforcement is adequately developed in the ends of girders, the positive moment connection will yield before excessive positive moments can develop and the behavior for positive restraint moment will be acceptable

4.3.3.2.2 Design Recommendations. Based on the above review of research, the following recommendations are made for design of multi-span DBT girders made continuous for live load:

1. For negative moment, and for positive moment at strength limit states, design the girders and connections based on fully continuous elastic, gross section analysis for live load. The effect of secondary continuity moments can be ignored.

2. For positive moment service level stresses, design the girders based on analysis as simple supported spans. The effect of secondary continuity moments can be ignored.

3. Provide a positive moment connection with minimum reinforcement for a moment equal to $0.6M_{cr}$ where M_{cr} is the cracking moment of the connection. Also, the design positive moment should not exceed 1.2 $M_{cr.}$

4. If mild reinforcing bars are used for the positive moment reinforcement, extend the bars into the bottom bulb a full development length beyond the transfer length of the bonded prestressing strands in the bottom bulb. Check the level of prestress in the bottom of the girder at the transfer length to ensure that it is greater than the sum of the bottom bending stresses due to girder dead load acting on a simple supported span plus a potential positive restraint moment assuming full yield stress in the positive moment reinforcement applied to the end of the girder. If the level of prestress is not sufficient to resist this combined positive moment, reduce the amount of positive moment reinforcement.

4.4 PRESTRESSING LAYOUT

4.4.1 Pretensioning

4.4.1.1 Draped Strands

Draped strand patterns tend do a better, more efficient job at controlling end stresses in girders than do straight patterns with debonding. They also tend to result in more efficient vertical shear designs. The LRFD Specifications require that longitudinal steel requirements be met. Unlike debonded patterns, a larger percentage of the strands in the pattern tend to be available to contribute to the provided capacity of the required tension tie.

Drawbacks of draped patterns include the added complexity in prestressed bed design and the safety issues associated with the sometimes very large hold-down forces that are generated. Figure 4-3 shows devices t hold down harped strand.

4.4.1.2 End Debonding

As an alternative to draping strands to control the stresses in the ends of the beam at release, debonding can be used. Debonding consists of wrapping or sleeving individual strands to break the bond between the strand and the concrete for a specified distance. Typically, debonding starts at the end of the girder and runs along the strand towards the interior of the girder. This method of controlling girder end stresses in

girders is favored by some precast fabricators because it eliminates the safety risks and expenses associated with draping strands.

Debonding is covered in LRFD Art. 5.11.4.3. In summary: The number of debonded strands should not exceed 25 percent of the total number of strands in the strand pattern. For any given row of strands, no more than 40 percent of the strands should be debonded. Debonding patterns should be symmetric and the end strands of each row should not be debonded. Figure 4-4 illustrates types or debonding.

4.4.1.3 Temporary Top Strands vs. Midspan Debonding

To control release stresses in a girder, temporary top strands can be used. These are post-tensioned strands that are stressed after the prestensioned strands are released. Once the girders are erected into their final locations in the bridge, the temporary strands can be detensioned.

Alternatively, fully-stressed straight pretensioned strands are sometimes placed near the top of the beam to control top tensile stresses near the ends of the girder at release. However, these strands tend to reduce the bottom prestress near the midspan region and thus may require that strands be added to the bottom region of the beam to offset the effect of the top strands. To avoid adding additional strands to the pattern, the technique of midspan debonding can be employed. Here debonding or sleeving is applied to the top strands over the midspan region of the girder and an access pocket is cast into the top flange of the girder, which is centered on midspan of the girder. Once the girders are placed into their locations in the bridge, the strands are cut via the access pockets, thus disabling their effect for the length of the debonding. Note that the access pockets must be cleaned out and grouted after the detensioning operation.

4.5 PRESTRESS LOSSES

The level of prestress in a prestressed concrete beam does not remain constant throughout the life of the beam. The prestress level varies during the various stages of the loading of the girder as a function of time and the material properties of both the concrete and the prestressing steel.

4.5.1 Loss Components

In accordance with the AASHTO Specifications, several components of prestress loss are evaluated:

- Elastic shortening (instantaneous effect)
- Anchor set (post-tensioning tendons only)
- Friction (post-tensioning tendons only)
- Relaxation of prestressing steel (time-dependent)
- Shrinkage of concrete (time-dependent)
- Creep of concrete (time-dependent)

Of these four components, elastic shortening, anchor set, and friction loss are the only non-time-dependent components.

4.5.1.1 Instantaneous

4.5.1.1.1 Elastic Shortening. Elastic shortening (ES) loss occurs as the girder shortens when the strands are detensioned (i.e., cut) after the concrete has reached its specified minimum release strength. As the strands are detensioned, either by being individually cut, detensioned together as a gang, or by some other method, the prestress is imparted into the girder. When this force acts on the girder, the girder itself shortens a small amount and the prestressing steel embedded in the girder shortens with it, reducing the stress level in the strands. The amount of prestress loss attributed to this elastic shortening is a function of the level of prestress, area of the concrete cross section, and the modulus of elasticity of both the concrete and the steel.

4.5.1.1.2 Anchor Set. After a post-tensioning tendon has been stressed to its required level, each strand must be anchored using a chuck. Typically, for a strand to fully anchor, it shifts by an amount equal to the anchor set.

4.5.1.1.3 Friction. During the stressing operation of post-tensioning tendons, friction causes some portion of the prestress to be lost. This loss occurs as a function of

the wobble coefficient (K), the friction coefficient (μ), the length of the tendon, and the total angle change of the tendon.

4.5.1.2 Time-Dependent

4.5.1.2.1 Relaxation of Prestressing. Steel. If a prestressing strand were stretched some distance and its ends were anchored a fixed distance apart, over time the steel would gradually relax and the stress level in the strand would decrease. This phenomenon is called steel relaxation.

4.5.1.2.2 Shrinkage of Concrete. After casting, over time, concrete gradually shrinks due to water loss. The amount of shrinkage is a function of the ambient relative humidity at the project site.

4.5.1.2.3 Creep of Concrete. When a load is applied to concrete, it gradually moves, or creeps. In the case of a prestressed concrete girder, under permanent loads (i.e., dead load and prestress), there is a component of creep in the direction of the prestressing strands, which causes the strands to shorten over time. This, in turn, results in a loss of prestress.

4.5.2 Simplified Methods

The simplified method specified in the Specs consists of computing instantaneous, elastic losses, but lumping time-dependent losses into a single value.

4.5.3 Detailed Method

The detailed loss method involves computing elastic losses and separate calculations for each time-dependent component.

When post-tensioning is introduced into a pretensioned girder, there is interaction between the PT and the pretensioning. Essentially this means that the losses in the pretensioned strands are increased due to the extra force applied to the girder during the post-tensioning operation. The method of computing losses described in NCHRP Report 517 (32) is recommended.

4.6 STRESSES

4.6.1 Concrete Stress Limits

4.6.1.1 Service Limit State After Losses

LRFD Section 5.9.4.2.2 allows $0.19\sqrt{f'_c}$ (ksi) tensile stress in the precompressed tensile zone of fully prestressed components. However, as discussed in Section 4.3.1, nominally high calculated flexural tensile stresses were determined in the study of the effects camber leveling forces in DBT girders. Therefore, an allowable of 0 tensile stress is included in these design guidelines. This criterion provides a margin of tensile capacity to help compensate for camber leveling tensile stresses rather than attempting to calculate the effects of camber leveling in the design process.

4.6.1.2 Stress Limit State for Future Re-Decking

If future full deck replacement is required as an option, stress limits during deck removal and after replacement with a cast-in place deck need to be considered in the original design calculations in addition to stress limit states for the original girder. As discussed in Section 3.5.1.2, with deck removal and replacement, the girder section is converted from a fully prestressed system to a composite system as illustrated in Figure 3-19. Overall dimensions of each system are identical. However, in the first case the entire system in prestressed whereas in the second case, only the lower portion is prestressed. Therefore, the stress history in the girder is more complex. Stresses will need to be checked at the application of each load and when section properties change. Higher stresses are expected in the lower portion during deck removal and after the CIP section is cast since there is less area over which the prestressing force is applied. At this stage, however, all prestress losses would have occurred. In addition, at this stage, camber leveling forces are no longer applicable. Therefore, the allowable of 0 tensile stress to provide a margin of tensile capacity to help compensate for camber leveling tensile stresses, as discussed in Section 4.6.1.1, is not needed. The LRFD Section 5.9.4.2.2 allowable of $0.19\sqrt{f'_c}$ (ksi) tensile stress in the precompressed tensile zone would be applicable.

4.7 FLEXURAL STRENGTH

4.7.1 Flexural Capacity - Reinforcement Limits

Previous editions of the LRFD Specifications specified limits on the reinforcement that can be placed in a beam. However, as of the 4th edition, that limit has been eliminated. A unified approach in which phi is now variable has been introduced (Art. 5.5.4.2.1), which effectively covers this check. For prestressed members, the variation in phi is computed according to the following:

$$0.75 \le f = 0.583 + 0.25\left(\frac{d_t}{c} - 1\right) \le 1.0 \qquad \text{(LRFD Eq. 5.5.4.2.1-1)}$$

4.8 SHEAR DESIGN

4.8.1 Vertical Shear

4.8.1.1 Critical Section for Shear

Due to the structural system configuration and the orientation of loads on precast girder bridges, compression is introduced into the end regions of the girders due to applied loads. For such cases, LRFD Art. 5.8.3.2 states that the critical section for shear shall be taken as the larger of $0.5d_v\cot(q)$ or d_v from the internal face of the support, since d_v is a fixed value and since it is conservative to adopt a section closer to the support.

LRFD Art. 5.8.2.9 defines the parameter d_v as the effective shear depth, which is taken as the distance between the resultants of the compressive and tensile forces. In practical terms, d_v is the distance between the centroid of the compression block and the centroid of the tensile force, taking into account the effects of both prestressed strand and non-prestressed reinforcement (i.e., rebar). However, d_v need not be taken to be less than the greater of $0.9d_e$ and $0.72h$, where d_e is defined above (see Section 5.8) and h is the total section height.

4.8.1.2 Sectional design model

One of the biggest changes introduced in the LRFD Specifications is the procedure used to compute the concrete contribution to the vertical shear strength of the beam. While the basic steps to designing shear steel are the same as for the Standard Specifications (33), the procedure for determining V_c has completely changed. V_c must be determined using the Modified Compression Field Theory method (34), or the

Sectional Design Model (Art. 5.8.3), as it is termed in the LRFD Specs. This method is a trial-and-error procedure, the basic steps of which are outlined below.

Step 1: Compute the factored shear, V_u

Step 2: Compute the shear stress at the section using:

$$v = \frac{\left|V_u - f V_p\right|}{f b_v d_v} \qquad \text{(LRFD Eq. 5.8.2.9-1)}$$

Step 3: Assume a value of q, the crack angle.

Step 4: Compute the strain in the longitudinal reinforcement using:

$$e_x = \frac{\left(\frac{|M_u|}{d_v} + 0.5N_u + 0.5\left|V_u - V_p\right|\cot q - A_{ps} f_{po}\right)}{2(E_c A_c + E_s A_s + E_p A_{ps})} \qquad \text{(LRFD Eq. 5.8.3.4.2-3)}$$

Step 5: Using Table 5.8.3.4.2-1, look up a revised value of theta.

Step 6: If the new value of theta differs from the assumed value by more than 0.1 degrees, continue iterating by re-computing e_x and looking up a new value of q.

Step 7: Once the value of q has converged, beta can be determined from Table 5.8.3.4.2-1. Once b is known, V_c can be computed using:

$$V_c = 0.0316\ b\sqrt{f_c'}\, b_v d_v \qquad \text{(LRFD Eq. 5.8.3.3-3)}$$

4.9 TOP FLANGE DESIGN

4.9.1 Flanges with Conventional Weld Plate Joints

As discussed in Section 4.3.2.1, the conventional DBT construction with welded shear connections is considered “not sufficiently connected”. For transverse analysis of decks with flexural discontinuity through which essentially only shear may be transmitted, the locations of the discontinuities should be modeled as hinges. Two conditions must be checked for the top flange design: the case where a truck wheel is

placed directly over an interior joint and the case where the wheel load is placed on the exterior side of the exterior girder.

4.9.1.1 Typical Interior Girder

Flange connections are generally designed to transmit shear via a grouted keyway. Because of this, it is reasonable to assume half of a wheel load is distributed to the flange of each adjacent girder (Fig. 4-5a). The equivalent strip method (Figure 4-5b) is then used to design the required amount of transverse reinforcement that must be placed in the flange to resist the applied loads. The basic steps required for this analysis are as follows:

1. Determine the width of the top flange that resists the applied moment. AASHTO LRFD Article 4.6.2.1.3 provides guidance on the equivalent strip width. The DBT flange can be assumed to act as an overhang. From AASHTO LRFD Table 4.6.2.1.3-1, the equivalent strip width is:

   $E = 45.0 + 10.0X$

   Where,
   E = Equivalent strip width (in.)
   X = Distance from load to point of support (ft.)

2. Compute the required factored moment at the section on per unit width basis.

3. Determine the flexural resistance of a unit width strip.

4.9.1.2 Typical Exterior Girder

The flange of an exterior girder must be checked for the full wheel load. But the wheel load need not be placed any closer to the barrier than as required by code. That distance is typically one foot from the face of the barrier (Figure 4-5c). As with an interior flange, the equivalent strip method (Figure 4-5d) is then used to perform the design. The steps to design the exterior overhang of an exterior girder are similar to those for an interior girder.

4.9.2 Flanges With Headed Bar Joints

For construction with the proposed alternate longitudinal joint with spliced headed bars, the deck is considered continuous for moment and shear. With the exception of the longitudinal joint region, it is recommended that an approximate method with equivalent strips be used for design of the flanges per LRFD Art. 4.6.2. Design loads are determined per LRFD Section 3.6.1.3.3. The reinforcement for the headed bar longitudinal joint region is discussed in Section 4.12.2.2.

For design of the flanges using the optimized section with the re-decking option, the sub-flange is considered as a slab in parallel with the top flange rather than composite with the top flange for spans in the transverse direction. Reinforcement for the sub-flange is illustrated in Figure 4-6. It is recommended that the outside edges of the sub-flange be tied to the top flange for deformations that would tend to lift the top flange up away from the edge of the sub-flange. This reinforcement may also be used to add to the reinforcement for horizontal shear in the longitudinal direction as discussed in Section 4.13 of this report. However, it is not intended to make the sub-flange composite with the top flange in the transverse direction.

4.10 REINFORCEMENT DETAILING

This section of the Guidelines contains some figures that include specific details. These details are provided for concept only and should not be considered as final designs.

4.10.1 Typical Reinforcement

4.10.1.1 Near end of girder

Figures 4-7 and 4-8 illustrate an example of elevation and section views of typical reinforcement required near ends of girders. Figures 4-9 to 4-12 show example plan views of the various layer of typical reinforcement required near ends of girders.

4.10.1.2 Near midspan of girder

Figure 4-13 illustrates an example of typical reinforcement near midspan of a girder

4.10.2 Bursting Reinforcement

Bursting reinforcement is computed in accordance with LRFD 5.10.10.1. The bursting force, P_r, is computed as 4 percent of the total prestressing force. The relationship between P_r and the bursting reinforcement is as follows:

$$P_r = f_s A_s \qquad (5.10.10.1\text{-}1)$$

Where:

f_s = stress in steel not exceeding 20 ksi

A_s = total area of vertical reinforcement located within the distance h/4 from the end of the beam ($in.^2$)

h = overall depth of the precast member (in.)

The reinforcement is typically the same shape as vertical shear reinforcement. However; a larger bar size may be necessary to enable the required area of reinforcement to be contained within the end zone. The first stirrup is to be placed as close to the end of the beam as practical.

4.10.3 Confinement Reinforcement

In practice, the design of confinement is empirical. LRFD 5.10.10.2 stipulates that for a distance 1.5d from the end of the beam, deformed reinforcement no smaller than a No. 3 bar shall be placed to confine the prestressing strand in the bottom bulb of the girder. Confinement bars shall be shaped to enclose the strands and shall not be spaced farther apart than 6 in.

4.11 CAMBER AND DEFLECTIONS

Camber and long-term deflections are estimated using the PCI Multiplier method. Prestress uplift is computed using the moment-area method, which permits beams that contain debonding to be accurately handled. Instantaneous deflections due to applied loads are computed using closed-form solutions. To obtain long-term prestress uplift and load deflections, growth multipliers are applied to the instantaneous values.

In the LRFD Specs, live load deflection criteria are optional. If the Owner chooses to invoke such criteria, the deflection limit for concrete superstructures is specified as L/800 for normal vehicular loads. When pedestrians are present, deflection is limited to L/1000.

Minimum girder depths are often prescribed with the intention of controlling superstructure deflections. LRFD Table 2.5.2.6.3-1 indicates that the traditional minimum depth for precast I-beam superstructures of constant depth is 0.045 L for simple spans and 0.040 L for continuous structures. Theses minimum depths are presented by the Specifications as guidelines, subject to Owner adoption.

4.12 CONNECTION DESIGN

4.12.1 Lifting Loops

Figure 4-14 illustrates an example of typical lifting loop details

4.12.2 Longitudinal Joint

4.12.2.1 Conventional Weld Plate Joints

This section of the Guidelines contains some figures that include specific details. These details are provided for concept only and should not be considered as final designs.

Longitudinal joints between DBTs consist of two structural components: a grouted shear key and regularly spaced mechanical connectors embedded in the tips of abutted flanges, which are welded together in the field.

Vertical shear forces acting on longitudinal joints arise from rectifying differential cambers between beams during construction, from differential temperature effects, and from truck loads. In addition, tension or compression occurs when multi-stemmed members try to twist about their shear centers, which are above the flange. Also, shrinkage and temperature changes will cause forces which tend to separate the precast members. Other parameters to be considered in determining the connection forces are the effect of diaphragms; effect of skews; local lateral forces caused by vehicles changing lanes, and the “spreading” effects of vertical cyclic loading.

The recommended approach for designing the longitudinal joint is to design the grout key to carry all vertical shears applied after grouting (i.e., truck loading and differential temperature effects). The connectors should then be designed to carry the locked-in shear from leveling during construction, the tension due to restraint of twisting and the tension needed to mobilize the shear resistance of the connection after cracking. The spacing and strength of steel flange connectors should be based on shear forces induced before grouting and tension and moments induced afterwards. Twisting of the girders under live loads is shown to induce tension in the connectors along the joint between the two outer members of a bridge. However, this tension arises largely from compatibility and not equilibrium requirements, and its value is significantly reduced by small deformations of the connectors.

Stanton and Mattock made the following recommendations for the design of connections:

1. The edge thickness of the precast member flanges should be:

$$t_{edge} = 6\sqrt{\frac{5000}{f'_c}} \geq 6.00 \text{ in.}$$

2. The shape of the grout key should be as shown in Figure 4-15.

3. The spacing of the welded connectors should not be more than the lesser of 5 ft and the width of the flange of the precast member.

4. Welded connectors should be located within the middle third of the slab thickness.

5. The tensile strength of each connector and of its anchors should be not less than

$$T_n = T_1 + T_2 \text{ kip}$$

where:

$$T_1 = 16(\sin a - m_1 \cos a)/(\cos a + m_1 \sin a) \geq 6.00 \text{ kip and}$$

$$T_2 = 0.5sW_mN_m\mu_2 \text{ kip}$$

6. If the connector is to be used to resist shears due to the elimination of differential camber before grouting the keyway, both the shear strength of the metal connector and the resistance to shear of the anchors should be calculated using

$$V_n = N_a(2.5d_e - 3.5) \text{ kip}$$

must not be less than twice the calculated shear per connector due to the leveling operation.

In the above,

f_c' = Compressive strength of concrete;

T_1 = anchor force required to develop a shear resistance of 16 kip, in a length s of grouted connection

T_2 = maximum probable tension force per connector due to restraint of lateral shrinkage in bridge deck;

α = maximum inclination of sloping faces of grout key (see Figure 4-15);

μ_1 = coefficient of friction between grout key and concrete (to be taken as 0.5);

μ_2 = coefficient of friction between precast beams and their bearings (0.80 for concrete on concrete, 0.50 for concrete on elastomeric bearing pad);

s = longitudinal spacing of welded connector, in ft;

W_m = weight per foot length of each precast member and any topping its supports, in kip/ft;

N_m = number of members in width of bridge;

N_a = number of anchor bars or studs attached to connector in each flange; and

d_e = distance from centerline of anchor to nearest face of precast member flange in which it is embedded.

Figure 4-15 shows the shape of the shear key recommended by Stanton and Mattock (35). Figures 4-16 through 4-18 show typical weld tie details in common use. However, rather than headed studs, Jones (36) recommend that #4 rebar at least 18 in. long be used to anchor the plates to improve the capacity of the connection. The minimum thickness of the field-welded plate should be ¾" (37).

4.12.2.2 Headed Bar Joints

For construction with the proposed alternate longitudinal joint with spliced headed bars, the deck is considered continuous for moment and shear. Section 4.5.2.2 of LRFD Article 4.5 for mathematical modeling indicates that the stiffness properties shall be based on cracked and/or uncracked sections consistent with the anticipated behavior. The analytical study carried out in NCHRP Project 12-69 for live load demands on the proposed alternate joint indicated that the joint would be expected to crack under maximum moments calculated using uncracked stiffness in the model. While the commentary for Section 4.5.2.2 indicated that, for bridges within the elastic range of behavior, the cracking of concrete seems to have little effect of the global behavior, the maximum moments in the longitudinal joints in the analytical study occur in a local region in the joints when the wheel loads are at or near the joints. Therefore further analyses were carried out in the analytical study using a cracked flexural section at the longitudinal joint locations. (See also Appendix H of the main report for NCHRP Project 12-69 for further details on computer modeling of bridge decks with proposed alternate longitudinal joint with spliced headed bars.)

The proposed alternate longitudinal joint with spliced headed bars is described in Section 3.4.3 of this report. The geometry and the reinforcement for the alternate joint are shown in Figures 3-15 and 3-16. As described in the main report for NCHRP Project

12-69, extensive analytical studies were carried out to define the live load demands on the joint. In addition, laboratory testing indicated that this longitudinal joint detail has sufficient strength, fatigue characteristics, and crack control for the maximum loads determined from the analytical studies for all combinations of span length, girder spacing, girder depth, and bridge skew used in the analytical studies. Therefore, based on the analyses and tests carried out in the NCHRP Project 12-69,, the improved longitudinal joint shown in Figures 3-15 and 3-16 and described in Section 3.4.3 is a viable connection system to transfer the forces between the adjacent decked bulb tee (DBT) girders for all DBT girder bridges with 6 in. thick top flanges and girder spacing of 4 to 8 ft..

4.13 DESIGNING AND DETAILING FOR FUTURE RE-DECKING

Bridges constructed of conventional DBT girders have not typically been re-decked as a girder bridge with a cast-in-place deck might be. The primary reason for this is that bridges built to date with DBTs have largely been low-volume, non-interstate bridges. Therefore, deck wear would be minimal. Additionally, the quality of the concrete in the top region of a DBT is much higher than the quality of ready mix concrete used in CIP decks.

To be considered viable candidates for high-volume roads with high ADTTs, it was considered that a viable redecking scheme has been needed for DBT girders. Recent research has been conducted on conventional precast girder bridges with CIP decks in which details have been developed that greatly facilitate deck removal (21, 22). These details have been adapted for use with DBTs.

A re-deckable DBT would cast in two stages as indicated in Figure 4-20. The bottom stage would be cast first with a shear key formed along the top surface of the girder (Figure 4-21). Shear reinforcement would be placed at an increment of the shear key spacing and be detailed to fit within the available space (Figure 4-22). Figure 4-23 shows a photograph of pans used to form shear keys ion the top of the sub-flange. Figure 4-24 shows the resulting shear keys. A bond-breaking agent would then be applied to the top surface prior to the top flange being cast. Figure 4-25 the girder form with reinforcement prior to casting the top flange.

The initial design of a re-deckable DBT system is typically governed by the re-decking phase of the bridge, although this phase may be quite far into the life of the bridge. The stresses in the girder must be able to be maintained within the code-specified limits when the deck is removed. Careful consideration should be given to possible modeling the sub-flange as a reduced shape as a result of any damage that occurs during top flange removal.

Stability of the sub-girders must be maintained during the recasting of the deck. At this stage, the girder now begins to act more like a conventional composite girder bridge. Stresses in the girder should be computed for each load applied in accordance with whether the load acts on the non-composite or composite section.

4.13.1 Flange Width

The width of the top flange of a re-deckable system is governed by the overall framing plan. However, consideration must be given to the width of the sub-flange of the girder. Generally, issues that must be addressed when determining the width of the sub-flange include:

- Development of the transverse reinforcement in the top of the sub-flange,
- Shear key strength,
- Forming needs, and
- System stability during future re-decking.

4.13.2 Shear Key Design

Methodology for design of the shear key is base on the procedures in Reference 13. Shear key dimensions are shown in Figures 4-26 and 4-27. The required shear key geometry is based on bearing capacity of the transverse width and depth, b_{sk} and t_{sk} and on the nominal shear strength of the interface surface area determine from b_{sk} and the smaller of w'_{sk1} or w'_{sk2}. Required reinforcement crossing the interface is designed based on shear friction. Design examples for the shear key and interface shear reinforcement are provided in Appendix C of this report.

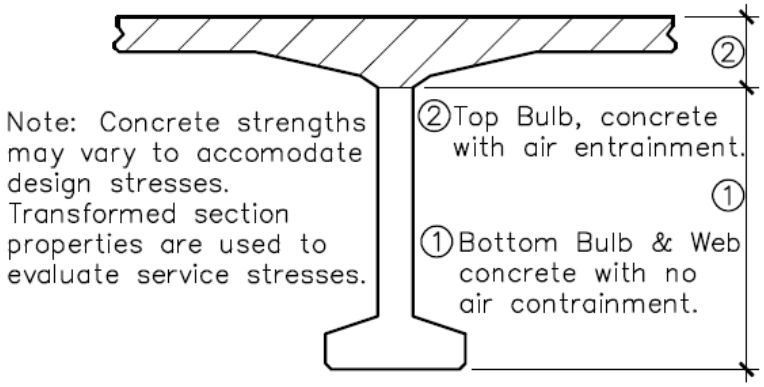

Figure 4-1. Section properties are impacted when different strengths of materials are used in the top and bottom portions of the girder.

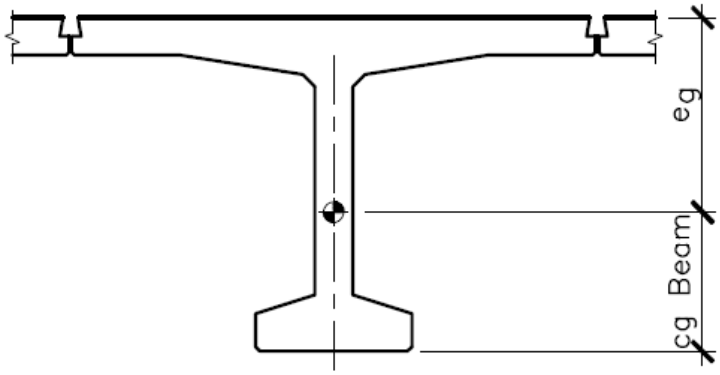

Figure 4-2. Definition of "e_g".

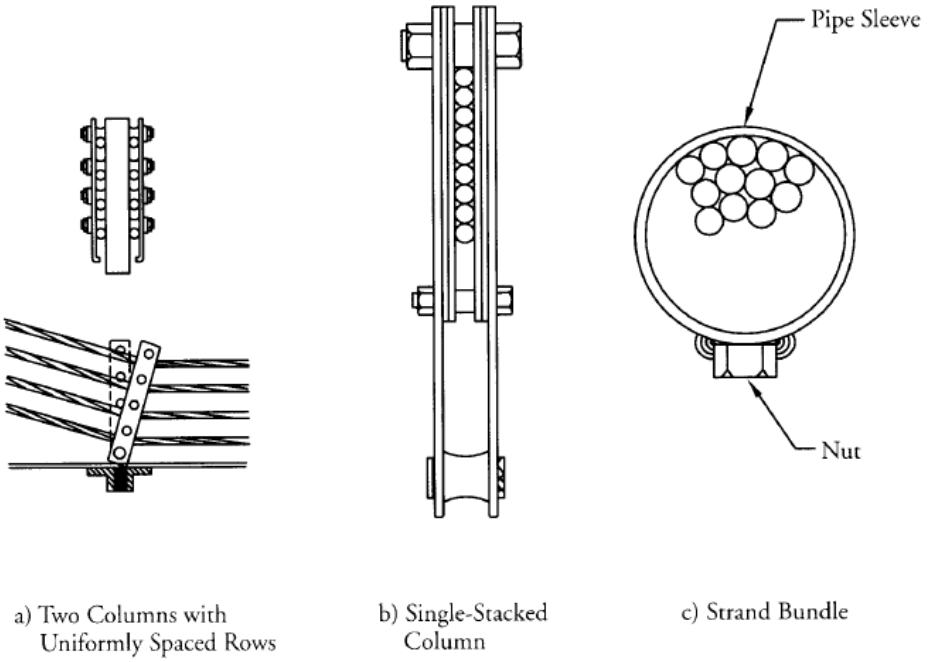

Figure 4-3. Devices used to harp strands.

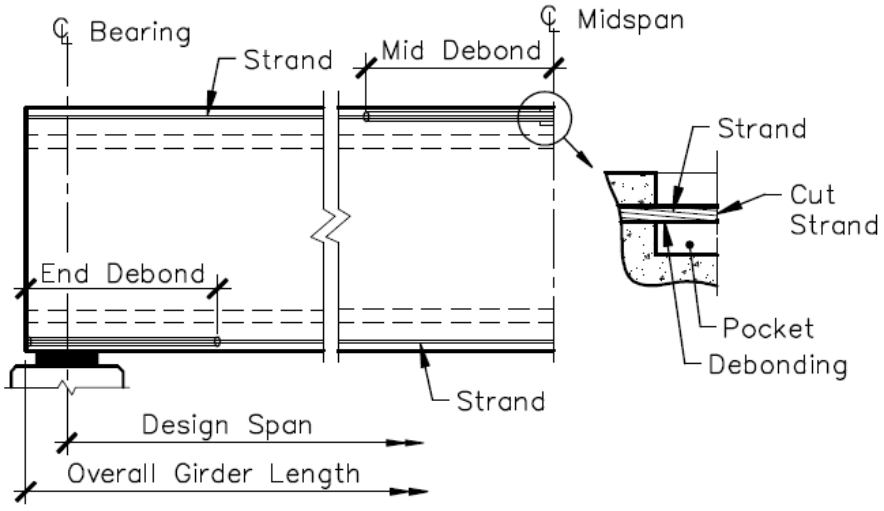

Figure 4-4. Types of debonding.

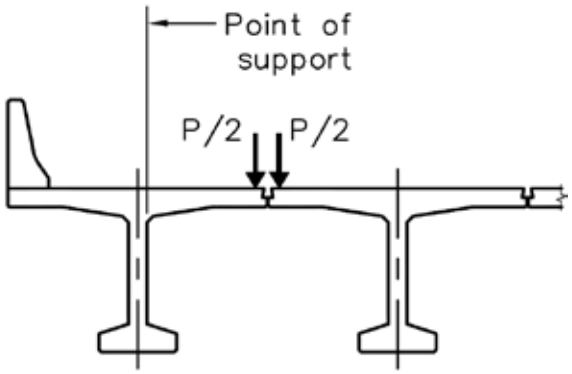

Figure 4-5 a. Wheel load applied to top flange of interior girder.

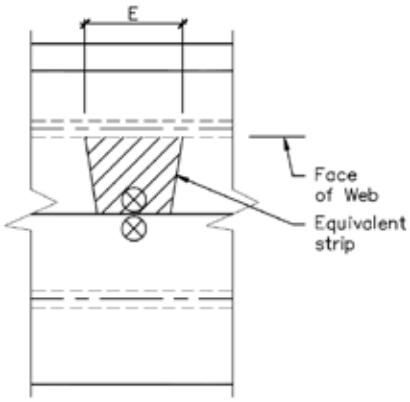

Figure 4-5 b. Equivalent strip for interior girder.

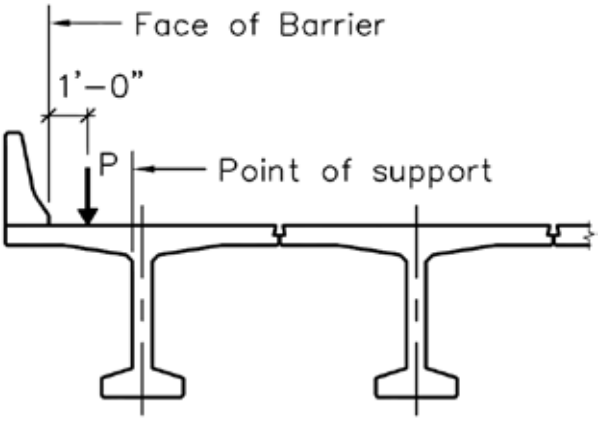

Figure 4-5 c. Wheel load applied to top flange of exterior girder.

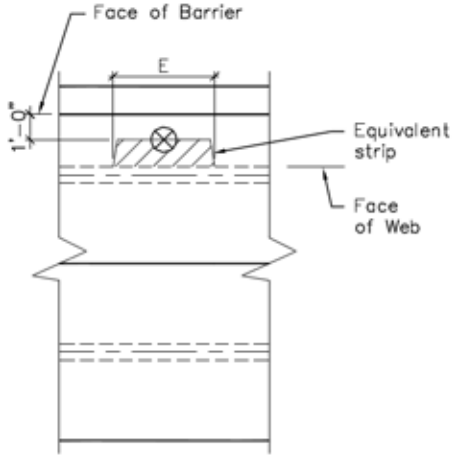

Figure 4-5 d. Equivalent strip for exterior girder.

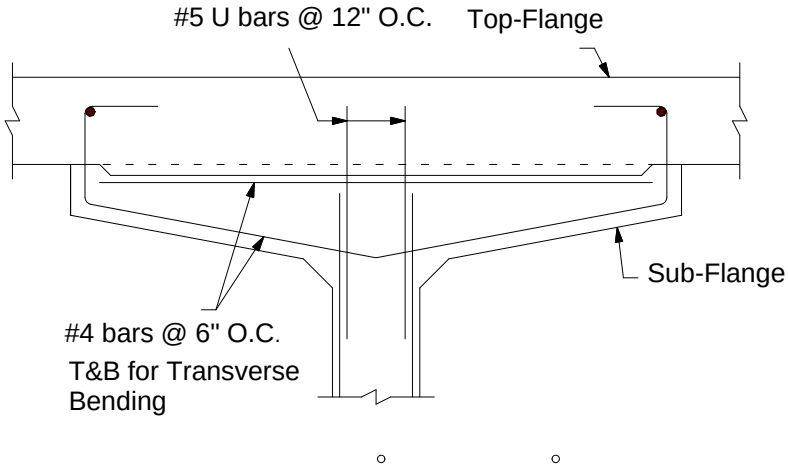

Figure 4-6. Reinforcement for in Sub-flange of Optimized Section.

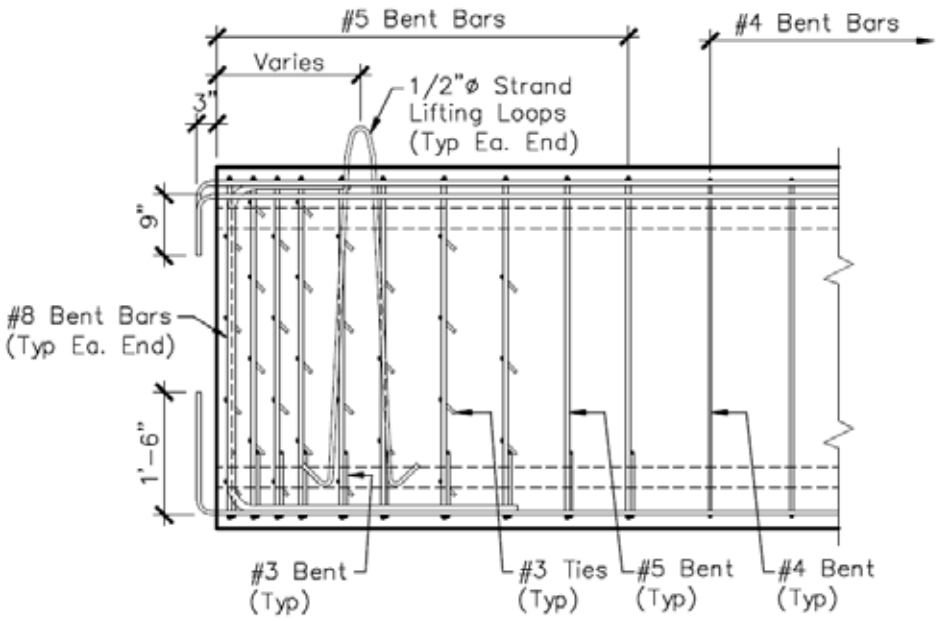

Figure 4-7. Typical reinforcement required – elevation view.

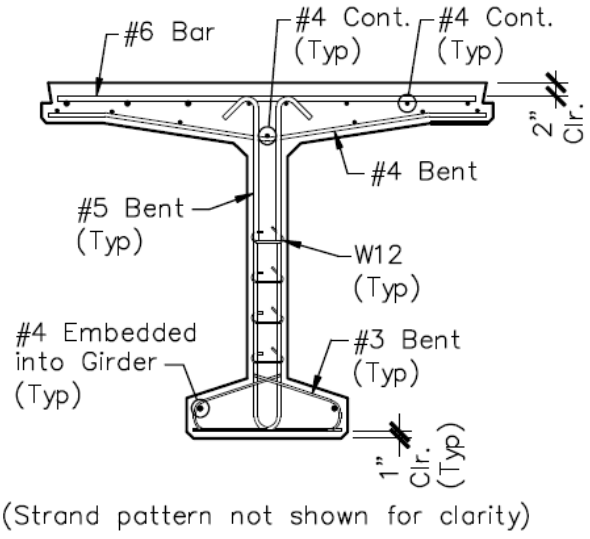

Figure 4-8. Typical reinforcement required near ends of girder.

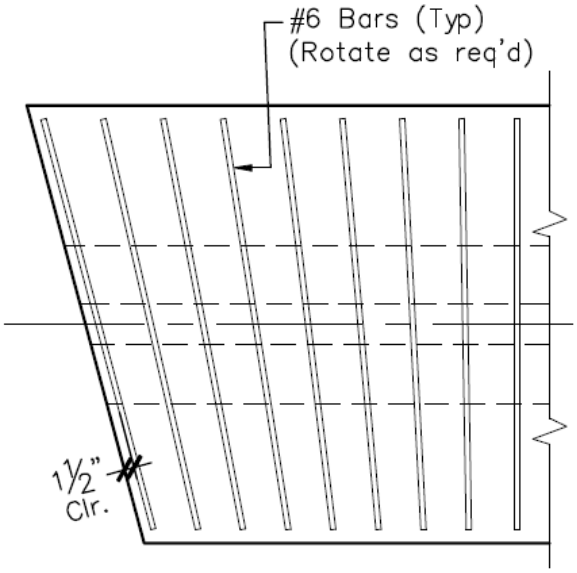

Figure 4-9. Typical top layer of flange reinforcement near end of girder – interior girder.

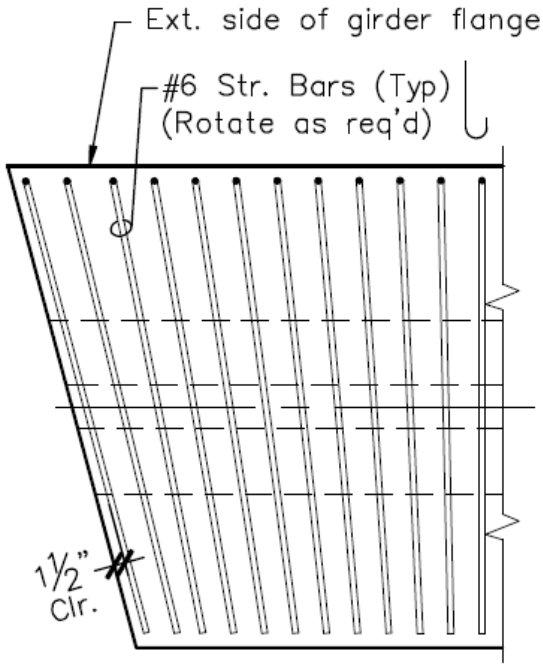

Figure 4-10. Typical top layer of flange reinforcement near end of girder – exterior girder.

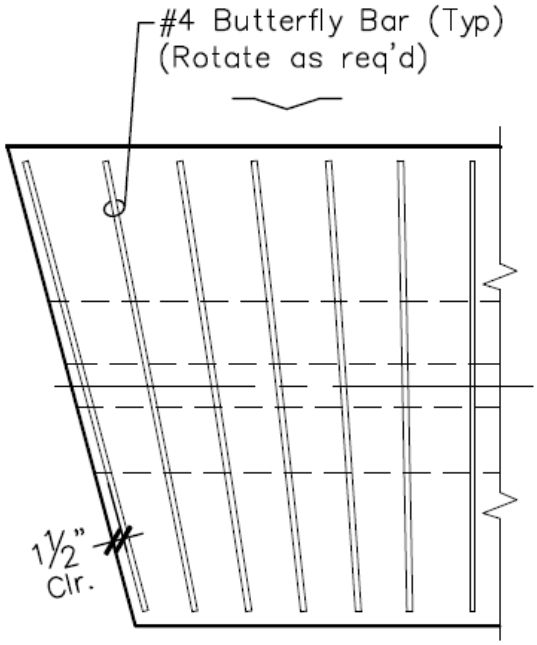

Figure 4-11. Typical bottom layer of flange reinforcement at end of girder – plan view.

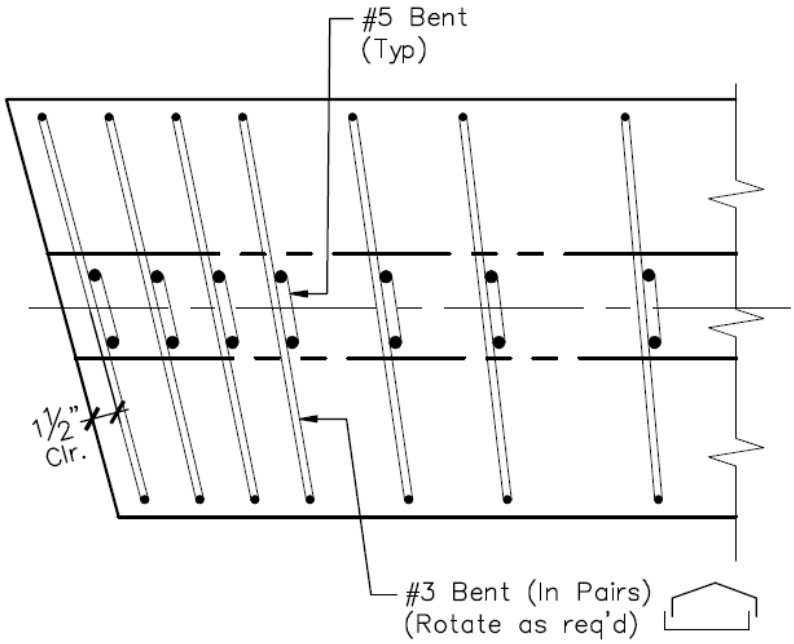

Figure 4-12. Typical bulb reinforcement near end of girder – plan view.

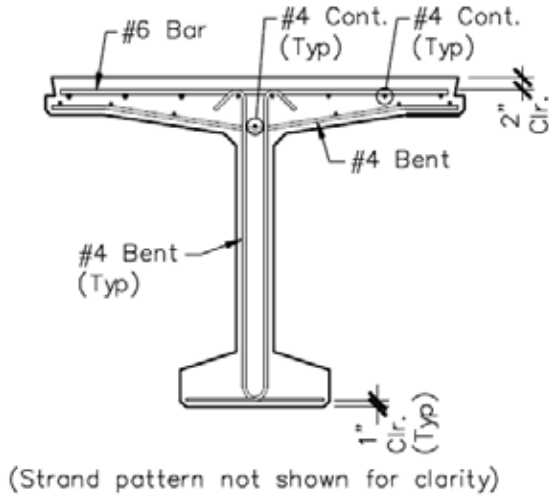

Figure 4-13. Typical reinforcement required near midspan of girder.

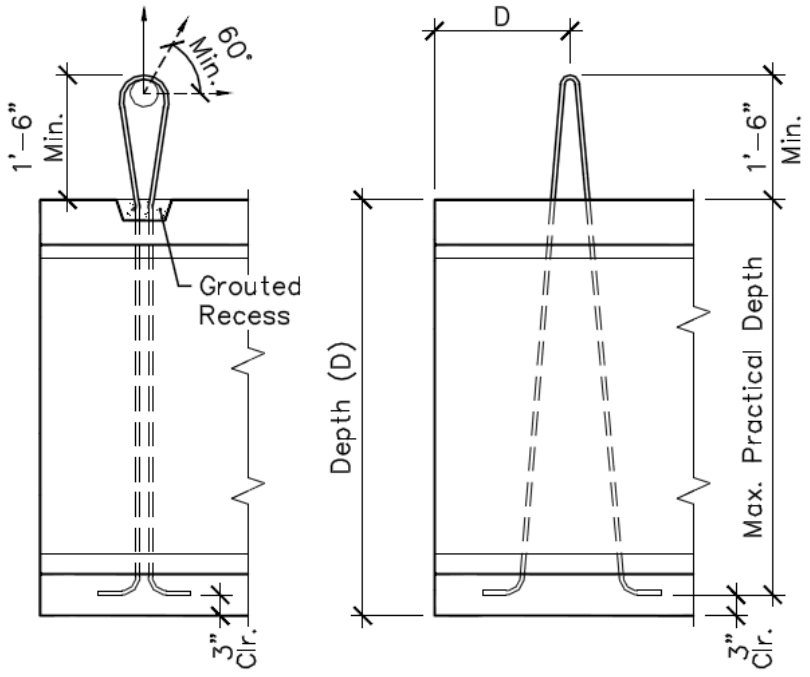

Figure 4-14. Typical lifting loop details.

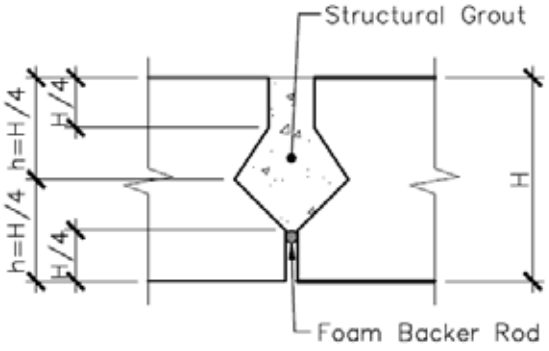

Figure 4-15. Shape of shear key recommended by Stanton and Mattock.

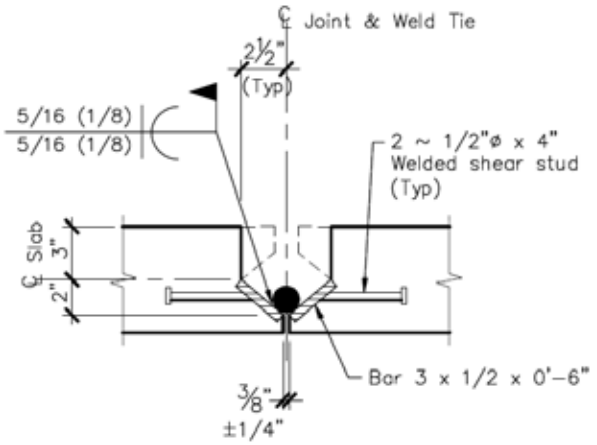

Figure 4-16. Weld tie Alternate 1.

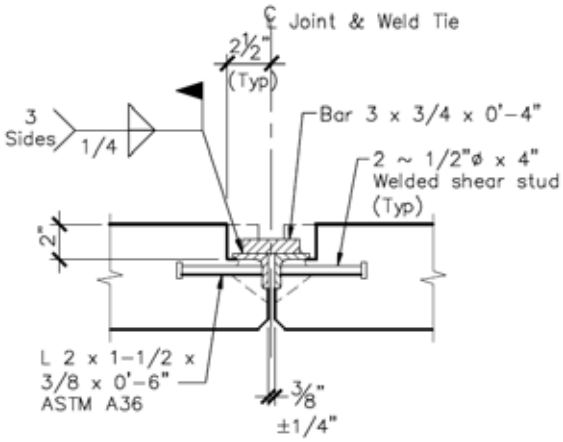

Figure 4-17. Weld tie Alternate 2.

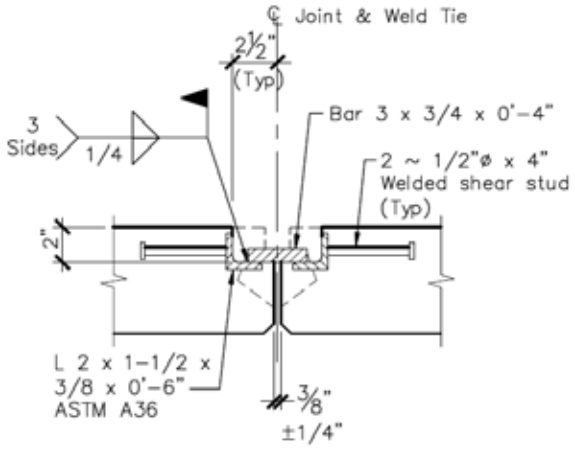

Figure 4-18. Weld tie Alternate 3.

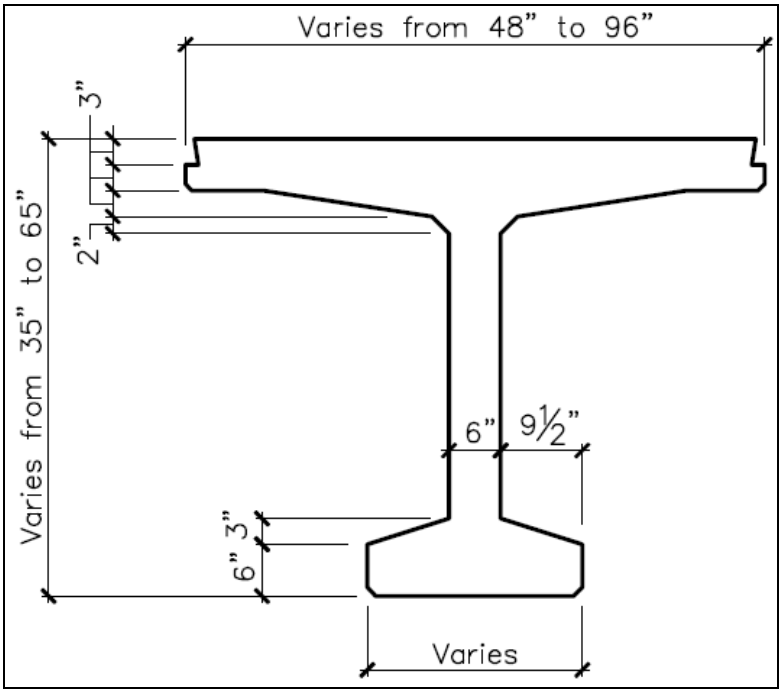

Figure 4-19. Conventional DBT girder.

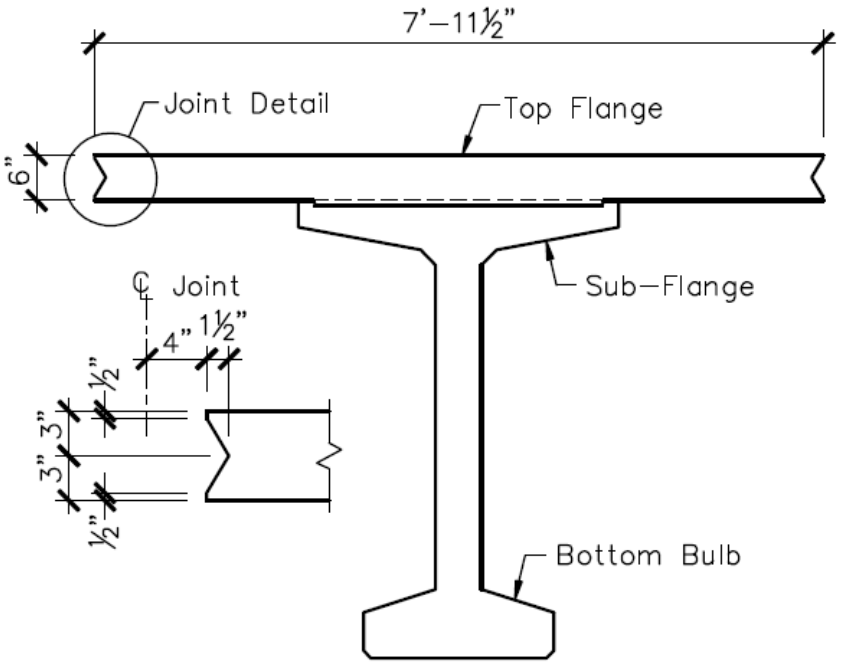

Figure 4-20. Re-deckable system with top flange and sub-girder.

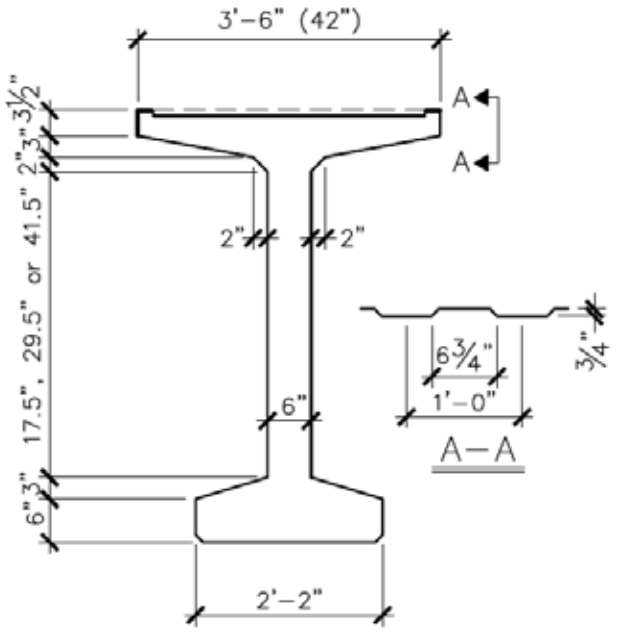

Figure 4-21. Sub-girder (Stage 1).

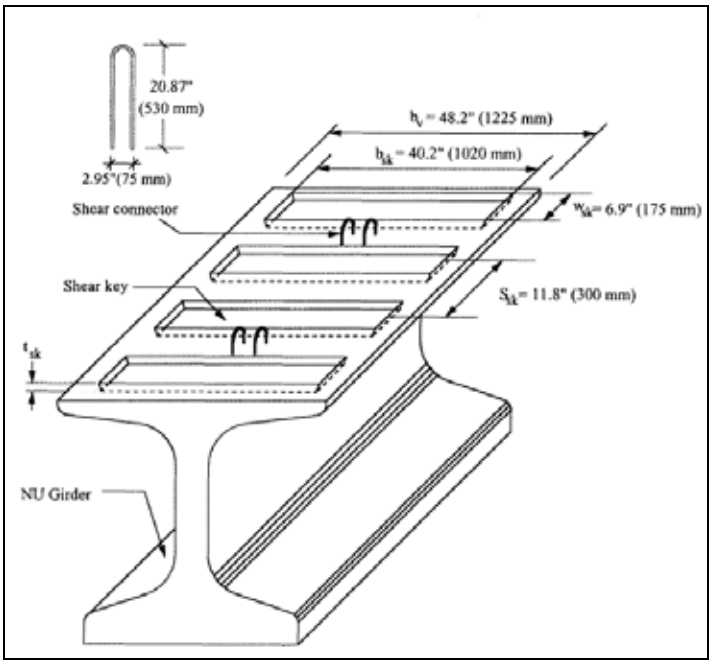

Figure 4-22. Isometric view of sub-girder showing shear keys formed in sub-flange.

Figure 4-23. Pans used to form shear keys in sub-flange.

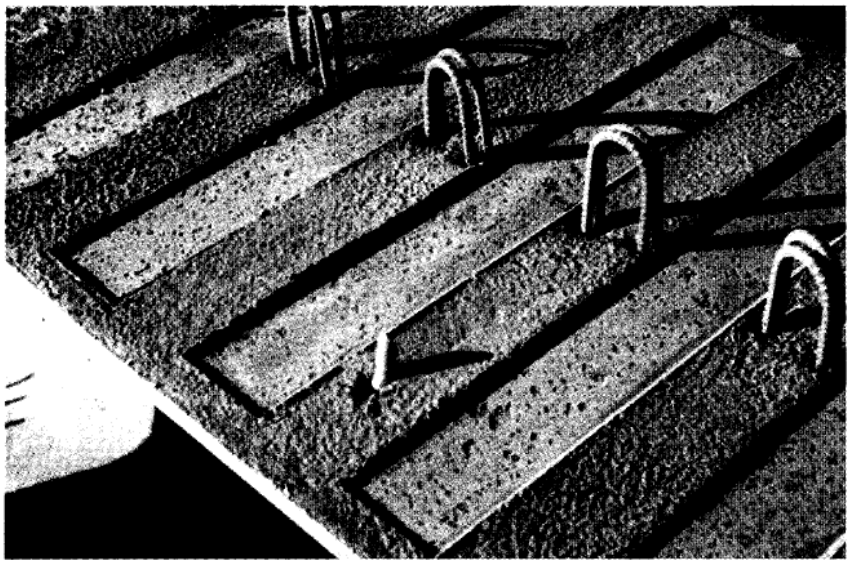

Figure 4-24. Shear key close-up.

Figure 4-25. Girder form with reinforcement prior to casting.

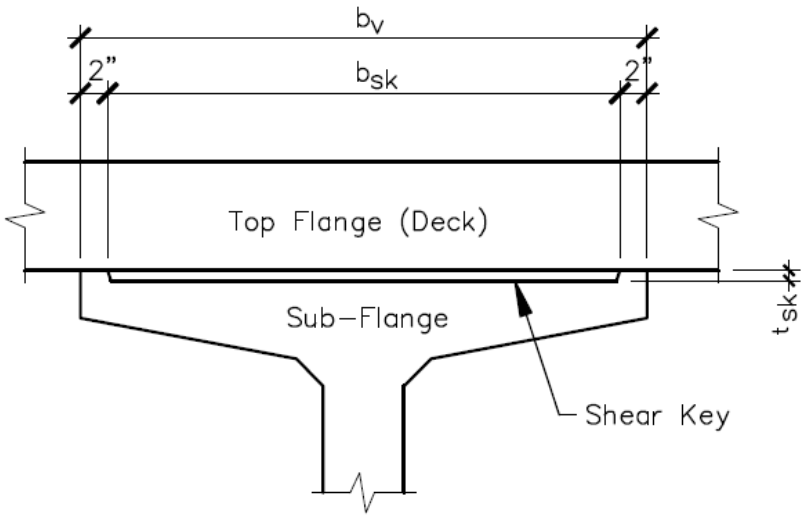

Figure 4-26. Sub-flange dimensions.

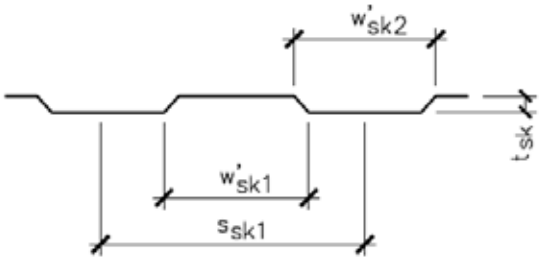

Figure 4-27. Shear key dimensions.

REFERENCES

1. AASHTO LRFD Bridge Design Specifications, Fourth Edition, American Association of State Highway and Transportation Officials, Inc., 2007.

2. Gilbertson ,C. G. and Ahlborn ,T. M., “A Probabilistic Comparison of Prestress Loss Methods in Prestressed Concrete Beams, PCI JOURNAL, Journal of the Precast/Prestressed Concrete Institute, Vol. 49, No. 5, p. 52-69, (Sept-Oct. 2004).

3. Precast/Prestressed Concrete Institute, Precast/Prestressed Concrete Bridge Design Manual, Chicago, IL, 1997.

4. State of the Art of Precast/Prestressed Integral Bridges, PCI, 2001.

5. Nicholls, Jerome J., and Prussack, Chuck, Innovative Design and Erection Methods Solve Construction of Rock Cut Bridge, PCI Journal, Vol. 42, No. 4. (July–August 1997) pp. 42–55.

6. Mattock, A.H., and Kaar, P.H., “Precast Prestressed Concrete Bridges-6, Test of Half Scale Highway Bridge Continuous over Two Spans,” Journal of PCA Research and Development Laboratory, Vol. 3, No. 3, 1961, pp.30-70.

7. Kostem, C.N., and deCastro, E.S., “Effects of Diaphragms on Lateral Load Distribution in Beam-Slab Bridges,” Transportation Research Record, Report No. 645, 1977.

8. McCathy, W., White, K.R., and Minor, J., “Interior Diaphragms Omitted on the Gallup East Interchange Bridge- Interstate 40,” Journal of Civil Engineering Design, Vol. 1, No. 1, 1979, pp. 95-112.

9. Sengupta, S., and Breen, J.E., “The Effects of Diaphragms in Prestressed Concrete Girders and Slab Bridges,” Research Report 158-1F, Center for Highway Research, The University of Texas at Austin, October, 1973.

10. Tokerud, R., “Precast Prestressed Concrete Bridge for Low-Volume Roads,” PCI Journal, Vol. 24, No.4, 1979.

11. Ma, Z., Chaudhury, S., Millam, J., and Hulsey, J. L., “Field Test and 3D FE Modeling of Decked Bulb-Tee Bridges,” ASCE Journal of Bridge Engineering, Vol. 12, No. 3, 2007, pp. 306 – 314.

12. Millam, J. and Ma, Z., “Single Lane Live Load Distribution Factor for Decked Precast/Prestressed Concrete Girder Bridges,” Journal of Transportation Research Board, No. 1928, 2005, TRB of the National Academies, Washington, D.C., pp.142 - 152.

13. Chaudhury, S. and Ma, Z., “Effect of Connections between Adjacent Units on Decked Precast, Prestressed Concrete Girder Bridges,” Proceedings of PCI NBC 2004, Atlanta, October, 2004.

14. Martin, L.D., and Osborn, A.E.N., “Connections for Modular Precast Concrete Bridge Decks,” Report No. FHWA/RD-82/106, US DOT, Federal Highway Administration, August, 1983, 117 pp.

15. Buth, C. Eugene, Williams, William F., Menges, Wanda L and Schoeneman, Sandra K.; “NCHRP Report 350 Tests 4-10 Through 4-12 of the Alaska Multi-State Bridge Rail”, Texas Transportation Institute, December 1998.

16. Nicholls, Jerome J., and Prussack, Chuck, Prestressed Full Deck Girder Construction Problem and Solutions, Unpublished work.

17. Mast, R. F., Lateral Stability of Long Prestressed Beams – Part 1, PCI Journal, V. 34, No. 1, Jan. – Feb., 1989, pp. 34-53.

18. Mast, R. F., Lateral Stability of Long Prestressed Beams – Part 2, PCI Journal, V. 38, No. 1, Jan. – Feb., 1993, pp. 70-88.

19. Ma, Z., Huo, X., Tadros, M. K., and Baishya, M., “Restraint Moments in Precast/Prestressed Concrete Continuous Bridges,” PCI Journal, Vol. 43, No. 6, Nov-Dec., 1998, pp. 40 – 57.

20. Noppakunwijai, Panya, Jongpitakseel, Nipon, Ma, Z., Yehia, Sherif A., Tadros, Maher K.;”Pullout Capacity of Non-Prestressed Bent Strands for Prestressed Concrete Girders”, PCI Journal, V.47, No. 4, July-August, 2002, pp. 90-103.

21. Tadros, M. K. and Baishya, M. C., Rapid Replacement of Bridge Decks, NCHRP Report 407, Transportation Research Board, National Cooperative Highway Research Program, 1998.

22. Tadros, M. K., Badie, S. S., and Kamel, M. R., Girder/Deck Connection for Rapid Removal of Bridge Decks, PCI Journal, Vol. 47, No. 3, May-June, 2002, pp. 58-69.

23. Alaska Department of Transportation and Public Facilities, Standard Specifications for Highway Construction 2004 http://www.dot.state.ak.us/stwddes/dcsspecs/assets/pdf/hwyspecs/english/2004sshc.pdf

24. Prestressed Concrete Institute, "PCI Design Handbook," 6th Edition, Chicago, 2004.

25. Washington State Department of Transportation, Standard Specifications for Road, Bridge, and Municipal Construction, 2006.

26. Rosa, M., Stanton, J. F., and Eberhard, M. O. "Improving Predictions for Camber in Precast, Prestressed Concrete Bridge Girders," University of Washington, Seattle, Washington, March, 2007.

27. Sethi, V., "Unbonded Monostrands for Camber Adjustment," Master Thesis, Virginia Polytechnic Institute and State University, Blacksburg, Virginia, 2006.

28. Oesterle, R.G., Mehrabi, A.B., Tabatabai, H., Scanlon, A., and Ligozio, C.A., "Continuity Considerations in Prestressed Concrete Jointless Bridges," Proceedings of the 2004 Structures Congress & Exposition, ASCE Structures Congress, Nashville, TN, May, 2004, pp. 23-26.

29. Oesterle, R.G., Mehrabi, A.B., Tabatabai, H., Scanlon, A., and Ligozio, C.A., "Evaluation of Continuity in Prestressed Concrete Jointless Bridges," Proceedings of the 2004 Concrete Bridge Conference, Charlotte, N.C. 2004, 20 pp.

30. Oesterle, R.G., Glikin, J.D., and Larson, S.C., "Design of Precast Prestressed Bridge Girders Made Continuous," NCHRP Report 322, Transportation Research Board, 1989, 97 pp.

31. Miller, R.A., Castrodale, R., Mirmiran, A., and Hastak, M., “Connection of Simple-Span Precast Concrete Girders for Continuity,” NCHRP Report 519, Transportation Research Board, 2004, 55pp.

32. Castrodale, R.W. and White, C.D., Extending Span Ranges of Precast, Prestressed Concrete Girders, NCHRP Report 517, TRB, National Research Council, Washington D.C., 2004.

33. Standard Specifications for Highway Bridges, 17th Edition, American Association of State Highway and Transportation Officials. Washington, DC, 2002.

34. Collins, Michael P. and Mitchell, Denis, Prestressed Concrete Structures, Prentice Hall, Englewood Cliffs, NJ, 1991.

35. Stanton, J., and Mattock, A.H. “Load Distribution and Connection Design for Precast Stemmed Multibeam Bridge Superstructures” NCHRP Rep. 287. 1986

36. Jones, “Lateral Connections For Double Tee Bridges,” Report 1856 – 2, Texas Transportation Institute, April, 2001.

37. Prestressed Concrete Institute, “Precast Prestressed Concrete Short Span Bridges – Spans to 100 Ft,” Chicago, Ill., 1975.

APPENDIX A

SUBTASK 6.3-B – DESIGN EXAMPLE FOR SIMPLE SPAN BRIDGE

This example problem presents the steps required to design a typical interior girder of a simple-span bridge with a superstructure that consists of four 53" deep by 7'-0" wide non-composite decked bulb tee girders. Girders are prestressed with 0.6" diameter pretensioned strands. The design is in accordance with the *AASHTO LRFD Bridge Design Specifications 4th edition, including 2008 Interim Revisions.*

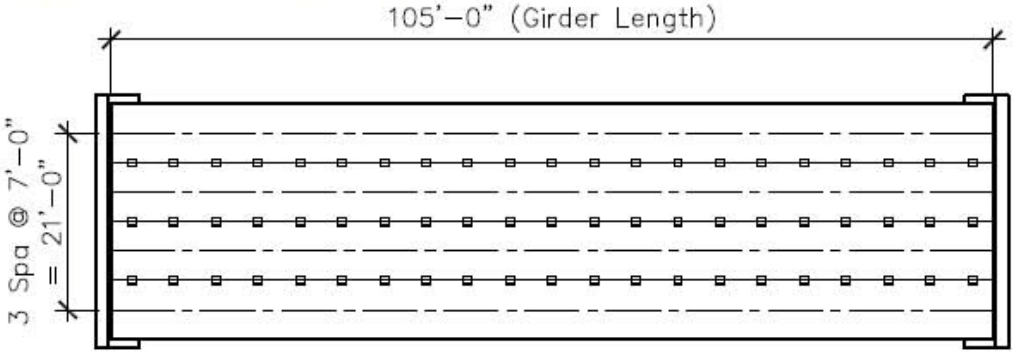

Figure 1: Bridge framing plan and elevation with four 53" deep by 84" wide decked bulb tee girders.

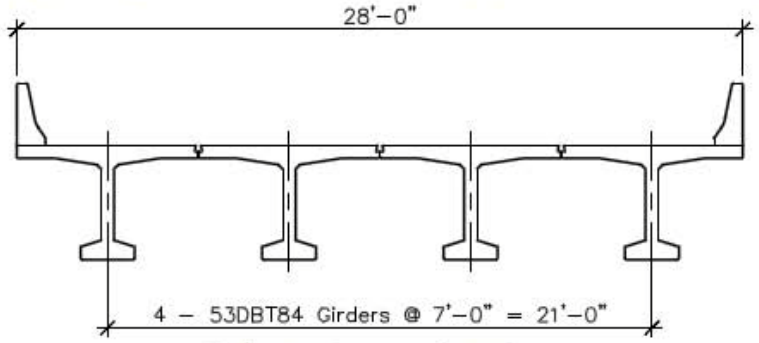

Figure 2: Cross section of bridge.

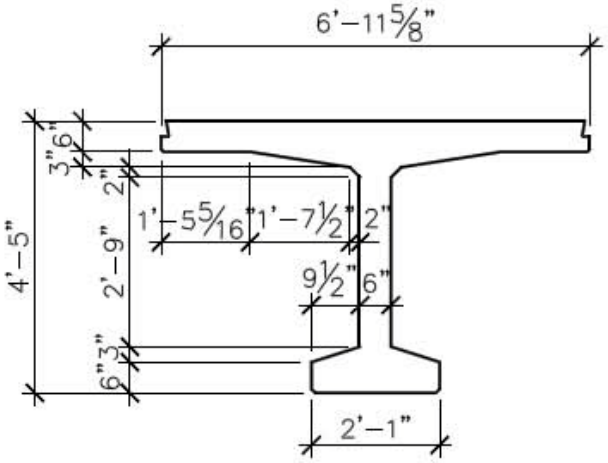

Figure 4: Typical girder cross section.

1 Design Parameters

Units:

	$kcf := kip \cdot ft^{-3}$	Defined unit: kips per cubic foot
	$ksf := kip \cdot ft^{-2}$	Defined unit: kips per square foot

Materials:

Concrete:	$f'_c := 7.0 \cdot ksi$	Concrete strength at 28 days
	$f'_{ci} := 6.0 \cdot ksi$	Concrete strength at release of prestressing force
	$H := 70$	Average ambient relative humidity
Strand:	$A_{strand} := 0.217 \cdot in^2$	Area of one prestressing strand.
	$d_b := 0.6 \cdot in$	Nominal diameter of prestressed strand.
	$f_{pu} := 270 \cdot ksi$	Tensile strength of prestressing steel
	$E_p := 28500 \cdot ksi$	Modulus of elasticity of prestressing steel
	$f_{py} := 0.9 \cdot f_{pu}$	Yield strength of prestressing steel
	$Pull := 0.75$	Pull of strands expressed as a fraction of f_{pu}
	$Dep\_Frac := 0.40$	Drape point of strands expressed as a fraction of design span
	$t := 18 \cdot hr$	Time from tensioning to detensioning of strands
Rebar:	$f_y := 60 \cdot ksi$	Yield stress of non-prestressed reinforcement
	$E_s := 29000 \cdot ksi$	Modulus of elasticity of non-prestressed reinforcement

Geometry:

Beam:	$Section := "DBT"$	Girder section name
	$h := 53.0 \cdot in$	Height of girder
	$A := 999.0 \cdot in^2$	Gross area of girder cross section
	$I := 350965 \cdot in^4$	Gross moment of inertia of girder cross section about cenroidal x-x axis
	$I_{yy} := 308449 \cdot in^4$	Gross moment of inertia of girder cross section about cenroidal y-y axis
	$y_b := 35.61 \cdot in$	Center of gravity of gross girder cross section
	$b_f := 84.0 \cdot in$	Width of top flange of girder

	$t_{flg} := 6.00 \cdot in$	Effective thickness of top flange
	$b_v := 6.00 \cdot in$	Shear width of girder (web width)
	$A_c := 450 \cdot in^2$	Area of concrete on flexural tension side of member (see LRFD 5.8.4.3.2-1)
	$VS_b := 3.44 \cdot in$	Volume to surface ratio of girder
Span:	$L_{ovr} := 105.0 \cdot ft$	Overal length of girder
	$L_{des} := 104.0 \cdot ft$	Design span of girder
	$L_{pad} := 12 \cdot in$	Length of bearing pad
Bridge:	$S := 7.00 \cdot ft$	Girder spacing
	$N_g := 4$	Number of girders in bridge cross section
	$Width_{overall} := 28.0 \cdot ft$	Overall width of bridge
	$Width_{ctc} := 24.0 \cdot ft$	Curb to curb width of bridge
	$N_l := 2$	Number of lanes

Loads:

Dead:	$N_{barriers} := 2$	Number of barriers
	$w_{barrier} := 0.300 \cdot klf$	Weight of single barrier
	$w_{fws} := 0.025 \cdot ksf$	Weight of future wearing surface allowance
Live:	HL-93	Notional live load per LRFD Specs

Load & Resistance Factors:

ϕ_f (variable)	Resistance factor for flexure
$\phi_v := 0.90$	Resistance factor for shear
$DLA := 0.33$	Dynamic load allowance (LRFD 3.6.2.1-1)

Construction Timing:

$t_{transfer} := 1.00 \cdot day$	Time from release tensioning of strands to release of prestress
$t_{deck} := 90 \cdot day$	Time to placement of superimposed dead load (SDL)
$t_{final} := 20000 \cdot day$	Time final

Strand Pattern:

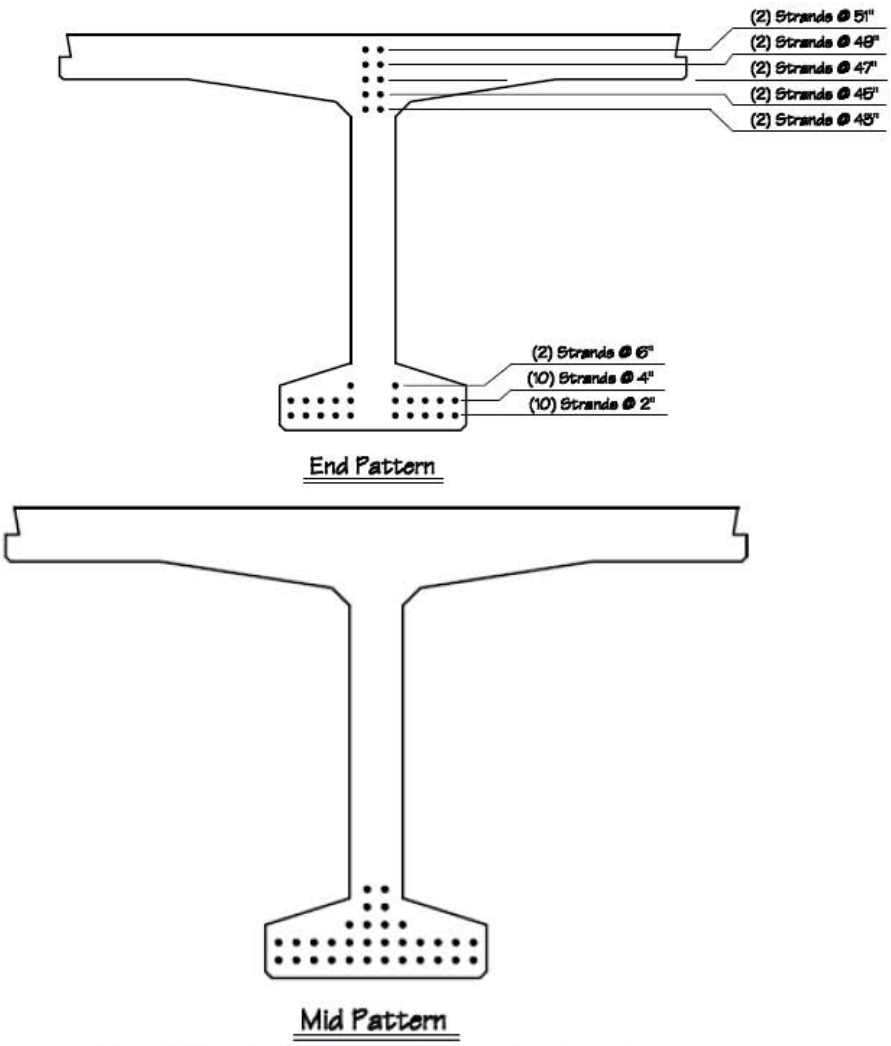

Figure 5: Strand pattern and end of girder and at depression point.

$$Dep\_Pt := Dep\_Frac \cdot L_{des} + \left(L_{ovr} - L_{des}\right) \cdot 0.5 \qquad Dep\_Pt = 42.1 \cdot ft$$

End Pattern $EPat\_n := \begin{pmatrix} 2 \\ 2 \\ 2 \\ 2 \\ 2 \\ 0 \\ 0 \\ 0 \\ 2 \\ 10 \\ 10 \end{pmatrix}$ $EPat\_h := \begin{pmatrix} 51 \\ 49 \\ 47 \\ 45 \\ 43 \\ 12 \\ 10 \\ 8 \\ 6 \\ 4 \\ 2 \end{pmatrix} \cdot in$

Mid Pattern $MPat\_n := \begin{pmatrix} 0 \\ 0 \\ 0 \\ 0 \\ 0 \\ 0 \\ 2 \\ 2 \\ 4 \\ 12 \\ 12 \end{pmatrix}$ $MPat\_h := \begin{pmatrix} 22 \\ 20 \\ 18 \\ 16 \\ 14 \\ 12 \\ 10 \\ 8 \\ 6 \\ 4 \\ 2 \end{pmatrix} \cdot in$

2 Material Properties

Modulus of Elasticity of Concrete:

$$E_c := 33000 \cdot K_1 \cdot w_c^{1.5} \cdot \sqrt{f'_c}$$ (LRFD 5.4.2.4-1)

K_1 = Correction factor for source of aggregate, taken as 1.0 unless a more accurate value is known

$K_1 := 1.0$

w_c = Density of concrete (kcf), computed using the following equation:

$$w_c := \left(0.14 + \frac{f'_c}{1000 \cdot ksi}\right) \cdot kcf \qquad w_c = 0.147 \cdot kcf$$ (LRFD Table 3.5.1-1)

The equation for w_c can be substituted into the equation for E_c to obtain:

$$E_{ci} := 33000 \cdot K_1 \cdot \left(0.14 + \frac{f'_c}{1000 \cdot ksi}\right)^{1.5} \cdot \sqrt{\frac{f'_{ci}}{ksi}} \cdot ksi \qquad E_{ci} = 4555.8 \cdot ksi$$

$$E_c := 33000 \cdot K_1 \cdot \left(0.14 + \frac{f'_c}{1000 \cdot ksi}\right)^{1.5} \cdot \sqrt{\frac{f'_c}{ksi}} \cdot ksi \qquad E_c = 4920.8 \cdot ksi$$

3 Check Points

Two sets of check points are used for calculations: one for release and the other for final conditions since the locations of interest are different at release as compared to final conditions.

At transfer, there are three locations along the girder of interest:

1. Transfer point of strands: $x_{r_1} := 60 \cdot d_b$ (LRFD 5.8.2.3)
2. Depression point: $x_{r_2} := Dep\_Frac \cdot L_{des} + \frac{L_{ovr} - L_{des}}{2}$
3. Midspan of beam: $x_{r_3} := \frac{L_{ovr}}{2}$

$x_r^T = (3 \;\; 42.1 \;\; 52.5) \cdot ft$

At final conditions, 10th points of the span (to midspan) plus the critical section for shear will be investigated.

1. The critical section for shear is d_v from the face of the support. At this point in the calculations d_v is not known, so a reasonable value must be assumed. Assume d_v equals 90% of the height of the section. Thus, from the centerline of bearing, the critical point for shear is estimated as:

   $x_{f_2} := 3.80 \cdot ft$

2. 10th points

   $x_{f_1} := 0.0 \cdot ft \qquad x_{f_3} := 0.1 \cdot L_{des} \qquad x_{f_4} := 0.2 \cdot L_{des} \qquad x_{f_5} := 0.3 \cdot L_{des} \qquad x_{f_6} := 0.4 \cdot L_{des} \qquad x_{f_7} := 0.5 \cdot L_{des}$

$x_f^T = (0 \;\; 3.8 \;\; 10.4 \;\; 20.8 \;\; 31.2 \;\; 41.6 \;\; 52) \, ft$

4 Strand Pattern Properties

$No\_Strands := \sum EPat\_n$ $No\_Strands = 32$ $A_{ps} := No\_Strands \cdot A_{strand}$ $A_{ps} = 6.944 \cdot in^2$

$i := 1 .. last(EPat\_n)$

$$y_{end} := \frac{\sum_i \left(EPat\_n_i \cdot EPat\_h_i\right)}{No\_Strands} \quad y_{end} = 16.9375 \cdot in \qquad y_{mid} := \frac{\sum_i \left(MPat\_n_i \cdot MPat\_h_i\right)}{No\_Strands} \quad y_{mid} = 4.13 \cdot in$$

$j := 1 .. 3$

$$y_{cg\_r_j} := if\left[x_{r_j} \le Dep\_Pt, y_{end} - \left(\frac{x_{r_j}}{Dep\_Pt}\right) \cdot \left(y_{end} - y_{mid}\right), y_{mid}\right]$$

$$y_{cg\_r} = \begin{pmatrix} 16.0245 \\ 4.125 \\ 4.125 \end{pmatrix} \cdot in$$

$ecc\_r_j := y_b - y_{cg\_r_j}$

$$ecc\_r = \begin{pmatrix} 19.5855 \\ 31.485 \\ 31.485 \end{pmatrix} \cdot in$$

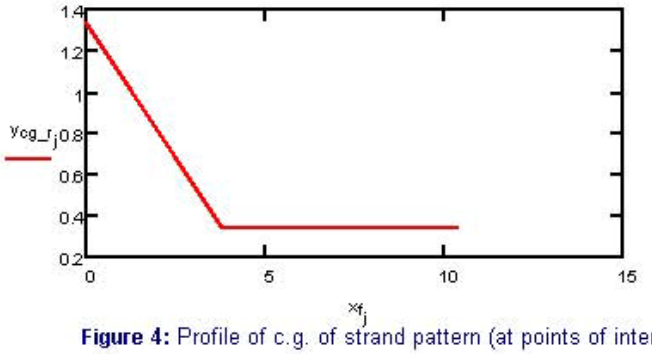

Figure 4: Profile of c.g. of strand pattern (at points of interest).

C.G. and Eccentricity of Strand Pattern at Final Check Points:

$$y_{cg\_f_j} := if\left[x_{f_j} \le x_{f_2}, y_{end} - \left(\frac{x_{f_j} + \frac{L_{ovr} - L_{des}}{2}}{x_{f_2} + \frac{L_{ovr} - L_{des}}{2}}\right) \cdot \left(y_{end} - y_{mid}\right), y_{mid}\right] \qquad y_{cg\_f} = \begin{pmatrix} 15.448 \\ 4.125 \\ 4.125 \end{pmatrix} \cdot in$$

$ecc\_f_j := y_b - y_{cg\_f_j}$ $ecc\_f^T = (20.162 \quad 31.485 \quad 31.485) \cdot in$

5 Section Properties

Non-Composite Section Properties:

$S_b := \frac{I}{y_b}$ $S_b = 9855.8 \cdot in^3$

$y_t := h - y_b$ $S_t := \frac{I}{y_t}$ $S_t = 20182 \cdot in^3$

Gross Girder Properties (ignore strands):

$A_g := A$ $y_{bg} := y_b$ $I_g := I$

$y_{tg} := h - y_{bg}$ $y_{tg} = 17.39 \cdot in$

$S_{bg} := \frac{I_g}{y_{bg}}$ $S_{bg} = 9855.8 \cdot in^3$

Section Properties Nomenclature

y_{btfc}

- non-composite (blank) or composite
- Time-frame: release or final
- gross, net, or transformed
- Variable: A, y_b, y_t, I, S_b, S_t

$S_{tg} := \frac{I_g}{y_{tg}}$ $S_{tg} = 20182 \cdot in^3$

Transformed Properties (girder + strands transformed into concrete):

release:

$n_{pci} := \frac{E_p}{E_{ci}}$ $n_{pci} = 6.25574868$

$A_{tr} := A_g + (n_{pci} - 1) \cdot A_{ps}$ $A_{tr} = 1035.5 \cdot in^2$

$y_{btr_j} := \frac{A_g \cdot y_{bg} + (n_{pci} - 1) \cdot A_{ps} \cdot y_{cg\_f_j}}{A_{tr}}$ $y_{btr}^T = (34.9 \;\; 34.5 \;\; 34.5) \cdot in$

$y_{ttr} := h - y_{btr}$ $y_{ttr}^T = (18.1 \;\; 18.5 \;\; 18.5) \cdot in$

$I_{tr_j} := I_g + A_g \cdot (y_{btr_j} - y_{bg})^2 + (n_{pci} - 1) \cdot A_{ps} \cdot (y_{btr_j} - y_{cg\_f_j})^2$

$I_{tr}^T = (365278 \;\; 385868 \;\; 385868) \cdot in^4$

$S_{btr_j} := \frac{I_{tr_j}}{y_{btr_j}}$ $S_{btr}^T = (10466.6 \;\; 11184.5 \;\; 11184.5) \cdot in^3$

$S_{ttr_j} := \frac{I_{tr_j}}{y_{ttr_j}}$ $S_{ttr}^T = (20180.4 \;\; 20858.1 \;\; 20858.1) \cdot in^3$

final:

$n_{pc} := \frac{E_p}{E_c}$ $n_{pc} = 5.7917$ (Note that this value is smaller than n_{pci})

$A_{tf} := A_g + (n_{pc} - 1) \cdot A_{ps}$ $A_{tf} = 1032.3 \cdot in^2$

$y_{btf_j} := \frac{A_g \cdot y_{bg} + (n_{pc} - 1) \cdot A_{ps} \cdot y_{cg\_f_j}}{A_{tf}}$ $y_{btf}^T = (34.96 \;\; 34.6 \;\; 34.6) \cdot in$

$y_{ttf_j} := h - y_{btf_j}$ $y_{ttf}^T = (18.04 \;\; 18.4 \;\; 18.4) \cdot in$

$I_{tf_j} := I_g + A_g \cdot (y_{btf_j} - y_{bg})^2 + (n_{pc} - 1) \cdot A_{ps} \cdot (y_{btf_j} - y_{cg\_f_j})^2$

$I_{tf}^T = (364055 \;\; 382886 \;\; 382886) \cdot in^4$

$S_{btf_j} := \frac{I_{tf_j}}{y_{btf_j}}$ $S_{btf}^T = (10413.5 \;\; 11067.6 \;\; 11067.6) \cdot in^3$

$S_{ttf_j} := \frac{I_{tf_j}}{y_{ttf_j}}$ $S_{ttf}^T = (20180.6 \;\; 20803.5 \;\; 20803.5) \cdot in^3$

6 Moments and Shears

At Release:

Girder self-weight at release:

$w_{sw} := w_c \cdot A$ $\quad w_{sw} = 1.0198 \cdot klf$

$i := 1 .. 3$

$M_{swr_i} := \frac{w_{sw} \cdot x_{r_i}}{2} \cdot \left(L_{ovr} - x_{r_i}\right)$ $\quad M_{swr}^{T} = (156 \;\; 1350.3 \;\; 1405.4) \cdot kip \cdot ft$

At Final Conditions:

Girder self-weight at final:

At final conditions, there are also three points of interest:

1. The critical section for shear is d_v from the face of the support, with d_v taken as 0.72h (see discussion in Theory section)

$$x_{f_1} := 0.72 \cdot h + \frac{L_{pad}}{2}$$

2. Depression point: $x_{f_2} := Dep\_Frac \cdot L_{des}$

3. Midspan of beam: $x_{f_3} := 0.5 \cdot L_{des}$ $\quad x_f^{T} = (3.68 \;\; 41.6 \;\; 52 \;\; 20.8 \;\; 31.2 \;\; 41.6 \;\; 52) \cdot ft$

$j := 1 .. 3$

$M_{swf_j} := \frac{w_{sw} \cdot x_{f_j}}{2} \cdot \left(L_{des} - x_{f_j}\right)$ $\quad M_{swf}^{T} = (188.2 \;\; 1323.6 \;\; 1378.8) \cdot kip \cdot ft$

$V_{swf_j} := w_{sw} \cdot \left(\frac{L_{des}}{2} - x_{f_j}\right)$ $\quad V_{swf}^{T} = (49.3 \;\; 10.6 \;\; 0) \cdot kip$

Barrier Weight (Composite Dead Load):

$w_{barrier} = 0.3 \cdot klf$ $\quad$ Per barrier: $w_b := \frac{N_{barriers} \cdot w_{barrier}}{N_g}$ $\quad w_b = 0.15 \cdot klf$

$M_{barrier_j} := \frac{w_b \cdot x_{f_j}}{2} \cdot \left(L_{des} - x_{f_j}\right)$ $\quad M_{barrier}^{T} = (27.7 \;\; 194.7 \;\; 202.8) \cdot kip \cdot ft$

$V_{barrier_j} := w_b \cdot \left(\frac{L_{des}}{2} - x_{f_j}\right)$ $\quad V_{barrier}^{T} = (7.2 \;\; 1.6 \;\; 0) \cdot kip$

Future Wearing Surface:

$w_{fws} = 0.025 \cdot ksf$ $\quad$ Per Beam: $w_f := \frac{Width_{ctc} \cdot w_{fws}}{N_g}$ $\quad w_f = 0.15 \cdot klf$

$M_{fws_j} := \frac{w_f \cdot x_{f_j}}{2} \cdot \left(L_{des} - x_{f_j}\right)$ $\quad M_{fws}^{T} = (27.7 \;\; 194.7 \;\; 202.8) \cdot kip \cdot ft$

$V_{fws_j} := w_f \cdot \left(\frac{L_{des}}{2} - x_{f_j}\right)$ $\quad V_{fws}^{T} = (7.2 \;\; 1.6 \;\; 0) \cdot kip$

Live Load:

LL distribution factor for moment:

Bridge Type (j), connected only enough to prevent relative vertical displacement at interface.

$k := 2.0$ (preliminary T-Beam) (LRFD Table 4.6.2.2.2a-1)

Compute J for stocky open sections

$I_p := I + I_{yy}$ $I_p = 659414 \cdot in^4$

$J := \frac{A^4}{40 \cdot I_p}$ $J = 37761 \cdot in^4$ (LRFD C4.6.2.2.1-2)

$\mu := 0.20$ Poisson's ratio (LRFD 5.4.2.5)

$k := \sqrt{\frac{(1+\mu) \cdot I}{J}}$ $k = 3.3396$

$C := k \cdot \left(\frac{Width_{overall}}{L_{des}} \right)$ $C = 0.8991$

$D := \left\lceil 11.5 - N_l + 1.4 \cdot N_l \cdot (1 - 0.2 \cdot C)^2 \right\rceil \cdot ft$ $D = 11.384\,ft$

$DF_m := \frac{S}{D}$ $DF_m = 0.6149$

Check single lane loading: $N_l := 1$

$D := \left\lceil 11.5 - N_l + 1.4 \cdot N_l \cdot (1 - 0.2 \cdot C)^2 \right\rceil \cdot ft$ $D = 11.442\,ft$

$DF_m := \frac{S}{D}$ $DF_m = 0.6118$

LL distribution factor for shear:

User Lever Rule: (LRFD Table 4.6.2.2.3a-1)

Assume each wheel is 0.5 and one wheel is positioned 1' from the face of the barrier. Summing moments about the interior wheel yields:

$DF_v := \left(\frac{5.5}{3.5} \right) \cdot 0.5$ $DF_v = 0.7857$

Live Load Moments (HL-93):

Maximum Moments Due to Design Truck and Design Lane:

Due to the Design Truck:

However, for convenience in checking, a closed-form solution for the maximum moment at any point along a simply-supported beam due to the LRFD design truck is given below. There are two formulae, one which is valid for the region between the support and the L/3 point of the beam, and the other which is valid between L/3 and midspan. These two formulae correspond to different orientations of the truck (i.e., when it faces one way or the other).

$L := L_{des}$ (purely to condense the expression)

$$M_{truck_j} := if\left[x_{f_j} \le \frac{L}{3}, \frac{8\cdot kip\cdot x_{f_j}}{L}\cdot\left(9\cdot L - 9\cdot x_{f_j} - 84\cdot ft\right), \frac{8\cdot kip}{L}\cdot\left[-9\cdot\left(x_{f_j}\right)^2 + 9\cdot x_{f_j}\cdot L - 42\cdot ft\cdot x_{f_j} - 14\cdot ft\cdot L\right]\right]$$

$M_{truck}^T = (231.8 \quad 1550.7 \quad 1592)\cdot kip\cdot ft$

Due to the Design Lane:

$w_{lane} := 0.64\cdot klf$

$$M_{lane_j} := \frac{w_{lane}\cdot x_{f_j}}{2}\cdot\left(L - x_{f_j}\right) \qquad M_{lane}^T = (118.1 \quad 830.7 \quad 865.3)\cdot kip\cdot ft$$

Maximum Service Live Load Moments (HL-93):

The dynamic load allowance (DLA) is applied to the truck portion only: (LRFD 3.6.2.1-1)

$$M_{LL_j} := DF_m\cdot\left[M_{lane_j} + (1 + DLA)\cdot M_{truck_j}\right] \qquad M_{LL}^T = (260.9 \quad 1770 \quad 1824.8)\cdot kip\cdot ft$$

Live Load Shears:

$$V_{truck_j} := \frac{8\cdot kip}{L}\cdot\left(9\cdot L - 9\cdot x_{f_j} - 84\cdot ft\right) \qquad V_{truck}^T = (63 \quad 36.7 \quad 29.5)\cdot kip$$

$$V_{lane_j} := \frac{w_{lane}\cdot\left(L - x_{f_j}\right)^2}{2\cdot L} \qquad V_{lane}^T = (31 \quad 12 \quad 8.3)\cdot kip$$

$$V_{LL_j} := DF_v\cdot\left[V_{lane_j} + (1 + DLA)\cdot V_{truck_j}\right] \qquad V_{LL}^T = (90.2 \quad 47.8 \quad 37.4)\cdot kip$$

7 Flexural Stress Check

At Release:

Beam Self-Weight Stresses:

$$f_{swt_j} := \frac{M_{swr_j}}{S_t} \qquad f_{swt} = \begin{pmatrix}0.093\\0.803\\0.836\end{pmatrix}\cdot ksi \qquad f_{swb_j} := -\frac{M_{swr_j}}{S_b} \qquad f_{swrb} = \begin{pmatrix}-0.19\\-1.644\\-1.711\end{pmatrix}\cdot ksi$$

Note: Since for a simple-span structural system of this type, it is unlikely that compression at the top of the deck at a given section would exceed its allowable value, calculation of those stresses will be omitted for simplicity. Only the stresses at the bottom and top of the precast beam itself will be computed.

Self-Weight:

$$f_{swt_j} := \frac{M_{swf_j}}{S_t} \qquad f_{swt} = \begin{pmatrix}0.112\\0.787\\0.82\end{pmatrix}\cdot ksi \qquad f_{swb_j} := -\frac{M_{swf_j}}{S_b} \qquad f_{swb} = \begin{pmatrix}-0.229\\-1.612\\-1.679\end{pmatrix}\cdot ksi$$

Barriers:

$$f_{barriert_j} := \frac{M_{barrier_j}}{S_t} \qquad f_{barriert} = \begin{pmatrix}0.016\\0.116\\0.121\end{pmatrix}\cdot ksi \qquad f_{barrierb_j} := -\frac{M_{barrier_j}}{S_b} \qquad f_{barrierb} = \begin{pmatrix}-0.034\\-0.237\\-0.247\end{pmatrix}\cdot ksi$$

Future Wearing Surface:

$$f_{fwst_j} := \frac{M_{fws_j}}{S_t} \qquad f_{fwst} = \begin{pmatrix} 0.016 \\ 0.116 \\ 0.121 \end{pmatrix} \cdot ksi \qquad f_{fwsb_j} := -\frac{M_{fws_j}}{S_b} \qquad f_{fwsb} = \begin{pmatrix} -0.034 \\ -0.237 \\ -0.247 \end{pmatrix} \cdot ksi$$

Live Load:

$$f_{LLt_j} := \frac{M_{LL_j}}{S_b} \qquad f_{LLt} = \begin{pmatrix} 0.318 \\ 2.155 \\ 2.222 \end{pmatrix} \cdot ksi \qquad f_{LLb_j} := -\frac{M_{LL_j}}{S_b} \qquad f_{LLb} = \begin{pmatrix} -0.318 \\ -2.155 \\ -2.222 \end{pmatrix} \cdot ksi$$

Transformed:

At Release:

Self-Weight:

$$f_{tswtr_j} := \frac{M_{swr_j}}{S_{ttr_j}} \qquad f_{tswtr}^{T} = (0.093 \quad 0.777 \quad 0.809)\ ksi$$

$$f_{bswtr_j} := \frac{-M_{swr_j}}{S_{btr_j}} \qquad f_{bswtr}^{T} = (-0.179 \quad -1.449 \quad -1.508)\ ksi$$

At Final Conditions:

Self-Weight: $j := 1 .. 3$

$$f_{tsw_j} := \frac{M_{swf_j}}{S_{ttf_j}} \qquad f_{tsw}^{T} = (0.112 \quad 0.764 \quad 0.795)\ ksi$$

$$f_{bsw_j} := -\frac{M_{swf_j}}{S_{btf_j}} \qquad f_{bsw}^{T} = (-0.217 \quad -1.435 \quad -1.495)\ ksi$$

Barriers:

$$f_{tbarrier_j} := \frac{M_{barrier_j}}{S_{ttf_j}} \qquad f_{tbarrier}^{T} = (0.016 \quad 0.112 \quad 0.117)\ ksi$$

$$f_{bbarrier_j} := -\frac{M_{barrier_j}}{S_{btf_j}} \qquad f_{bbarrier}^{T} = (-0.032 \quad -0.211 \quad -0.22)\ ksi$$

Future Wearing Surface:

$$f_{tfws_j} := \frac{M_{fws_j}}{S_{ttf_j}} \qquad f_{tfws}^{T} = (0.016 \quad 0.112 \quad 0.117)\ ksi$$

$$f_{bfws_j} := -\frac{M_{fws_j}}{S_{btf_j}} \qquad f_{bfws}^{T} = (-0.032 \quad -0.211 \quad -0.22)\ ksi$$

Live Load I:

$$f_{LL\_It_j} := \frac{M_{LL_j}}{S_{ttf_j}} \qquad f_{LL\_It}^{T} = (0.1551 \quad 1.021 \quad 1.0526)\ ksi$$

Live Load III:

$$f_{LL\_IIIb_j} := -\frac{(0.8 \cdot M_{LL})_j}{S_{btf_j}} \qquad f_{LL\_IIIb}^{T} = (-0.241 \quad -1.535 \quad -1.583)\ ksi$$

8 Prestress Losses

Total Loss of Prestress:

$$\Delta f_{pT} := \Delta f_{pES} + \Delta f_{pLT}$$ (LRFD 5.9.5.1-1)

where:

Δf_{pES} = Sum of all losses due to elastic shortening at time of application of prestress load (ksi). Note that in accordance with LRFD C5.9.5.2.3a, the effects of losses due to elastic shortening are implicitly accounted for when transformed section properties are used. That is, Δf_{pES} should not be included in the loss calulations as a separate quantity. Therefore, Δf_{pES} need not be computed separately since it is implicitly accounted for in the calculations.

Δf_{pLT} = Total loss due to long-term effects, which include shrinkage and creep of the concrete and relaxation of the prestressing steel (ksi).

In pretensioned bridge girder design, stresses have traditionally been assessed at two timeframes: at release of prestress (i.e., when the prestress force is applied to the girder) and at final (long-term) conditions. Therefore, loss of prestress has been evaluated at these two periods in the life of the girder. However, with the new prestress loss procedure introduced in the 2005 Interim Revisions, long-term losses are computed in two steps: (a) The time period between prestress transfer and placement of the cast-in-place concrete deck and (b) the time period between deck placement and the end of the service life of the girder. These two periods correspond to the non-composite and composite phases of the structural system. The rate of stress change in the strands can differ significantly in each phase, hence the need to subdivide the long-term losses into two components.

In non-composite precast girder systems, such as the non-composite adjacent box beams used in this example, some modifications to the loss procedure are necessary to properly apply it. After the girders are erected, no deck is cast; significant loads are introduced to the bridge nonetheless. Barriers and an asphalt wearing course are typcally applied, which result in a significant stress change in the girder. Hence, the same two time periods will be used as for a composite system, except that the "deck placement" stage will be called superimposed dead loads (SDL) placement.

Loss at Release:

The principal component of prestress loss when the strands are released and the prestress force in the strands is imparted into the girder is elastic shortening. This reduction in prestress (prestress loss) occurs essentially instantaneously. However, as noted above, since transformed properties (i.e., the prestressing steel is transformed into an equivalent area of concrete) are used in this example problem, a separate calculation need not be performed to compute the effects of elastic shortening; the effects are implicit in the stress calculations.

Loss at Final Conditions:

The time-dependent loss of prestress consists of three distinct components. Loss due to:

1. Creep of girder concrete,
2. Relaxation of prestressing strands, and
3. Shrinkage of girder concrete.

These are computed in two stages:

1. From time prestress force is imparted to the girder to the time the girder is erected and
2. From the time the barriers and wearing surface are applied to final time.

Mathematically, this is expressed as:

$$\Delta fpLT = (\Delta f_{pSR}+\Delta f_{pCR}+\Delta f_{pR1})_{id} + (\Delta f_{pSD}+\Delta f_{pCD}+\Delta f_{pR2}-\Delta f_{pSS})_{df}$$ (LRFD 5.9.5.4.1-1)

Since there is no CIP slab in this system, the last term of this expression should be omitted:

$$\Delta fpLT = (\Delta f_{pSR}+\Delta f_{pCR}+\Delta f_{pR1})_{id} + (\Delta f_{pSD}+\Delta f_{pCD}+\Delta f_{pR2})_{df}$$

Materials Properties:

The shrinkage and creep properties of the girder need to be computed in preparation for the actual prestress loss computations. These are addressed in LRFD Article 5.4.2.3. Creep coefficients are computed in accordance with Article 5.4.2.3.2 and shrinkage strains are computed in accordance with Article 5.4.2.3.3.

Creep Coefficients

Girder creep coefficient at final time due to loading at transfer:

$$\psi_b(t_f, t_i) := 1.9 \cdot k_{vs} \cdot k_{hc} \cdot k_f \cdot k_{td} \cdot t_i^{-0.118}$$ (LRFD Eq. 5.4.2.3.2-1)

where:

ψ_b Ratio of creep strain to elastic strain.

k_{vs} = Factor for the effect of volume to surface ratio.

k_{hc} = Humidity factor for creep.

k_f = Factor for strength of concrete.

k_{td} = Factor for time development.

$$k_{vs} := 1.45 - 0.13\frac{VS_b}{in} \qquad k_{vs} = 1.003$$ Note: k_{vs} must be greater than or equal to 0.0. (LRFD 5.4.2.3.2-1)

$$k_{hc} := 1.56 - 0.008H \qquad k_{hc} = 1.000$$ (LRFD Eq. 5.4.2.3.2-3)

$$k_f := \frac{5}{1 + \frac{f'_{ci}}{ksi}} \qquad k_f = 0.714$$ (LRFD 5.4.2.3.2-4)

$t_f := t_{final}$ $t_i := t_{transfer}$

$t := t_f - t_i$ $t = 19999 \cdot day$

$$k_{td} := \frac{\frac{t}{day}}{61 - \frac{4 \cdot f'_{ci}}{ksi} + \frac{t}{day}} \qquad k_{td} = 0.996$$ (LRFD 5.4.2.3.2-5)

$$\psi_{bfi} := 1.9 \cdot k_{vs} \cdot k_{hc} \cdot k_f \cdot k_{td} \cdot \left(\frac{t_i}{day}\right)^{-0.118} \qquad \psi_{bfi} = 1.358$$

Girder creep coefficient at time of SDL placement due to loading at transfer:

$t_i := t_{transfer}$ $t_d := t_{deck}$

$t := t_d - t_i$ $t = 89 \cdot day$

$$k_{td} := \frac{\frac{t}{day}}{61 - \frac{4 \cdot f'_{ci}}{ksi} + \frac{t}{day}} \qquad k_{td} = 0.706$$

$$k_{vs} := 1.45 - 0.13\frac{VS_b}{in} \qquad k_{vs} = 1.003$$

Note: k_{vs} must be greater than or equal to 0.0. (LRFD 5.4.2.3.2-1)

$k_{hc} := 1.56 - 0.008H$ $k_{hc} = 1.000$ (LRFD Eq. 5.4.2.3.2-3)

$$k_f := \frac{5}{1 + \frac{f'_{ci}}{ksi}} \qquad k_f = 0.714$$ (LRFD 5.4.2.3.2-4)

$$\psi_{bdi} := 1.9 \cdot k_{vs} \cdot k_{hc} \cdot k_f \cdot k_{td} \cdot \left(\frac{t_i}{day}\right)^{-0.118} \qquad \psi_{bdi} = 0.961$$

Girder creep coefficient at final time due to loading at SDL placement:

$t_i := t_{deck}$

$t := t_f - t_i$ $t = 19910 \cdot day$

$$k_{td} := \frac{\frac{t}{day}}{61 - \frac{4 \cdot f'_{ci}}{ksi} + \frac{t}{day}} \qquad k_{td} = 0.998$$

$$k_{vs} := 1.45 - 0.13\frac{VS_b}{in} \qquad k_{vs} = 1.003$$

Note: k_{vs} must be greater than or equal to 0.0. (LRFD 5.4.2.3.2-1)

$k_{hc} := 1.56 - 0.008H$ $k_{hc} = 1.000$ (LRFD Eq. 5.4.2.3.2-3)

$$k_f := \frac{5}{1 + \frac{f'_{ci}}{ksi}} \qquad k_f = 0.714$$ (LRFD 5.4.2.3.2-4)

$$\psi_{bfd} := 1.9 \cdot k_{vs} \cdot k_{hc} \cdot k_f \cdot k_{td} \cdot \left(\frac{t_i}{day}\right)^{-0.118} \qquad \psi_{bfd} = 0.799$$

Shrinkage Strains

Girder concrete shrinkage strain between transfer and final time:

The concrete shrinkage strain, ε_{bid}, is computed in accordance with Art. 5.4.2.3.3:

$$\varepsilon_{sh} := -k_{vs} \cdot k_{hs} \cdot k_f \cdot k_{td} \cdot 0.48 \cdot 10^{-3}$$ (LRFD 5.4.2.3.3-1)

where:

k_{vs} = Factor for the effect of volume to surface ratio.

k_{hs} = Factor for humidity.

k_f = Factor for strength of concrete.

k_{td} = Factor for time development.

$k_{vs} := 1.45 - 0.13 \frac{VS_b}{in}$ $k_{vs} = 1.003$ Note: kvs must be greater than or equal to 0.0. (LRFD 5.4.2.3.2-1)

$k_{hs} := 2.00 - 0.014 \cdot H$ $k_{hs} = 1.020$ (LRFD 5.4.2.3.3-2)

$k_f := \frac{5}{1 + \frac{f'_{ci}}{ksi}}$ $k_f = 0.714$ (LRFD 5.4.2.3.2-4)

$t_f := t_{final}$ $t_i := t_{transfer}$

$t := t_f - t_i$ $t = 19999 \cdot day$

$k_{td} := \frac{\frac{t}{day}}{61 - \frac{4 \cdot f'_{ci}}{ksi} + \frac{t}{day}}$ $k_{td} = 0.998$ (LRFD 5.4.2.3.2-5)

$\varepsilon_{bif} := -k_{vs} \cdot k_{hs} \cdot k_f \cdot k_{td} \cdot 0.48 \cdot 10^{-3}$ $\varepsilon_{bif} = -350 \times 10^{-6}$

Girder concrete shrinkage strain between transfer and SDL placement:

$k_{vs} := 1.45 - 0.13 \frac{VS_b}{in}$ $k_{vs} = 1.003$ (LRFD 5.4.2.3.2-1)

$k_{hs} := 2.00 - 0.014 \cdot H$ $k_{hs} = 1.020$ (LRFD 5.4.2.3.3-2)

$k_f := \frac{5}{1 + \frac{f'_{ci}}{ksi}}$ $k_f = 0.714$ (LRFD 5.4.2.3.2-4)

$t := t_d - t_i$ $t = 89 \cdot day$

$k_{td} := \frac{\frac{t}{day}}{61 - \frac{4 \cdot f'_{ci}}{ksi} + \frac{t}{day}}$ $k_{td} = 0.706$ (LRFD 5.4.2.3.2-5)

$\varepsilon_{bid} := -k_{vs} \cdot k_{hs} \cdot k_f \cdot k_{td} \cdot 0.48 \cdot 10^{-3}$ $\varepsilon_{bid} = -248 \times 10^{-6}$

Girder concrete shrinkage strain between SDL placement and final time:

The girder concrete shrinkage between deck placement and final time is the difference between the shrinkage at time of deck placement and the total shrinkage at final time.

$\varepsilon_{bdf} := \varepsilon_{bif} - \varepsilon_{bid}$ $\varepsilon_{bdf} = -102 \times 10^{-6}$

Loss from Transfer to SDL Placement:

The prestress loss from transfer of prestress to placement of SDL consists of three loss components: shrinkage of the girder concrete, creep of the girder concrete, and relaxation of the strands. That is,

Time-Dependent Loss from Transfer to SDL Placement = $\Delta f_{pSR} + \Delta f_{pCR} + \Delta f_{pR1}$

Shrinkage of Concrete Girder:

$\Delta f_{pSR} := \varepsilon_{bid} \cdot E_p \cdot K_{id}$ (LRFD5.9.5.4.2a-1)

where:

ε_{bid} = Concrete shrinkage strain of girder between transfer and SDL placement. Computed using LRFD Eq. 5.4.2.3.3-1

E_p = Modulus of elasticity of prestressing strand (ksi).

K_{id} = Transformed steel coefficient that accounts for time-dependent interaction between concrete and bonded steel in the section being considered for the time period between transfer and SDL placement.

The transformed section coefficient, k_{id}, is computed using:

$$K_{id} := \frac{1}{1 + \frac{E_p}{E_{ci}} \cdot \frac{A_{ps_7}}{A_g} \cdot \left(1 + \frac{A_g \cdot e_{pg}^2}{I_g}\right) \cdot \left(1 + 0.7 \cdot \psi_b(t_f, t_i)\right)}$$ (LRFD Eq. 5.9.5.4.2a-2)

where:

e_{pg} = Eccentricity of strands with respect to centroid of girder (in).

$\psi_b(t_f, t_i)$ = Creep coefficient at final time due to loading introduced at transfer.

Note: The eccentricity of the strand pattern is stored in the vectors ecc_r and ecc_f. Vector ecc_r contains values at check points relative to release (i.e., the end of the girder), and vector ecc_r is relative to final check points (i.e., relative to the left bearing of the girder). The eccentricity at the midspan of the girder is the value of interest.

$e_{pg} := ecc\_r_3$ $e_{pg} = 31.48 \cdot in$ $A_g := A$ $I_g := I$

$A_{psm} := No\_Strands \cdot A_{strand}$ $A_{psm} = 6.944 \cdot in^2$ (Area of strand at midspan)

$$K_{id} := \frac{1}{1 + \frac{E_p}{E_{ci}} \cdot \frac{A_{psm}}{A_g} \cdot \left(1 + \frac{A_g \cdot e_{pg}^2}{I_g}\right) \cdot \left(1 + 0.7 \cdot \psi_{bfi}\right)}$$ $K_{id} = 0.7552$

Therefore, the prestress loss due to shrinkage of the girder concrete between time of transfer and SDL placement is:

$\Delta f_{pSR} := -\varepsilon_{bid} \cdot E_p \cdot K_{id}$ $\Delta f_{pSR} = 5.331 \cdot ksi$

Creep of Concrete Girder:

$$\Delta f_{pCR} := \frac{E_p}{E_{ci}} \cdot f_{cgp} \cdot \psi_b(t_d, t_i) \cdot K_{id}$$ (LRFD 5.9.5.4.2b-1)

where:

f_{cgp} = Concrete stress at cg of prestress pattern due to the prestressing force immediately after transfer and the self-weight of the girder at the section of maximum moment (ksi).

Section modulus at cg of strand pattern:

$e_{pti} := y_{btr_3} - y_{cg\_r_3}$ $e_{pti} = 30.38 \cdot in$

$S_{cgp} := \frac{I_{tr_3}}{e_{pti}}$ $S_{cgp} = 12703 \cdot in^3$

Initial prestress force:

$f_{pj} := Pull \cdot f_{pu}$

$P_{init} := f_{pj} \cdot A_{ps}$ $P_{init} = 1406.2 \cdot kip$

$$f_{cgp} := P_{init} \cdot \left(\frac{1}{A_{tr}} + \frac{e_{pti}}{S_{cgp}} \right) - \frac{M_{swf_3}}{S_{cgp}}$$ $f_{cgp} = 3.418 \cdot ksi$

$$\Delta f_{pCR} := \frac{E_p}{E_{ci}} \cdot f_{cgp} \cdot \psi_{bdi} \cdot K_{id}$$ $\Delta f_{pCR} = 15.521 \cdot ksi$

Relaxation of Prestressing Strands:

The LRFD Specs provide two equations for predicting the loss of prestress due to strand relaxation:

$$\Delta f_{pR1} := \frac{f_{pt}}{K_L} \cdot \left(\frac{f_{pt}}{f_{py}} - 0.55 \right)$$ (LRFD 5.9.5.4.2c-1)

where:

f_{pt} = Stress in prestressing steel immediately after transfer (ksi), taken not less than $0.55 f_y$

f_{py} = Yield strength of prestressing steel (ksi) = $0.90 f_{pu}$ for low-relaxation strand.

K_L = Factor accounting for type of prestressing steel. Taken as 30 for low-relaxation strands and 7 for other types of prestressing steel.

$$\Delta f_{pR1} := \left[\frac{f_{pt}}{K'_L} \cdot \frac{\log(24 \cdot t)}{\log(24 \cdot t_i)} \cdot \left(\frac{f_{pt}}{f_{py}} - 0.55 \right) \right] \cdot \left[1 - \frac{3 \cdot (\Delta f_{pSR} + \Delta f_{pCR})}{f_{pt}} \right] \cdot K_{id}$$ (LRFD C5.9.5.4.2c-1)

where:

k'_L = Factor accounting for type of prestressing steel, equal to 45 for low-relaxation steel and 10 for stress-relieved steel.

Art. 5.9.5.4.2c also permits 1.2 ksi to be assumed as the loss for low-relaxation strands.

Using the first formula:

The parameter f_{pt} is the stress in the strands immediately after transfer. At that point in time, the loss associated with elastic shortening has already occurred. However, since transformed section properties are being used in this example, there has been no need to compute elastic shortening as a separate item since its effects are implicit in the calculations (see LRFD C5.9.5.2.3a). But to compute f_{pt}, the loss caused by elastic shortening must be computed since the stress in the strands--rather than the concrete--after release is needed. This can be computed by calculating the stress in the concrete immediately after release and multiplying by the modular ratio, n, to determine the change in strand stress. This change in strand stress can then be deducted from the jacking stress to obtain the net strand stress after release.

The stress in the concrete at the cg of the strands after transfer was computed above (using transformed section properties), which is f_{cgp}:

$f_{cgp} = 3.418 \cdot ksi$

Thus, the change in steel stress is:

$\Delta f_{pES} := n_i \cdot f_{cgp}$

where,

n_i = Ratio of steel modulus to concrete modulus at release.

$n_i := \frac{E_p}{E_{ci}}$ $\quad n_i = 6.2557$

$\Delta f_{pES} := n_i \cdot f_{cgp}$ $\quad \Delta f_{pES} = 21.381 \cdot ksi$

$f_{pt} := f_{pj} - \Delta f_{pES}$ $\quad f_{pt} = 181.1 \cdot ksi$

$K_L := 30$

$f_{py} := 0.90 \cdot f_{pu}$ $\quad f_{py} = 243 \cdot ksi$

$\Delta f_{pR1} := \frac{f_{pt}}{K_L} \cdot \left(\frac{f_{pt}}{f_{py}} - 0.55 \right)$ $\quad \Delta f_{pR1} = 1.1794 \cdot ksi$

Using the second formula:

$K'_L := 45$

$t := t_d$

$\Delta f_{pR1} := \left[\frac{f_{pt}}{K'_L} \cdot \frac{\log\left(24 \cdot \frac{t}{day}\right)}{\log\left(24 \cdot \frac{t_i}{day}\right)} \cdot \left(\frac{f_{pt}}{f_{py}} - 0.55 \right) \right] \cdot \left[1 - \frac{3 \cdot \left(\Delta f_{pSR} + \Delta f_{pCR} \right)}{f_{pt}} \right] \cdot K_{id}$ $\quad \Delta f_{pR1} = 0.939 \cdot ksi$

Since, according to LRFD C5.9.5.4.2c, the second equation is the more accurate equation, Δf_{pR1} should be computed using the second. However, for this example, it will be assumed to be equal to 1.2 ksi (Article 5.9.5.4.2b permits this).

$\Delta f_{pR1} := 1.2 \cdot ksi$

Total prestress loss at time of SDL placement:

$\Delta f_{pLTid} := \Delta f_{pSR} + \Delta f_{pCR} + \Delta f_{pR1}$

Calculated above:

$\Delta f_{pSR} = 5.33\cdot ksi$ $\Delta f_{pCR} = 15.52\cdot ksi$ $\Delta f_{pR1} = 1.20\cdot ksi$

$\Delta f_{pLTid} = 22.053\cdot ksi$

Loss from SDL Placement to Final:

The prestress loss from placement of SDL to final conditions consists of four loss components: shrinkage of the girder concrete, creep of the girder concrete, and relaxation of the strands. That is,

Time-Dependent Loss from SDL Placement to Final = $\Delta f_{pSD} + \Delta f_{pCD} + \Delta f_{pR2}$

Shrinkage of Concrete Girder:

$\Delta f_{pSD} := \varepsilon_{bdf} E_p \cdot K_{df}$ (LRFD5.9.5.4.3a-1)

where:

ε_{bdf} = Concrete shrinkage strain of girder between time of SDL placement and final time. Computed using LRFD Eq. 5.4.2.3.3-1

K_{df} = Transformed steel coefficient that accounts for time-dependent interaction between concrete and bonded steel in the section being considered for the time period between the time of SDL placement and final time.

Compute K_{df}:

$$K_{df} := \frac{1}{1 + \frac{E_p}{E_{ci}} \cdot \frac{A_{ps}}{A_c} \cdot \left(1 + \frac{A_c \cdot e_{pc}^2}{I_c}\right) \cdot \left(1 + 0.7\,\psi_b(t_f, t_i)\right)}$$ (LRFD 5.9.5.4.3a-2)

where:

e_{pc} = Eccentricity of strands with respect to centroid of composite section

A_c = For composite sections, the gross area of the composite section should be used. However, since this girder is non-composite, the gross area of the non-composite section is used.

I_c = Gross area of composite section for composite systems, gross area of bare beam for non-composite systems.

$\psi_b(t_f, t_i)$ = Girder creep coefficient

$e_{pc} := y_{bg} - y_{cg\_f_3}$ $e_{pc} = 31.485\cdot in$

A_c: $A_g = 999\cdot in^2$

I_c: $I_g = 350965\cdot in^4$

$$K_{df} := \frac{1}{1 + \frac{E_p}{E_{ci}} \cdot \frac{A_{ps}}{A_g} \cdot \left(1 + \frac{A_g \cdot e_{pc}^2}{I_g}\right) \cdot \left(1 + 0.7\,\psi_{bfi}\right)}$$ $K_{df} = 0.755$

Therefore, prestress loss due to shrinkage of girder concrete between SDL placement and final is:

$\Delta f_{pSD} := -\varepsilon_{bdf} \cdot E_p \cdot K_{df}$ $\Delta f_{pSD} = 2.202 \cdot ksi$

Creep of Concrete Girder:

$$\Delta f_{pCD} := \frac{E_p}{E_{ci}} \cdot f_{cgp} \cdot \left(\psi_b(t_f, t_i) - \psi_b(t_d, t_i)\right) \cdot K_{df} + \frac{E_p}{E_c} \cdot \Delta f_{cd} \cdot \psi_b(t_f, t_d) \cdot K_{df} \geq 0.0$$ (LRFD5.9.5.4.3b-1)

where:

Δf_{cd} = Change in concrete stress at centroid of prestressing strands due to long-term losses between transfer and SDL placement combined with superimposed loads (ksi).

$\psi_b(t_f, t_d)$ = Girder creep coefficient at final time due to loading at SDL placement per Eq. 5.4.2.3.2-1.

Let:

$\Delta f_{pCD} := \Delta f_{pCD1} + \Delta f_{pCD2}$

compute Δf_{pCD1}:

$$\Delta f_{pCD1} := \frac{E_p}{E_{ci}} \cdot f_{cgp} \cdot \left(\psi_{bfi} - \psi_{bdi}\right) \cdot K_{df}$$ $\Delta f_{pCD1} = 6.412 \cdot ksi$

compute Δf_{pCD2}:

compute Δf_{cd}:

$$\Delta f_{cd} := \Delta P \cdot \left(\frac{1}{A_g} + \frac{e_{pg}^2}{I_g}\right) - \left(\frac{M_{fws_7} + M_{barrier_7}}{S_{cgp}}\right)$$

$\Delta P := -\Delta f_{pLTid} \cdot A_{ps}$ $\Delta P = -153.1 \cdot kip$

$e_{pg} := y_{bg} - y_{cg\_f_3}$ $e_{pg} = 31.485 \cdot in$

$$\Delta f_{cd} := \Delta P \cdot \left(\frac{1}{A_g} + \frac{e_{pg}^2}{I_g}\right) - \left(\frac{M_{fws_3} + M_{barrier_3}}{S_{cgp}}\right)$$ $\Delta f_{cd} = -0.969 \cdot ksi$

$\Delta f_{pCD2} := \frac{E_p}{E_c} \cdot \Delta f_{cd} \cdot \psi_{bfd} \cdot K_{df}$ $\Delta f_{pCD2} = -3.385 \cdot ksi$

Therefore,

$\Delta f_{pCD} := \Delta f_{pCD1} + \Delta f_{pCD2}$ $\Delta f_{pCD} = 3.027 \cdot ksi$

Relaxation of Prestressing Strands:

$\Delta f_{pR2} := \Delta f_{pR1}$ $\Delta f_{pR2} = 1.2 \cdot ksi$ (LRFD 5.9.5.4.3c-1)

Total prestress loss from SDL placement to final, therefore, is:

$\Delta f_{pLTdf} := \Delta f_{pSD} + \Delta f_{pCD} + \Delta f_{pR2}$

Calculated above:

$\Delta f_{pSD} = 2.2 \cdot ksi$ $\Delta f_{pCD} = 3.03 \cdot ksi$ $\Delta f_{pR2} = 1.2 \cdot ksi$

$\Delta f_{pLTdf} = 6.429 \cdot ksi$

Summary of Time-Dependent Losses

Losses from Transfer to SDL Placement

Girder shrinkage: $\Delta f_{pSR} = 5.33 \cdot ksi$

Girder creep: $\Delta f_{pCR} = 15.52 \cdot ksi$

Strand relaxation: $\Delta f_{pR1} = 1.2 \cdot ksi$

Total = $\Delta f_{pLTid} = 22.053 \cdot ksi$

Losses from SDL Placement to Final

Girder shrinkage: $\Delta f_{pSD} = 2.2 \cdot ksi$

Girder creep: $\Delta f_{pCD} = 3.03 \cdot ksi$

Strand relaxation: $\Delta f_{pR2} = 1.2 \cdot ksi$

Total = $\Delta f_{pLTdf} = 6.429 \cdot ksi$

Total Long-term Pretsress Losses:

$\Delta f_{pLT} := \Delta f_{pLTid} + \Delta f_{pLTdf}$

Transfer to SDL: $\Delta f_{pLTid} = 22.053 \cdot ksi$

SDL to Final $\Delta f_{pLTdf} = 6.429 \cdot ksi$

Total = $\Delta f_{pLT} = 28.48 \cdot ksi$

9 Stress Due to Prestress

Stress Due to Total Initial Prestress Force at Transfer

The stress in the concrete at transfer is computed directly by applying the total initial prestress force to the transformed girder properties at release:

Stress in top of girder at three points of interest (transfer point, depress point, and midspan):

$j := 1 .. 3$

$P_j := f_{pj} \cdot A_{ps}$ $\quad P_j^T = (1406.2 \quad 1406.2 \quad 1406.2)\ kip$

$$f_{tpstr_j} := P_j \cdot \left(\frac{1}{A_{tr}} - \frac{y_{btr_j} - y_{cg\_r_j}}{S_{ttr_j}} \right)$$

$f_{tpstr}^T = (0.043 \quad -0.690 \quad -0.690)\ ksi$

Stress in bottom of girder:

$$f_{bpstr_j} := P_j \cdot \left(\frac{1}{A_{tr}} + \frac{y_{btr_j} - y_{cg\_r_j}}{S_{btr_j}} \right)$$

$f_{bpstr}^T = (3.894 \quad 5.177 \quad 5.177)\ ksi$

Change in Concrete Stress Due to Prestress Loss

The change in concrete stress due to long-term losses is computed by applying the change in strand force due to long-term losses to the concrete cross section that resists the forces at the time. Recall that the long-term losses were computed in two parts: Δf_{pLTid}, the long-term loss between transfer and SDL placement, and Δf_{pLTdf}, the long-term losses from SDL placement to final time. For each of these changes in stress, the corresponding forces are computed. The changes in concrete stress are then computed by applying these forces to the gross precast section.

Change in prestress force due to long-term losses:

From initial to SDL placement:

$\Delta f_{pLTid} = 22.053\,ksi$

$\Delta P_{id_j} := -\Delta f_{pLTid} \cdot A_{ps}$

$\Delta P_{id}^{T} = (-153.1 \quad -153.1 \quad -153.1)\,kip$

From SDL placement to final:

$\Delta f_{pLTdf} = 6.429\,ksi$

$\Delta P_{df_j} := -\Delta f_{pLTdf} \cdot A_{ps}$

$\Delta P_{df}^{T} = (-44.6 \quad -44.6 \quad -44.6)\,kip$

To compute the changes in concrete stress, these forces are applied to their respective resisting cross sections, and the resulting stresses are summed.

Change in concrete stress in concrete at top of girder due to long-term prestress losses:

$$\Delta f_{tps_j} := \left(\Delta P_{id_j} + \Delta P_{df_j}\right) \cdot \left(\frac{1}{A_g} - \frac{y_{bg} - y_{cg\_f_j}}{S_{tg}}\right)$$

$\Delta f_{tps}^{T} = (-0 \quad 0.111 \quad 0.111)\,ksi$

Change in concrete stress in concrete at bottom of girder due to long-term prestress losses:

$$\Delta f_{bps_j} := \left(\Delta P_{id_j} + \Delta P_{df_j}\right) \cdot \left(\frac{1}{A_g} + \frac{y_{bg} - y_{cg\_f_j}}{S_{bg}}\right)$$

$\Delta f_{bps}^{T} = (-0.603 \quad -0.83 \quad -0.83)\,ksi$

7.10 Net Stress at Service

At Release Conditions:

Service Limit State I:

Top of girder (tension):

$f_{tr_j} := f_{tpstr_j} + f_{tswtr_j}$ $\quad f_{tr}^{T} = (0.136 \;\; 0.087 \;\; 0.119)\ ksi$

Bottom of girder (compression):

$f_{br_j} := f_{bpstr_j} + f_{bswtr_j}$ $\quad f_{br}^{T} = (3.715 \;\; 3.728 \;\; 3.669)\ ksi$

At Final Conditions:

Stress Due to Prestress + Full Dead Load + Live Load:

Service I (compressive stresses in top of beam):

$f_{ttf_j} := f_{tpstr_j} + \Delta f_{tps_j} + f_{tsw_j} + f_{tbarrier_j} + f_{tfws_j} + f_{LL\_It_j}$

$f_{ttf}^{T} = (0.342 \;\; 1.43 \;\; 1.503)\ ksi$

Service III Limit State (tensile stresses in precompressed tensile zone, i.e., bottom of beam):

$f_{btf_j} := f_{bpstr_j} + \Delta f_{bps_j} + f_{bsw_j} + f_{bbarrier_j} + f_{bfws_j} + f_{LL\_IIIb_j}$

$f_{btf}^{T} = (2.77 \;\; 0.954 \;\; 0.83)\ ksi$

Prestress Losses per LRFD 4th Edition (Approximate Method)

At Release:

Elastic Shortening:

$f_{pbt} := Pull \cdot f_{pu}$ $\quad f_{pj} = 202.5 \cdot ksi$ $\quad f_{py} = 243 \cdot ksi$

$f_{pbt} := f_{pj}$ (relaxation of steel between tensioning and detensioning ignored)

$E_{ci} := 33000 \cdot w_c^{1.5} \cdot kcf^{-1.5} \cdot \sqrt{f'_{ci} \cdot ksi^{-1}}$ $\quad E_{ci} = 4556 \cdot ksi$ (LRFD 5.4.2.4-1)

$A_{psm} := No\_Strands \cdot A_{strand}$ $\quad A_{psm} = 6.944 \cdot in^2$ (Area of strand at midspan)

$e_m := y_b - y_{mid}$ $\quad e_m = 31.48 \cdot in$

$$\Delta f_{pES} := \frac{A_{psm} \cdot f_{pbt} \cdot \left(1 + e_m^2 A\right) - e_m \cdot M_{swr_3} \cdot A}{A_{psm} \cdot \left(1 + e_m^2 A\right) + \frac{A \cdot I \cdot E_{ci}}{E_p}}$$ $\quad \Delta f_{pES} = 20.74 \cdot ksi$

$\Delta f_{pES} = 20.74 \cdot ksi$

Total Prestress Loss at Release:

$\Delta f_{sr} := \Delta f_{pES}$ $\Delta f_{sr} = 20.74 \cdot ksi$

$\%Loss := \frac{\Delta f_{sr}}{Pull \cdot f_{pu}} \cdot 100$ $\%Loss = 10.242$

$f_{per} := f_{pj} - \Delta f_{pES}$ $f_{per} = 181.8 \cdot ksi$

$P_r := f_{per} \cdot No\_Strands \cdot A_{strand}$ $P_r = 1262.1 \cdot kip$

At Final Conditions:

Total loss at final condition:

$\Delta f_{PT} := \Delta f_{pES} + \Delta f_{pLT}$

Elastic Shortening: Same as at release (see above)

Long-Term Losses:

$\Delta f_{pLT} := 10.0 \frac{f_{pj} \cdot A_{psm}}{A} \cdot \gamma_h \cdot \gamma_{st} + 12.0 \cdot ksi \cdot \gamma_h \cdot \gamma_{st} + \Delta f_{pR}$ (LRFD 5.9.5.3-1)

$\gamma_h := 1.7 - 0.01 \cdot H$ $\gamma_h = 1.00$ (LRFD 5.9.5.3-2)

$\gamma_{st} := \frac{5 \cdot ksi}{1 \cdot ksi + f'_{ci}}$ $\gamma_{st} = 0.714$ (LRFD 5.9.5.3-3)

$\Delta f_{pR} := 2.4 \cdot ksi$

$\Delta f_{pLT} := 10.0 \frac{f_{pj} \cdot A_{psm}}{A} \cdot \gamma_h \cdot \gamma_{st} + 12.0 \cdot ksi \cdot \gamma_h \cdot \gamma_{st} + \Delta f_{pR}$ $\Delta f_{pLT} = 21.03 \cdot ksi$

$\Delta f_{PT} := \Delta f_{pES} + \Delta f_{pLT}$ $\Delta f_{PT} = 41.77 \cdot ksi$

$\%Loss := \frac{\Delta f_{PT}}{Pull \cdot f_{pu}} \cdot 100$ $\%Loss = 20.62$

Check effective stress after losses:

$f_{pe} := Pull \cdot f_{pu} - \Delta f_{PT}$ $f_{pe} = 160.7 \cdot ksi$

$f_{allow} := 0.80 \cdot f_{py}$ $f_{allow} = 194.4 \cdot ksi$ (LRFD 5.9.3-1)

Stresses Due to Prestress (with LRFD 4th Edition Losses, Approx. Method)

At Release Conditions:

$j := 1 .. 3$

$f_{psrb_j} := P_r \left(\frac{1}{A} + \frac{ecc\_r_j}{S_b} \right)$ $f_{psrb}^T = (3.772 \quad 5.295 \quad 5.295) \cdot ksi$

$f_{psrt_j} := P_r \left(\frac{1}{A} - \frac{ecc\_r_j}{S_t} \right)$ $f_{psrt}^T = (0.039 \quad -0.706 \quad -0.706) \cdot ksi$

At Final Conditions:

$dist_j := x_{f_j} + \frac{L_{ovr} - L_{des}}{2}$ $\quad dist^T = (4.18 \;\; 42.1 \;\; 52.5)\ ft$

$L_t := 60 \cdot d_b$ $\quad L_t = 36 \cdot in$

$dt_j := if\left(dist_j > L_t, 1.0, \frac{dist_j}{L_t}\right)$ $\quad dt^T = (1 \;\; 1 \;\; 1)$ (Fraction strands are transferred.)

$j := 1 .. 3$

$P_{f_j} := f_{pe} \cdot dt_j \cdot No\_Strands \cdot A_{strand}$ $\quad P_f^T = (1116.1 \;\; 1116.1 \;\; 1116.1) \cdot kip$

$f_{psb_j} := P_{f_j} \cdot \left(\frac{1}{A} + \frac{ecc\_f_j}{S_b}\right)$ $\quad f_{psb} = \begin{pmatrix} 3.401 \\ 4.683 \\ 4.683 \end{pmatrix} \cdot ksi$ $\quad f_{pst_j} := P_{f_j} \cdot \left(\frac{1}{A} - \frac{ecc\_f_j}{S_t}\right)$ $\quad f_{pst} = \begin{pmatrix} 0.002 \\ -0.624 \\ -0.624 \end{pmatrix} \cdot ksi$

Service Stress Check (with LRFD 4th Edition Losses, Approx. Method)

At Release Conditions:

Top of girder (tension):

$f_{rt_j} := f_{psrt_j} + f_{swrt_j}$ $\quad f_{rt}^T = (0.131 \;\; 0.097 \;\; 0.13) \cdot ksi$

$f_{allow\_rt} := -0.0948 \cdot \sqrt{f'_{ci}} \cdot \sqrt{ksi}$ $\quad f_{allow\_rt} = -0.232 \cdot ksi$

$Status\_ServiceLSrt_j := if\left(f_{rt_j} \geq f_{allow\_rt}, "OK", "NG"\right)$ $\quad Status\_ServiceLSrt^T = ("OK" \;\; "OK" \;\; "OK")$

Bottom of girder (compression):

$f_{rb_j} := f_{psrb_j} + f_{swrb_j}$ $\quad f_{rb}^T = (3.582 \;\; 3.651 \;\; 3.584) \cdot ksi$

$f_{allow\_rc} := 0.6 \cdot f'_{ci}$ $\quad f_{allow\_rc} = 3.6 \cdot ksi$

$Status\_ServiceLSrc_j := if\left(f_{rt_j} \leq f_{allow\_rc}, "OK", "NG"\right)$ $\quad Status\_ServiceLSrc^T = ("OK" \;\; "OK" \;\; "OK")$

At Final Conditions:

Check Service Limit States:

Service III Limit State (Tensile Stresses in Bottom of Beam):

$f_{IIIb_j} := f_{psb_j} + f_{swb_j} + f_{barrierb_j} + f_{fwsb_j} + 0.8 \cdot f_{LLb_j}$ $\quad f_{IIIb}^T = (2.85 \;\; 0.873 \;\; 0.733) \cdot ksi$

$f_{allow\_ft} := -0.19 \cdot \sqrt{f'_c} \cdot \sqrt{ksi}$ $\quad f_{allow\_ft} = -0.503 \cdot ksi$ (LRFD 5.9.4.2.2b)

$Status\_ServiceLSft_j := if\left(f_{IIIb_j} \geq f_{allow\_ft}, "OK", "NG"\right)$ $\quad Status\_ServiceLSft^T = ("OK" \;\; "OK" \;\; "OK")$

Service I (Compressive Stresses in Top of Beam):

Compressive Stress Due to Permanent Loads:

$f_{idt_j} := f_{pst_j} + f_{swt_j} + f_{barriert_j} + f_{fwst_j}$ $f_{idt}^T = (0.1471 \quad 0.3946 \quad 0.437)\cdot ksi$

$f_{allow\_fcd} := 0.45\cdot f'_c$ $f_{allow\_fcd} = 3.15\cdot ksi$ (LRFD 5.9.4.2.1)

$Status\_ServiceLSfcd_j := if\left(f_{idt_j} \le f_{allow\_fcd}, "OK", "NG"\right)$ $Status\_ServiceLSfcd^T = ("OK" \quad "OK" \quad "OK")$

Compressive Stress Due to Full Dead Load + Live Load:

$f_{llt_j} := f_{pst_j} + f_{swt_j} + f_{barriert_j} + f_{fwst_j} + f_{LLt_j}$ $f_{llt}^T = (0.4647 \quad 2.5496 \quad 2.6587)\cdot ksi$

$f_{allow\_fcl} := 0.6\cdot f'_c$ $f_{allow\_fcl} = 4.2\cdot ksi$ (LRFD 5.9.4.2.1)

$Status\_ServiceLSfcl_j := if\left(f_{llt_j} \le f_{allow\_fcl}, "OK", "NG"\right)$ $Status\_ServiceLSfcl^T = ("OK" \quad "OK" \quad "OK")$

11 Flexural Strength Check

$M_{u_j} := 1.25\cdot\left(M_{swf_j} + M_{barrier_j}\right) + 1.5\cdot M_{fws_j} + 1.75\cdot M_{LL_j}$ $M_u^T = (768 \quad 5287 \quad 5475)\cdot kip\cdot ft$

$\beta_1 := if\left[f'_c \le 4\cdot(ksi), 0.85, if\left[f'_c \ge 8\cdot(ksi), 0.65, 0.85 - \left[\frac{f'_c - 4\cdot(ksi)}{1\cdot(ksi)}\cdot 0.05\right]\right]\right]$ $\beta_1 = 0.7$ (LRFD 5.7.2.2)

Preliminary estimate of L_d: $L_d := \left(270.0\cdot ksi - \frac{2}{3}\cdot f_{pe}\right)\cdot d_b\cdot ksi^{-1}$ $L_d = 97.71\cdot in$ (LRFD Eq. 5.11.4.2-1)

$K_{ld} := if(h \le 24\cdot in, 1.0, 1.6)$ $K_{ld} = 1.6$

$df_j := if\left[dist_j < L_t, \frac{dist_j}{L_t}\cdot\frac{f_{pe}}{f_{pu}}, if\left[dist_j < K_{ld}\cdot L_d, \frac{f_{pe} + \left(\frac{dist_j - L_t}{K_{ld}\cdot L_d - L_t}\right)\cdot\left(f_{pu} - f_{pe}\right)}{f_{pu}}, 1.0\right]\right]$

$df^T = (0.6429 \quad 1 \quad 1)$ (fraction strands are developed)

$A_{ps_j} := No\_Strands\cdot df_j\cdot A_{strand}$ $A_{ps}^T = (4.4645 \quad 6.944 \quad 6.944)\cdot in^2$

$b := b_f$

$d_{p_j} := h - y_{cg\_f_j}$ $d_p^T = (37.55 \quad 48.87 \quad 48.87)\cdot in$

$k := 2\cdot\left(1.04 - \frac{f_{py}}{f_{pu}}\right)$ $k = 0.28$ (LRFD 5.7.3.1.1-2)

$h_f := t_f$

$c_j := \frac{A_{ps_j}\cdot f_{pu}}{0.85\cdot f'_c\cdot\beta_1\cdot b + k\cdot A_{ps_j}\cdot\frac{f_{pu}}{d_{p_j}}}$ $c^T = (3.36 \quad 5.2 \quad 5.2)\cdot in$ (LRFD 5.7.3.1.1-4)

$t_f = 1.728 \times 10^9\ s$

$b_{w_j} := if(c_j \le t_{sg}, b, b_v)$ $\quad b_w^T = (84\ \ 84\ \ 84)\cdot in$

$$c_j := \frac{A_{ps_j}\cdot f_{pu} - 0.85\cdot f'_c\cdot\left(b - b_{w_j}\right)\cdot t_{sg}}{0.85\cdot f'_c\cdot\beta_1\cdot b_{w_j} + k\cdot A_{ps_j}\dfrac{f_{pu}}{d_{p_j}}}$$ $\quad c^T = (3.36\ \ 5.2\ \ 5.2)\cdot in$ (LRFD 5.7.3.1.1-3)

$$f_{ps_j} := f_{pu}\cdot\left(1 - k\frac{c_j}{d_{p_j}}\right)$$ $\quad f_{ps}^T = (263.2\ \ 262\ \ 262)\cdot ksi$ (LRFD 5.7.3.1.1-1)

$a_j := \beta_1\cdot c_j$ $\quad a^T = (2.3514\ \ 3.6395\ \ 3.6395)\cdot in$ (LRFD 5.11.4.1-1)

$$M_{n_j} := A_{ps_j}\cdot f_{ps_j}\cdot\left(d_{p_j} - \frac{a_j}{2}\right) + 0.85\cdot f'_c\cdot\left(b - b_{w_j}\right)\cdot t_{fg}\cdot\left(\frac{a_j}{2} - \frac{t_{fg}}{2}\right)$$ (LRFD 5.7.3.2.2-1)

$M_n^T = (3563\ \ 7133\ \ 7133)\cdot kip\cdot ft$

Compute phi for each section:

$$\phi_{f_j} := 0.583 + 0.25\cdot\left(\frac{d_{p_j}}{c_j} - 1\right)$$ $\quad \phi_f^T = (3.13\ \ 2.68\ \ 2.68)$ (LRFD Eq. 5.5.4.2.1-1)

$\phi_{f_j} := if\left(\phi_{f_j} \le 0.75, 0.75, if\left(\phi_{f_j} > 1.0, 1.0, \phi_{f_j}\right)\right)$ $\quad \phi_f^T = (1.00\ \ 1.00\ \ 1.00)$

$\phi M_{n_j} := \phi_{f_j}\cdot M_{n_j}$ $\quad M_{r_j} := \phi M_{n_j}$

$M_r^T = (3563\ \ 7133\ \ 7133)\cdot kip\cdot ft$ $\quad M_u^T = (768\ \ 5287\ \ 5475)\cdot kip\cdot ft$

$Status\_StrengthLS_j := if\left(M_{u_j} \le M_{r_j}, "OK", "NG"\right)$ $\quad Status\_StrengthLS^T = ("OK"\ \ "OK"\ \ "OK")$

Maximum Steel Check:

Note: The provisions contained in Art. 5.7.3.3.1 to check maximum reinforcement were deleted in 2005. This check is now effectively handled by varying phi, depending upon whether the section is compression or tension controlled. See Art. 5.5.4.2.1.

Minimum Steel Check:

Compute Cracking Moment at Midspan:

$f_r := -0.37\cdot\sqrt{f'_c}\cdot\sqrt{ksi}$ $\quad f_r = -0.979\cdot ksi$ $\quad f_{IIIb_3} = 0.733\cdot ksi$

$\Delta f := f_{IIIb_3} - f_r$ $\quad \Delta f = 1.712\cdot ksi$

$\Delta M := \Delta f\cdot S_b$ $\quad \Delta M = 1405.9\cdot kip\cdot ft$

$M_{cr} := M_{swf_3} + M_{barrier_3} + M_{fws_3} + 0.8\,M_{LL_3} + \Delta M$ $\quad M_{cr} = 4650.1\cdot kip\cdot ft$

$1.2\cdot M_{cr} = 5580.1\cdot kip\cdot ft$ $\quad$ Ref: $M_{r_3} = 7132.9\cdot kip\cdot ft$ (LRFD 5.7.3.3.2)

$Status\_MinStl := if\left(1.2\cdot M_{cr} < M_{r_3}, "OK", "NG"\right)$ $\quad Status\_MinStl = "OK"$

12 Vertical Shear Design

At each section the following must be satisfied for shear:

$V_u \le V_r$ (LRFD 5.8.2.1-2)

Note: Evaluation has been disabled for these three equations (as indicated by the small boxes) to enable them to be shown without first evaluating their parameters.

$V_r := \phi V_n$

$V_n := V_c + V_s + V_p$ (LRFD 5.8.3.3-1)

Critical Section for Shear: (LRFD 5.8.3.2)

The critical section for shear near a support in which the reaction force produces compression in the end of the member is, from the face of support (Fig. 2), the greater of:

a. $0.5 d_v \cot(\theta)$, or

b. d_v

where,

d_v = Effective shear depth = Distance between resultants of tensile and compressive forces = d_e - a/2

Compute A_{ps} & d_p

Note that A_{ps} in the equation used to compute ε_x is the area of the prestressing steel on the flexural tension side only. It is not the total area of strands. The variable A_{ps_ex} is introduced below to handle this.

$No_{Aps\_ft}(Pat\_n, Pat\_h, hc\_2) :=$
- $j \leftarrow last(Pat\_n)$
- $N \leftarrow 0$
- while $Pat\_h_j \le \frac{hc\_2}{2}$
  - $N \leftarrow N + Pat\_n_j$
  - $j \leftarrow j - 1$
  - break if $j = 0$
- N

$N_{Aps\_ft} := No_{Aps\_ft}(EPat\_n, EPat\_h, h)$ $N_{Aps\_ft} = 22$

$CG_{Aps\_ft}(Pat\_n, Pat\_h, hc\_2) :=$
- $j \leftarrow last(Pat\_n)$
- $N \leftarrow 0$
- $N\_cg \leftarrow 0$
- while $Pat\_h_j \le \frac{hc\_2}{2}$
  - $N \leftarrow N + Pat\_n_j$
  - $N\_cg \leftarrow N\_cg + Pat\_n_j \cdot Pat\_h_j$
  - $j \leftarrow j - 1$
  - break if $j = 0$
- $\frac{N\_cg}{N}$

$CG_{Aps\_ft} := CG_{Aps\_ft}(EPat\_n, EPat\_h, h)$ $CG_{Aps\_ft} = 3.2727 \cdot in$

$d_{pv} := h - CG_{Aps\_ft}$ $d_{pv} = 49.7273\cdot in$

$A_{ps\_ex} := dt_1 \cdot N_{Aps\_ft} \cdot A_{strand}$ $A_{ps\_ex} = 4.774\cdot in^2$ $dt_1 = 1$

Compute "a" based on Aps on Flexural-Tension Side:

$A_{ps\_a} := df_1 \cdot N_{Aps\_ft} \cdot A_{strand}$ $A_{ps\_a} = 3.069\cdot in^2$ $df_1 = 0.6429$

$$c_v := \frac{A_{ps\_a}\cdot f_{ps_1}}{0.85\cdot f'_c\cdot \beta_1\cdot b + k\cdot A_{ps\_a}\cdot \frac{f_{ps_1}}{d_{pv}}} \qquad c_v = 2.28\cdot in$$

$b_{wv} := if\left(c_v \le t_{flg}, b, b_v\right)$ $b_{wv} = 84\cdot in$

$$c_v := \frac{A_{ps\_a}\cdot f_{ps_1} - 0.85\cdot f'_c\cdot\left(b - b_{wv}\right)\cdot t_{flg}}{0.85\cdot f'_c\cdot \beta_1\cdot b_{wv} + k\cdot A_{ps\_a}\cdot \frac{f_{ps_1}}{d_{pv}}} \qquad c_v = 2.28\cdot in$$

$a_v := \beta_1 \cdot c_v$ $a_v = 1.5958\cdot in$

$$M_{nv} := A_{ps\_a}\cdot f_{ps_1}\cdot\left(d_{pv} - \frac{a_v}{2}\right) + 0.85\cdot f'_c\cdot\left(b - b_{wv}\right)\cdot t_{flg}\cdot\left(\frac{a_v}{2} - \frac{t_{flg}}{2}\right)$$

$M_{nv} = 3294\cdot kip\cdot ft$

Compute d_v:

$$d_v := \frac{M_{nv}}{A_{ps\_a}\cdot f_{ps_1}} \qquad d_v = 48.929\cdot in$$ (LRFD C5.8.2.9-1)

But d_v need not be taken less than the greater of $0.9d_e$ and 0.72h. Thus,

$0.9\cdot d_{p_1} = 33.797\cdot in$ $0.72\cdot h = 38.16\cdot in$

$Min\_d_v := if\left(0.9\cdot d_{p_1} \ge 0.72\cdot h, 0.9\cdot d_{p_1}, 0.72\cdot h\right)$ $Min\_d_v = 38.16\cdot in$

$d_v := if\left(d_v < Min\_d_v, Min\_d_v, d_v\right)$ $d_v = 48.929\cdot in$

To compute critical section, assume: $\theta := 30\cdot deg$

$0.5\cdot d_v\cdot \cot(\theta) = 42.3741\cdot in$

$Crit\_sec := if\left(d_v > 0.5\cdot d_v\cdot \cot(\theta), d_v, 0.5\cdot d_v\cdot \cot(\theta)\right)$ (LRFD 5.8.2.7)

$Crit\_sec = 48.93\cdot in$ $Crit\_sec = 4.077\,ft$

Assuming that the distance from the face of support to the centerline of bearing is half the bearing pad length, the critical section for shear is:

$$x_{f_1} := Crit\_sec + \frac{L_{pad}}{2} \qquad x_{f_1} = 4.577\,ft$$ (Note: Compare this to previous assumption)

At the critical section, the factored shear is:

$V_u := 1.25\cdot\left(V_{swf_1} + V_{barrier_1}\right) + 1.5\cdot V_{fws_1} + 1.75\cdot V_{LL_1}$

$V_u = 239.3\cdot kip$

Compute the vertical component of the prestressing force, V_p:

$P_{f_1} = 1116.1 \cdot kip$ (Note: This approach uses the total P/S force.)

$\alpha := \operatorname{atan}\left(\frac{y_{end} - y_{mid}}{x_{f_2}}\right)$ $\alpha = 1.4528 \cdot deg$

$V_p := P_{f_1} \cdot \sin(\alpha)$ $V_p = 28.3 \cdot kip$

Compute maximum permissible shear capacity at a section:

$V_{n\_max} := 0.25 \cdot f'_c \cdot b_v \cdot d_v + V_p$ $V_{n\_max} = 542.1 \cdot kip$ (LRFD 5.8.3.3-2)

$Status\_V_{nmax} := if(V_u \le V_{n\_max}, "OK", "NG")$ $Status\_V_{nmax} = "OK"$

The shear contribution from the concrete, V_c, is given by:

$V_c := 0.0316 \cdot \beta \cdot \sqrt{f'_c} b_v \cdot d_v$

Note: Evaluation has been disabled for this equations to enable it to be shown without first evaluating its parameters.

$\beta := \frac{4.8}{1 + 750 \cdot \varepsilon_s}$ (LRFD 5.8.3.4.2-1)

$\theta := 29 + 3500 \cdot \varepsilon_s$ (LRFD 5.8.3.4.2-3)

$$\varepsilon_x := \frac{\frac{M_{u_1}}{d_v} + 0.5 \cdot (V_u - V_p) \cdot \cot(\theta) - A_{ps\_ex} \cdot f_{po}}{E_c \cdot A_c + E_p \cdot A_{ps\_ex}}$$ (LRFD 5.8.3.4.2-4)

$M_{u_1} = 768.01 \cdot kip \cdot ft$

Compute f_{po}:

This can be taken as $0.70 f_{pu}$:

$f_{po} := 0.75 \cdot f_{pu}$ $f_{po} = 202.5 \cdot ksi$

(LRFD 5.8.3.4.2)

$E_c := 33000 \cdot w_c^{1.5} \cdot kcf^{-1.5} \cdot \sqrt{f'_c} \cdot ksi^{.5}$ $E_c = 4921 \cdot ksi$

$$\varepsilon_x := \frac{\frac{M_{u_1}}{d_v} + 0.5 \cdot (V_u - V_p) \cdot \cot(\theta) - A_{ps\_ex} \cdot f_{po}}{E_c \cdot A_c + E_p \cdot A_{ps\_ex}}$$ $\varepsilon_x = -0.000253$

$\beta := \frac{4.8}{1 + 750 \cdot \varepsilon_x}$ $\beta = 5.9264$

$V_c := 0.0316 \cdot \beta \cdot \sqrt{f'_c} b_v \cdot d_v$

Compute V_c:

$V_c := 0.0316 \cdot \beta \cdot \sqrt{f'_c} \sqrt{ksi} \cdot b_v \cdot d_v$ $V_c = 145.5 \cdot kip$

Required V_s is, therefore:

$V_s := \frac{V_u}{\phi_v} - V_c - V_p$ $V_s = 92.1 \cdot kip$

Assuming two vertical legs of No. #4 bars:

$$A_v := \frac{V_s}{f_y \cdot d_v \cdot \cot(\theta)} \qquad A_v = 0.217 \cdot \frac{in^2}{ft} \qquad \text{(LRFD C5.8.3.3-1)}$$

$$Spac := \frac{2 \cdot 0.2 \cdot in^2}{A_v} \qquad Spac = 22.1 \cdot in \qquad \text{(stirrup spacing)}$$

Check minimum transverse reinforcement:

$$A_{v\_min} := 0.0316 \cdot \sqrt{f'_c} \cdot \sqrt{ksi} \cdot \frac{b_v}{f_y} \qquad A_{v\_min} = 0.1 \cdot \frac{in^2}{ft} \qquad \text{(LRFD 5.8.2.5-1)}$$

Check maximum stirrup spacing:

$$V_{spc} := 0.1 \cdot f'_c \cdot b_v \cdot d_v \qquad V_{spc} = 205.5 \cdot kip \qquad \text{(LRFD 5.8.2.7-2)}$$

Ref: $V_u = 239.3 \cdot kip$ $\quad d_v = 48.93 \cdot in$

$$Max\_spac := if\left(V_u < V_{spc}, if\left(0.8 \cdot d_v < 24 \cdot in, 0.8 \cdot d_v, 24 \cdot in\right), if\left(0.4 \cdot d_v < 12 \cdot in, 0.4 \cdot d_v, 12 \cdot in\right)\right)$$

$Max\_spac = 12 \cdot in$

1.13 Longitudinal Reinforcement Check

LRFD requires that the longitudinal steel be checked at all locations along the girder. This requirement is made to ensure that the longitudinal reinforcement is sufficient to develop the required tension tie, which is required for equilibrium. Equation 5.8.3.5-1 is the general equation, applicable at all sections. However, for the special case of the inside edge of bearing at simple-end supports, the longitudinal reinforcement must be able to resist a tensile force of $(V_u/\phi - 0.5V_s - V_p)\cot(\theta)$. Note that when pretensioned strands are used to develop this force, only a portion of the full prestress force may be available near the support due to partial transfer. Additionally, only those strands on the flexural tension side of the member contribute to the tension tie force.

Required Tension Tie Force:

If only the minimum amount of transverse reinforcement that is required by design is provided, the required tension tie force is:

$$F_{L\_reqd} := \left(\frac{V_u}{\phi_v} - 0.5 \cdot V_s - V_p\right) \cdot \cot(\theta) \qquad F_{L\_reqd} = 331.7 \cdot kip \qquad \text{Eq. 5.8.3.5-2}$$

However, a greater amount of stirrup reinforcement is typically provided than is required, which increases the actual V_s. Note that by Eq. 5.8.3.5-2, increasing V_s decreases the required tension tie force. Hence, it is helpful to use the computed of V_s that results from the actual transverse reinforcement detailed in the design. In this case, the required tension tie force is:

Assume 2 legs of No. 4 bars at 12" on center (amount of steel at the critical section for shear):

$$A_{v\_actual} := 0.4 \cdot in^2$$

$$V_{s\_actual} := \frac{A_{v\_actual} \cdot f_y \cdot d_v \cdot \cot(\theta)}{12 \cdot in} \qquad V_{s\_actual} = 169.5 \cdot kip$$

Check the upper limit of V_s:

$$V_{s\_actual\_max} := \frac{V_u}{\phi_v} \qquad V_{s\_actual\_max} = 265.9 \cdot kip \qquad \text{LRFD 5.8.3.5}$$

Adopt the lesser of provided V_s and the upper limit of V_s:

$V_{s\_actual} := \text{if}(V_{s\_actual} < V_{s\_actual\_max}, V_{s\_actual}, V_{s\_actual\_max})$

$V_{s\_actual} = 169.5 \cdot \text{kip}$

The revised value of the required tension tie force is:

$$F_{L\_reqd} := \left[\left(\frac{V_u}{\phi_v}\right) - 0.5 \cdot V_{s\_actual} - V_p\right] \cdot \cot(\theta) \qquad F_{L\_reqd} = 264.7 \cdot \text{kip}$$

Provided Tension Tie Force:

The longitudinal reinforcement that contributes to the tension tie are strands that are on the flexural tension side of the girder. Near the ends of the girder, the strands are typically only partially effective. C5.8.3.5 of the 2006 Interim Revisions permits the strand stress in regions of partial development to be estimated using a bilinear variation, as shown in Fig. 4.

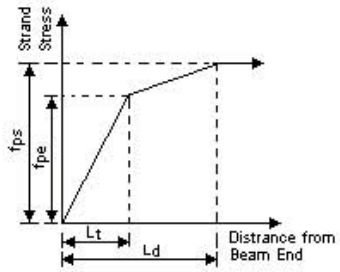

Figure 5: Variation in strand stress in relation to distance from girder end.

The stress in the strands at a given section depends on the location of the section with respect to the end of the girder. If the section is between the end of the girder and L_t (see Fig. 5), a linear interpolation is performed using a stress variation of 0.0 at the end of the girder to f_{pe} at a distance of L_t from the end of the girder. If the section is to the right of L_t but to the left of L_d, then the stress is interpolated between f_{pe} and f_{ps}. If the section is to the right of L_d, then the stress is assumed to be a constant value of f_{ps}.
At the face of bearing, the stress in the effective strands is:

$$x_{FB} := \frac{L_{ovr} - L_{des}}{2} + \frac{L_{pad}}{2} \qquad x_{FB} = 1.00\text{ft} \qquad \text{(Distance from physical end of girder to face of bearing)}$$

$$F_{L\_prov} := \text{if}\left[x_{FB} < L_t, N_{Aps\_ft} A_{strand} \cdot f_{pe} \cdot \frac{x_{FB}}{L_t}, \text{if}\left[x_{FB} < K_{ld} \cdot L_d, N_{Aps\_ft} A_{strand} \cdot \left[f_{pe} + \left(\frac{x_{FB} - K_{ld} \cdot L_d + L_t}{K_{ld} \cdot L_d - L_t}\right) \cdot (f_{ps} - f_{pe})\right], N_{Aps\_ft} A_{strand} \cdot f_{pe}\right]\right]$$

$F_{L\_prov} = 255.8 \cdot \text{kip}$

$\text{Status\_V}_l := \text{if}(F_{L\_prov} \geq F_{L\_reqd}, \text{"OK"}, \text{"NG"})$ $\qquad \text{Status\_V}_l = \text{"NG"}$

Refined Estimate of Provided Tension Tie Force:

If it is assumed that the point of intersection of the bearing crack (at angle theta) and c.g. of the strands is where the force in the strands is computed, then additional tensile capacity from the strands can be utilized.

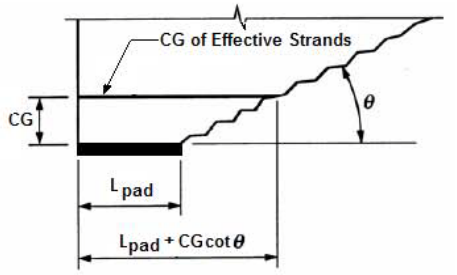

Figure 6: Elevation view of end of girder showing location where assumed failure crack crosses the c.g. of that portion of the strand pattern that is effective for resisting tensile forces caused by moment and shear.

Distance from bottom of girder to point of intersection of assumed crack and center of gravity of effective strands:

$$x_c := \left(\frac{L_{pad}}{2}\right) + CG_{Aps\_ft}\cdot\cot(\theta) \qquad x_c = 1\cdot ft \qquad \text{(Measured from L face of bearing)}$$

$$x_c := \left(\frac{L_{ovr} - L_{des}}{2}\right) + \left(\frac{L_{pad}}{2}\right) + CG_{Aps\_ft}\cdot\cot(\theta) \qquad x_c = 1.5\cdot ft \qquad \text{(Measured from L end of girder)}$$

$$F_{L\_prov} := \text{if}\left[x_c < L_t, N_{Aps\_ft}\cdot A_{strand}\cdot f_{pe}\cdot\frac{x_c}{L_t}, \text{if}\left[x_c < K_{ld}\cdot L_d, N_{Aps\_ft}\cdot A_{strand}\cdot\left[f_{pe} + \left(\frac{x_c - K_{ld}\cdot L_d + L_t}{K_{ld}\cdot L_d - L_t}\right)\cdot\left(f_{ps} - f_{pe}\right)\right], N_{Aps\_ft}\cdot A_{strand}\cdot f_{pe}\right]\right]$$

$F_{L\_prov} = 376.6\cdot kip$

1.14 Design Summary

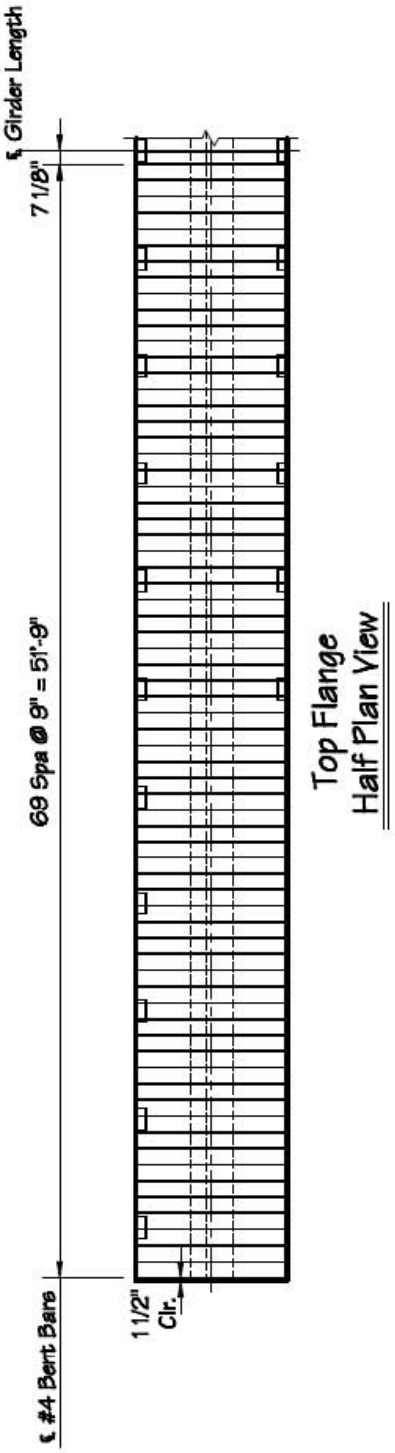

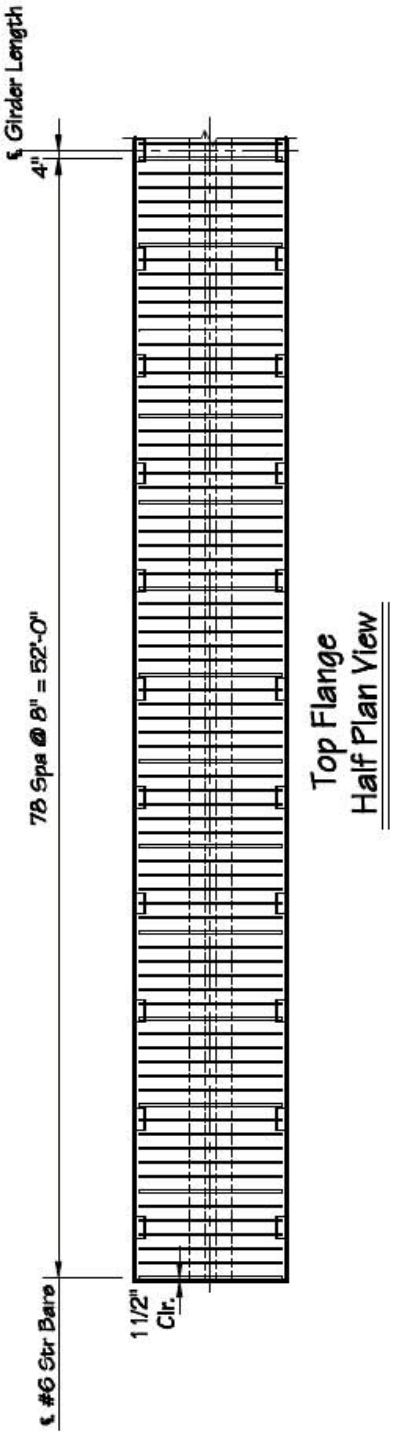

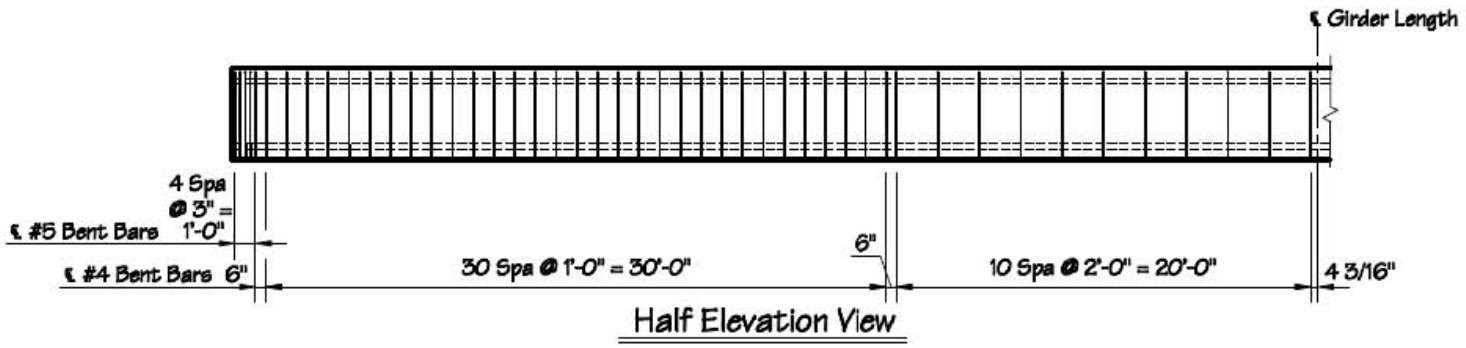

Half Elevation View

Bottom Flange
Half Plan View

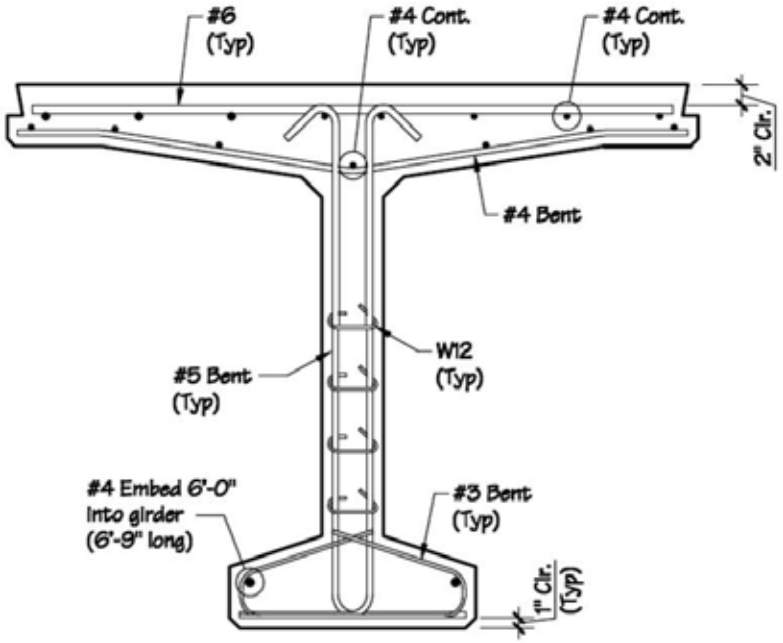

(Strand pattern not shown for clarity)

Typical Reinforcing
Section Near End

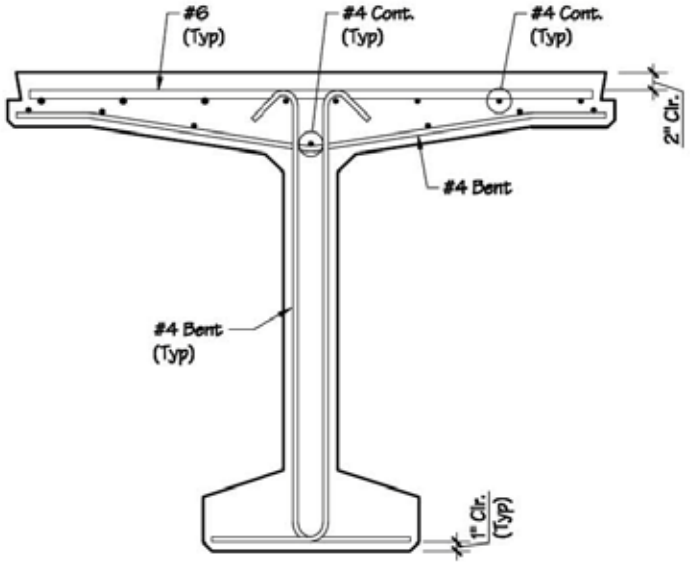

(Strand pattern not shown for clarity)

Typical Reinforcing
Section Near Mid

Prestress Losses per LRFD 3rd Edition

At Release:

At release, two components of prestress loss are significant: relaxation of the prestressing steel and elastic shortening. Elastic shortening is the loss of prestress that results when the strands are detensioned and the girder shortens in length due to the applied prestress. When the strands are tensioned in the prestress bed and anchored at the abutments, the steel gradually begins to relax as a function of time. By the time the strands are detensioned a small, but measurable, loss due to steel relaxation has occurred.

Steel Relaxation (short term):

$f_{pj} := Pull \cdot f_{pu}$ $\quad f_{pj} = 202.5 \cdot ksi$ $\quad f_{py} = 243 \cdot ksi$

$$\Delta f_{pR1} := \frac{\log\left(\frac{t}{hr}\right)}{40.0} \cdot \left(\frac{f_{pj}}{f_{py}} - 0.55\right) \cdot f_{pj} \qquad \Delta f_{pR1} = 4.783 \cdot ksi \qquad \text{(LRFD 5.9.5.4.4b-2)}$$

Elastic Shortening:

$$E_{ci} := 33000 \cdot w_c^{1.5} \cdot kcf^{-1.5} \cdot \sqrt{f'_{ci} \cdot ksi^{-1}} \cdot ksi \qquad E_{ci} = 4556 \cdot ksi \qquad \text{(LRFD 5.4.2.4-1)}$$

$A_{psm} := No\_Strands \cdot A_{strand}$ $\quad A_{psm} = 6.944 \cdot in^2$ (Area of strand at midspan)

$f_{pbt} := f_{pj} - \Delta f_{pR1}$ $\quad f_{pbt} = 197.7 \cdot ksi$

$e_m := y_b - y_{mid}$ $\quad e_m = 31.48 \cdot in$

$$\Delta f_{pES} := \frac{A_{psm} \cdot f_{pbt} \cdot \left(I + e_m^2 A\right) - e_m \cdot M_{swr_3} \cdot A}{A_{psm} \cdot \left(I + e_m^2 A\right) + \frac{A \cdot I \cdot E_{ci}}{E_p}} \qquad \Delta f_{pES} = 20.059 \cdot ksi$$

Total Prestress Loss at Release:

$\Delta f_{sr} := \Delta f_{pES} + \Delta f_{pR1}$ $\quad \Delta f_{sr} = 24.841 \cdot ksi$

$\%Loss := \frac{\Delta f_{sr}}{Pull \cdot f_{pu}} \cdot 100$ $\quad \%Loss = 12.2674$

$f_{per} := f_{pj} - \Delta f_{pES} - \Delta f_{pR1}$ $\quad f_{per} = 177.7 \cdot ksi$

$P_r := f_{per} \cdot No\_Strands \cdot A_{strand}$ $\quad P_r = 1233.7 \cdot kip$

At Final Conditions:

Elastic Shortening: Same as at release (see above)

Shrinkage:

$\Delta f_{pSH} := (17 - 0.150 \cdot H) \cdot ksi$ $\quad \Delta f_{pSH} = 6.5 \cdot ksi$ $\quad$ (LRFD 5.9.5.4.2-1)

Creep:

$S_{cgp} := \frac{I}{y_b - y_{cg\_f_3}}$ $\quad S_{cgp} = 11147.1 \cdot in^3$

$f_i := f_{pj} - \Delta f_{pR1} - \Delta f_{pES}$ $\quad f_i = 177.659 \cdot ksi$

$P_i := A_{psm} \cdot f_i$ $\quad P_i = 1234 \cdot kip$

$f_{cgp} := P_i \cdot \left(\frac{1}{A} + \frac{ecc\_f_3}{S_{cgp}} \right) - \frac{M_{swr_3}}{S_{cgp}}$ $f_{cgp} = 3.206 \cdot ksi$

$S_{c\_cg} := \frac{I}{y_b - y_{cg\_f_3}}$ $S_{c\_cg} = 11147 \cdot in^3$

$\Delta f_{cdp} := \frac{M_{barrier_3} + M_{fws_3}}{S_{cgp}}$ $\Delta f_{cdp} = 0.437 \cdot ksi$

$\Delta f_{pCR} := 12.0 \cdot f_{cgp} - 7.0 \cdot \Delta f_{cdp}$ $\Delta f_{pCR} = 35.421 \cdot ksi$ (LRFD 5.9.5.4.3-1)

Steel Relaxation (low-relaxation strands):

$\Delta f_{pR2} := 6 \cdot ksi - 0.12 \cdot \Delta f_{pES} - 0.06 \cdot (\Delta f_{pSH} + \Delta f_{pCR})$ $\Delta f_{pR2} = 1.078 \cdot ksi$ (LRFD 5.9.5.4.4c-1)

Total Prestress Loss:

$\Delta f_{pT} := \Delta f_{pES} + \Delta f_{pSH} + \Delta f_{pCR} + \Delta f_{pR2}$ $\Delta f_{pT} = 63.057 \cdot ksi$

$\%Loss := \frac{\Delta f_{pT}}{Pull \cdot f_{pu}} \cdot 100$ $\%Loss = 31.1392$

Check effective stress after losses:

$f_{pe} := Pull \cdot f_{pu} - \Delta f_{pT}$ $f_{pe} = 139.4 \cdot ksi$

$f_{allow} := 0.80 \cdot f_{py}$ $f_{allow} = 194.4 \cdot ksi$ (LRFD 5.9.3-1)

Stresses Due to Prestress (with LRFD 3rd Edition Losses)

At Release Conditions:

$j := 1 .. 3$

$f_{psrb_j} := P_r \cdot \left(\frac{1}{A} + \frac{ecc\_r_j}{S_b} \right)$ $f_{psrb}^T = (3.686 \quad 5.176 \quad 5.176) \cdot ksi$

$f_{psrt_j} := P_r \cdot \left(\frac{1}{A} - \frac{ecc\_r_j}{S_t} \right)$ $f_{psrt}^T = (0.038 \quad -0.69 \quad -0.69) \cdot ksi$

At Final Conditions:

$dist_j := x_{f_j} + \frac{L_{ovr} - L_{des}}{2}$ $dist^T = (5.0774 \quad 42.1 \quad 52.5)\ ft$

$L_t := 60 \cdot d_b$ $L_t = 36 \cdot in$

$dt_j := if\left(dist_j > L_t, 1.0, \frac{dist_j}{L_t} \right)$ $dt^T = (1 \quad 1 \quad 1)$ (Fraction strands are transferred.)

$j := 1 .. 3$

$P_{f_j} := f_{pe} \cdot dt_j \cdot No\_Strands \cdot A_{strand}$ $P_f^T = (968.3 \quad 968.3 \quad 968.3) \cdot kip$

$f_{psb_j} := P_{f_j} \cdot \left(\frac{1}{A} + \frac{ecc\_f_j}{S_b} \right)$ $f_{psb} = \begin{pmatrix} 2.95 \\ 4.063 \\ 4.063 \end{pmatrix} \cdot ksi$ $f_{pst_j} := P_{f_j} \cdot \left(\frac{1}{A} - \frac{ecc\_f_j}{S_t} \right)$ $f_{pst} = \begin{pmatrix} 0.002 \\ -0.541 \\ -0.541 \end{pmatrix} \cdot ksi$

Service Stress Check (with LRFD 3rd Edition Losses)

At Release Conditions:

Top of girder (tension):

$f_{rt_j} := f_{psrt_j} + f_{swrt_j}$ $\quad f_{rt}^{T} = (0.13 \;\; 0.113 \;\; 0.146)\cdot ksi$

$f_{allow\_rt} := -0.0948\cdot\sqrt{f'_{ci}}\cdot\sqrt{ksi}$ $\quad f_{allow\_rt} = -0.232\cdot ksi$

$Status\_ServiceLSrt_j := if\left(f_{rt_j} \geq f_{allow\_rt}, "OK", "NG"\right)$ $\quad Status\_ServiceLSrt^{T} = ("OK" \;\; "OK" \;\; "OK")$

Bottom of girder (compression):

$f_{rb_j} := f_{psrb_j} + f_{swrb_j}$ $\quad f_{rb}^{T} = (3.496 \;\; 3.532 \;\; 3.465)\cdot ksi$

$f_{allow\_rc} := 0.6\cdot f'_{ci}$ $\quad f_{allow\_rc} = 3.6\cdot ksi$

$Status\_ServiceLSrc_j := if\left(f_{rt_j} \leq f_{allow\_rc}, "OK", "NG"\right)$ $\quad Status\_ServiceLSrc^{T} = ("OK" \;\; "OK" \;\; "OK")$

At Final Conditions:

Check Service Limit States:

Service III Limit State (Tensile Stresses in Bottom of Beam):

$f_{IIIb_j} := f_{psb_j} + f_{swb_j} + f_{barrierb_j} + f_{fwsb_j} + 0.8\cdot f_{LLb_j}$ $\quad f_{IIIb}^{T} = (2.399 \;\; 0.253 \;\; 0.113)\cdot ksi$

$f_{allow\_ft} := -0.0\cdot\sqrt{f'_c}\cdot\sqrt{ksi}$ $\quad f_{allow\_ft} = 0\cdot ksi$ (LRFD 5.9.4.2.2b)

$Status\_ServiceLSft_j := if\left(f_{IIIb_j} \geq f_{allow\_ft}, "OK", "NG"\right)$ $\quad Status\_ServiceLSft^{T} = ("OK" \;\; "OK" \;\; "OK")$

Service I (Compressive Stresses in Top of Beam):

Compressive Stress Due to Permanent Loads:

$f_{Idt_j} := f_{pst_j} + f_{swt_j} + f_{barriert_j} + f_{fwst_j}$ $\quad f_{Idt}^{T} = (0.1468 \;\; 0.4772 \;\; 0.5197)\cdot ksi$

$f_{allow\_fcd} := 0.45\cdot f'_c$ $\quad f_{allow\_fcd} = 3.15\cdot ksi$ (LRFD 5.9.4.2.1)

$Status\_ServiceLSfcd_j := if\left(f_{Idt_j} \leq f_{allow\_fcd}, "OK", "NG"\right)$ $\quad Status\_ServiceLSfcd^{T} = ("OK" \;\; "OK" \;\; "OK")$

Compressive Stress Due to Full Dead Load + Live Load:

$f_{It_j} := f_{pst_j} + f_{swt_j} + f_{barriert_j} + f_{fwst_j} + f_{LLt_j}$ $\quad f_{It}^{T} = (0.4644 \;\; 2.6323 \;\; 2.7414)\cdot ksi$

$f_{allow\_fcl} := 0.6\cdot f'_c$ $\quad f_{allow\_fcl} = 4.2\cdot ksi$ (LRFD 5.9.4.2.1)

$Status\_ServiceLSfcl_j := if\left(f_{It_j} \leq f_{allow\_fcl}, "OK", "NG"\right)$ $\quad Status\_ServiceLSfcl^{T} = ("OK" \;\; "OK" \;\; "OK")$

APPENDIX B

DESIGN EXAMPLE FOR CAMBER LEVELING CLAMP

- Assume average camber leveling shear = 1.5 kip/ft
- Assume girders are clamped every 5 ft
- Leveling shear force transferred per clamp (V) = (5)(1.5) = 7.5 kip
- Proposed clamp geometry is shown in Figure 1
- Idealization of the force transfer is shown in Figure 2
- From equilibrium

$$P_1 - P_2 = V$$

$$P_1 - P_2 = 7.5$$

$$P_1(7) = P_2(13)$$

$$P_1 = 1.857P_2$$

$$1.857P_2 - P_2 = 7.5$$

$$P_2 = \frac{7.5}{0.857} = 8.75 \quad \text{kips}$$

$$P_1 = 7.5 + 8.75 = 16.25 \quad \text{kips}$$

$$T = P_1 + P_2$$

$$T = 16.25 + 8.75 = 25 \quad \text{kips}$$

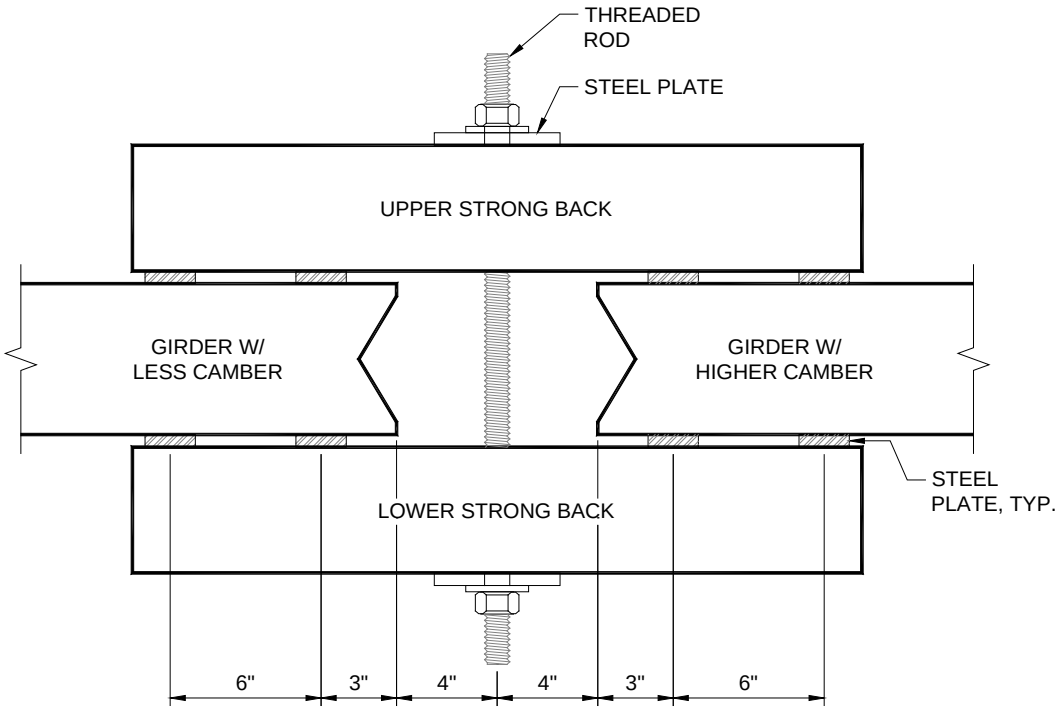

FIGURE 1

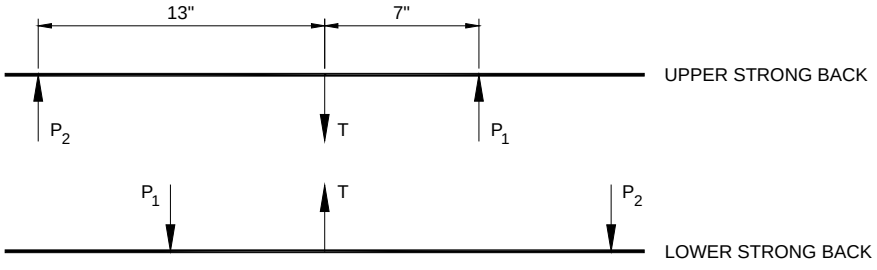

FIGURE 2

Design of strong back

- The reactions and internal forces diagrams for the upper strong back are shown in Figure 3.

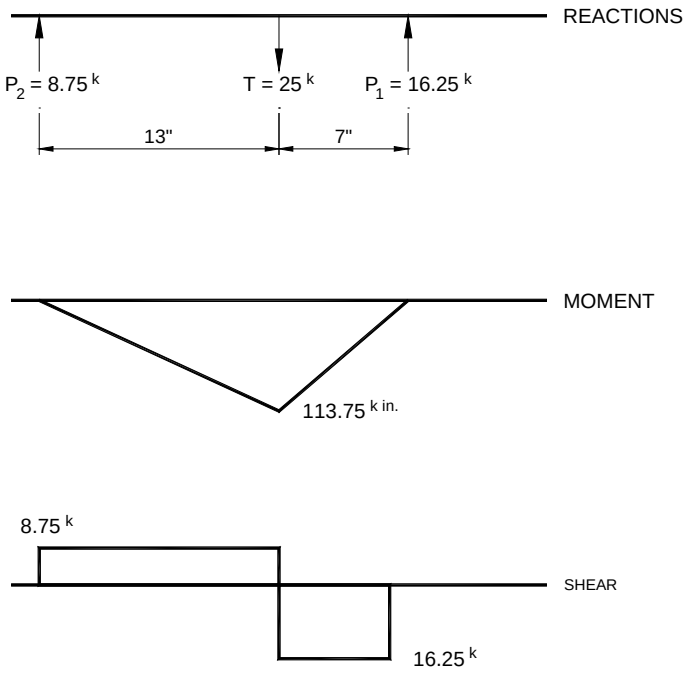

FIGURE 3

- Use a load factor of 1.6 for the design of the steel components of the temporary clamp.

$M_u = (113.75)(1.6) = 182$ kip-in

$V_u = (16.25)(1.6) = 26$ kips

- Use 2C5x9

$\phi V_n = \phi_v (0.6) F_y A_w$

$\phi V_n = 2(0.9)(0.6)(36)(5)(0.325)$

$\phi V_n = 63.18$ kips > V_u (Ok)

$Z = 4.36$ in^3 per channel

$M_p = (4.36)(36) = 156.96$ kip-in per channel

$r_y = 0.489$ in.

$$L_p = \frac{300 r_y}{\sqrt{F_{yf}}}$$

$$L_p = \frac{300(0.489)}{\sqrt{36}} = 24.45 \text{ in.}$$

$L_b = (2)(13) = 26$ in. $\cong L_p$

$\phi M_n = 0.9 M_p$

$\phi M_n = 0.9(2)(156.96) = 282.5$ kip-in > M_u (Ok)

- Check web crippling and local yielding

$T_u = 1.6(25) = 40$ kips

Using LRFD Tables

$\phi R = 2(60) = 120$ kips > T_u (no stiffeners are required)

Threaded rod design

- Use A193, grade B7 all thread rod, 1 in. diameter

$\phi R_n = 0.75(0.75 F_u) A_g$

$\phi R_n = 0.75\big((0.75)(120)\big)(0.7854) = 53.0$ kips > T_u (Ok)

Bearing plate design

- Figure 4 shows a cross section of the strong back.
- Assume reaction is at the center point of the web and plate is acting as simply supported beam.

$$M_u = \frac{40(1.5+0.325)}{4} = 18.25 \qquad \text{kip-in}$$

- Use 5in. x 5in. x 1in. plate

$$Z = \frac{bt^2}{4}$$

$$b = 5-(1+0.125) = 3.875$$

$$Z = \frac{(3.875)(1)^2}{4} = 0.969 \qquad \text{in}^3$$

$$\phi M_n = 0.9(0.969)(36) = 31.39 \qquad \text{kip-in} \quad > M_u \quad \text{(Ok)}$$

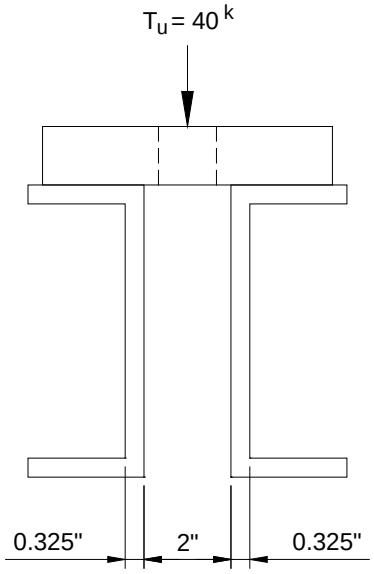

FIGURE 4

Check bearing on concrete

- Load factor for construction loads is 1.5 per LRFD Article 3.4.2.
- Assume support plate is 2in.×5in.

$P_u = 1.5(16.25) = 24.375$ kips

$P_n = 0.85 f_c' A_1 m$ LRFD Eq. (5.7.5-2)

$A_1 = 2(5) = 10$ in^2 (see Figure 5)

$A_2 = (2+4)(5+4) = 54$ in^2 (see Figure 5)

$m = \sqrt{\frac{A_1}{A_2}} \le 2$ LRFD Eq. (5.7.5-3)

$\sqrt{\frac{A_1}{A_2}} = \sqrt{\frac{54}{10}} = 2.33$ > 2

Use $m = 2$

$f_c' = 7$ ksi

$P_n = 0.85(7)(10)(2) = 119$ kips

$P_r = \phi P_n$ LRFD Eq. (5.7.5-1)

$P_r = 0.7(119) = 83.3$ kips > P_u (Ok)

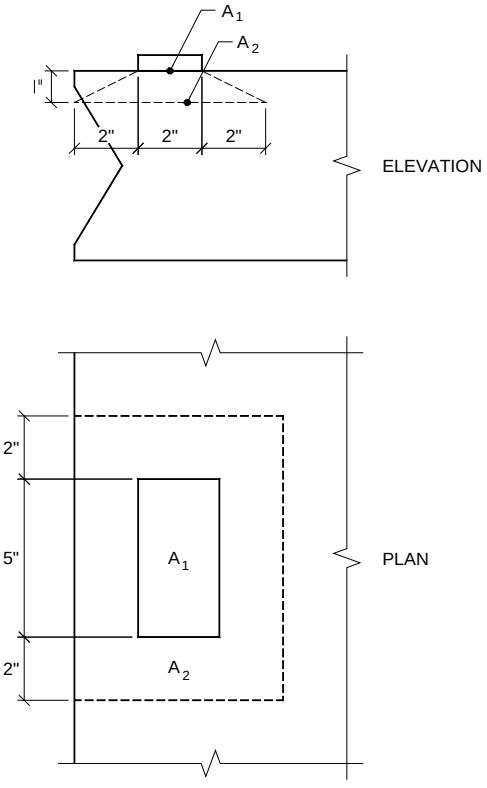

FIGURE 5

Check punching shear

$$V_n = \left(0.063 + \frac{0.126}{\beta_c}\right)\sqrt{f_c'}\,b_o d_v \le 0.126\sqrt{f_c'}\,b_o d_v \qquad \text{LRFD Eq. (5.13.3.6.3-1)}$$

With no. 4 rebars and 1 in. clear cover on the bottom

$$d_v = 6 - 1 - \frac{0.5}{2} = 4.75 \text{ in.}$$

$$b_o = 9.75 + 2(6.375) = 22.5 \quad \text{in. (see Figure 6)}$$

$$\beta_c = \frac{5}{2} = 2.5$$

$$\left(0.063 + \frac{0.126}{\beta_c}\right) = 0.063 + \frac{0.126}{2.5} = 0.113 < 0.126$$

$$V_n = 0.113\sqrt{f_c'}\,b_o d_v = 0.113\sqrt{7}(22.5)(4.75) = 31.95 \text{ kips}$$

$$\phi V_n = 0.9(31.95) = 28.8 \quad \text{kips} \quad > P_u \quad \text{(Ok)}$$

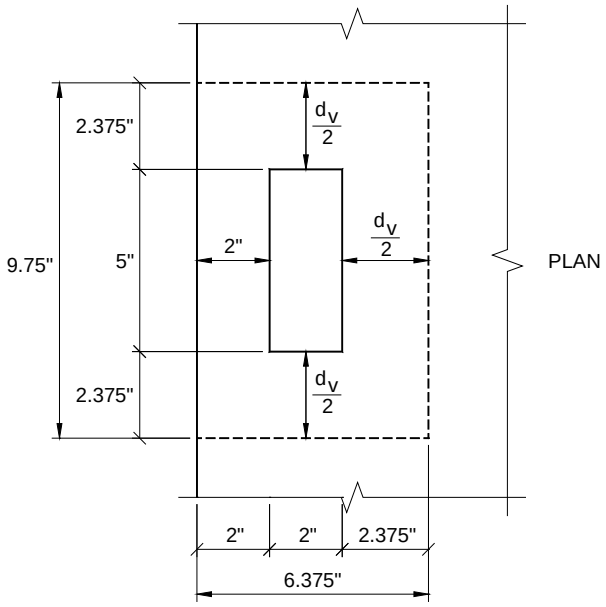

FIGURE 6

Check top flange transverse flexure

- Typical top flange reinforcement is #5 at 4 in. spacing for top reinforcement and #4 at 6 in. spacing for bottom reinforcement.
- Top cover is 2.5 in. and bottom cover is 1 in.

For negative bending of top flange

$$d = 6 - 2.5 - \frac{0.625}{2} = 3.19 \quad \text{in.}$$

$$A_s = 0.31\left(\frac{12}{4}\right) = 0.93 \ \text{in}^2/\text{ft}$$

$$a = \frac{(0.93)(60)}{0.85(7)(12)} = 0.78 \quad \text{in.}$$

$$\phi M_n = 0.9(0.93)(60)\left(3.19 - \frac{0.78}{2}\right)\Big/12 = 11.72 \quad \text{kip-ft/ft}$$

For positive bending of top flange

$$d = 6 - 1 - \frac{0.5}{2} = 4.75 \ \text{in.}$$

$$A_s = 0.2\left(\frac{12}{6}\right) = 0.4 \quad \text{in}^2/\text{ft}$$

$$a = \frac{(0.4)(60)}{0.85(7)(12)} = 0.34 \quad \text{in.}$$

$$\phi M_n = 0.9(0.4)(60)\left(4.75 - \frac{0.34}{2}\right)\Big/12 = 8.24 \ \text{kip-ft/ft}$$

- Figure 7 shows the leveling forces and the dimensions for 8 ft girder spacing.
- It should be noted that the forces will be reversed on the top flange of the opposite girder.
- Assuming the top flange is acting as an overhang, the width of the design strip is $45.0 + 10.0X$ per LRFD Table (4.6.2.1.3-1)

$$M_{L1} = \pm\frac{16.25(6)}{45+10(6/12)} = \pm 1.95 \qquad \text{kip-ft/ft}$$

$$M_{L2} = \pm\frac{16.25(41)-8.75(35)}{45+10(35/12)} = \pm 4.85 \qquad \text{kip-ft/ft}$$

Section 2 is more critical

$$w_d = 0.15\left(\frac{6}{12}\right) = 0.075 \qquad \text{kip/ft/ft}$$

$$M_{D2} = -\frac{0.075(41/12)^2}{2} = -0.44 \qquad \text{kip-ft/ft}$$

$M_{u2-ve} = 1.25(-0.44)+1.5(-4.85) = -7.83$ kip-ft/ft $< \phi M_n$ (Ok)

$M_{u2+ve} = 1.25(-0.44)+1.5(4.85) = 6.73$ kip-ft/ft $< \phi M_n$ (Ok)

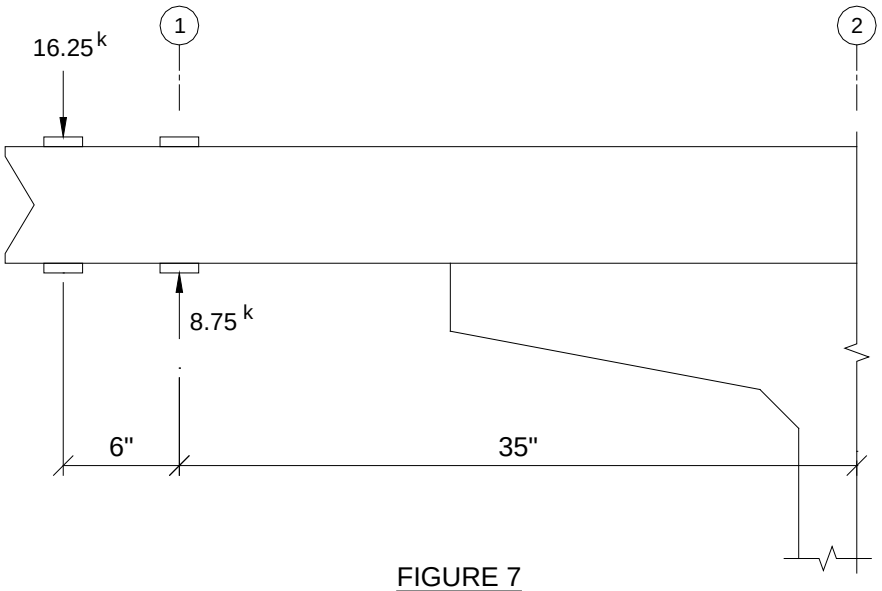

FIGURE 7

APPENDIX C

SUBTASK 6.3-C – DESIGN EXAMPLES FOR FUTURE RE-DECKING

Introduction

The objective of Subtask 6.3-C was to demonstrate the design of the interface between deck and girder considering the option of future deck replacement. The interface was designed using the detail discussed in Subtask 6.1-A Full Depth Deck Replacement, which incorporates a debonded joint between the deck and the girder to facilitate deck removal and shear keys with reinforcement for horizontal shear transfer across the interface. The design horizontal shear was based the maximum horizontal shear anticipated for this type of bridge girder as obtained from the parametric studies in Subtask 6.1-B Optimized Girder Study. Two examples are presented. The first considers the optimized section developed in Subtask 6.1-B and the second considers a typical AASHTO type section. These designs demonstrate the maximum reinforcement and shear key geometry required for selected connection details.

Interface Design for Optimized Section

The parametric study conducted on the optimized girder section indicated that the maximum factored horizontal shear stress across the interface between the sub-flange and the upper flange is 186 psi. The purpose of this example is to demonstrate the design of the horizontal shear key under the highest possible interface shear for all feasible bridge configurations using the optimized section. Dimensions of the shear key are shown in Figure C-1. The following steps summarize the design process.

General data:

CIP deck concrete strength	$f'_c = 6000$	psi
Steel yield stress	$f_y = 60$	ksi
ϕ for shear	$\phi_v = 0.9$	
ϕ for bearing	$\phi_b = 0.7$	
Top flange width	$b_v = 42$	in.
Shear key thickness	$t_{sk} = 0.75$	in.

Shear key spacing $s_{sk} = 12$ in.

Factored shear stress $v_{uh} = 186$ psi

Check bearing strength on shear key:

Shear key width $b_{sk} = b_v - 2(2)$

$= 42 - 2(2) = 38$ in.

Bearing strength $v_{nhb} = \dfrac{\phi_b (0.85) f_c' t_{sk} (b_{sk} - t_{sk})}{b_v s_{sk}}$

$= \dfrac{0.7(0.85)(6000)(0.75)(38 - 0.75)}{(42)(12)} = 198$ psi

$v_{nhb} \geq v_{uh}$ OK

Check maximum limit on nominal interface shear resistance:

Maximum resistance $v_{ni} \leq K_1 f_c' \leq K_2$

$K_1 = 0.3$ $K_2 = 1.5$ ksi

$K_1 f_c' = 0.3(6) = 1.8$ ksi $< K_2$

$v_{ni} = K_2 = 1.5$ ksi (acting over the base of the shear key)

Length of shear key $w_{sk} = 0.5 s_{sk} + t_{sk}$

$= 0.5(12) + 0.75 = 6.75$ in

$v_{nhs} = \phi_v \dfrac{v_{ni} b_{sk} w_{sk}}{b_v s_{sk}}$

$= 0.9 \dfrac{(1500)(38)(6.75)}{(42)(12)} = 687$ psi

$v_{nhs} \geq v_{uh}$ OK

Compute required reinforcement:

Required reinforcement $A_{vf,req} = \frac{v_{uh} b_v s_{sk}}{\phi_v f_y}$

$= \frac{(0.186)(42)(12)}{0.9(60)} = 1.74$ in^2/ft

Use 2#5 hairpins at 12 in. spacing as shown in Figure C-2.

$A_{vf,prov} = 4(0.31) = 1.24$ in^2/ft

$< A_{vf,req} = 1.74$ in^2/ft NG

Include reinforcement connecting the sub-flange to the top-flange near the outside tips of the sub-flange (see Figure C-2)

$A_{vf,prov}$ = 4 legs of #5 at 12 in. + 2 legs of #4 at 6 in.

$= 4(0.31) + 2(0.2)(12/6) = 2.04$ in^2/ft

$> A_{vf,req} = 1.74$ in^2/ft OK

It should be noted that the sub-flange is not acting composite with the top flange for transverse bending. However, connecting reinforcement such as shown in Figure C-2 is needed so that the sub-flange can work in parallel with the top-flange for transverse bending moments that put the bottom of the sub-flange in tension. The bars crossing the interface near sub-flange tips will serve as both connecting reinforcement for transverse bending and horizontal shear reinforcement for longitudinal bending.

Interface Design for a Typical AASHTO type section

The purpose of this example is to demonstrate the design of the interface between the two casting stages considering a typical AASHTO type section. Using an AASHTO type section results in a narrow interface between the two casting stages compared to the optimized section developed in this research. For this example, an AASHTO Type II section is considered with top surface width of 12 inches compared to 42 inches for the optimized section used in the example above. Dimensions of the top portion of the section and the shear key are shown in Figure C-3 and C-4. The narrow interface results in high horizontal shear stress demand. Analysis of a bridge with AASHTO Type II section with a span of 74 ft, which is typical for this

section, indicates that the expected horizontal shear stress is 320 psi. In order to accommodate such high shear stress, the shear keys are spaced at a shorter distance than used with the optimized section as shown in Figure C-4. The following steps summarize the design process.

General data:

CIP deck concrete strength	$f_c' = 6000$	psi
Steel yield stress	$f_y = 60$	ksi
ϕ for shear	$\phi_v = 0.9$	
ϕ for bearing	$\phi_b = 0.7$	
Top flange width	$b_v = 12$	in.
Shear key thickness	$t_{sk} = 0.75$	in.
Shear key spacing	$s_{sk} = 6$	in.
Factored shear stress	$v_{uh} = 320$	psi

Check bearing strength on shear key:

Shear key width $b_{sk} = b_v - 2(1)$

$= 12 - 2(1) = 10$ in.

Bearing strength $v_{nhb} = \dfrac{\phi_b (0.85) f_c' t_{sk} (b_{sk} - t_{sk})}{b_v s_{sk}}$

$= \dfrac{0.7(0.85)(6000)(0.75)(10 - 0.75)}{(12)(6)} = 344$ psi

$v_{nhb} \geq v_{uh}$ OK

Check maximum limit on nominal interface shear resistance:

Maximum resistance $v_{ni} \leq K_1 f_c' \leq K_2$

$K_1 = 0.3$ $K_2 = 1.5$ ksi

$K_1 f_c' = 0.3(6) = 1.8$ ksi $< K_2$

$v_{ni} = K_2 = 1.5$ ksi (acting over the base of the shear key)

Length of shear key $w_{sk} = 0.5s_{sk} + t_{sk}$

$= 0.5(6) + 0.75 = 3.75$ in

$$v_{nhs} = \phi_v \frac{v_{ni} b_{sk} w_{sk}}{b_v s_{sk}}$$

$$= 0.9 \frac{(1500)(10)(3.75)}{(12)(6)} = 703 \text{ psi}$$

$v_{nhs} \geq v_{uh}$ OK

Compute required reinforcement:

Required reinforcement $A_{vf,req} = \frac{v_{uh} b_v s_{sk}}{\phi_v f_y}$

$$= \frac{(0.320)(12)(6)}{0.9(60)} = 0.43 \quad \text{in}^2\text{/shear key}$$

Use 1#5 hairpin at each shear key as shown in Figure C-4.

$A_{vf,prov} = 2(0.31) = 0.62$ in^2

$> A_{vf,req} = 0.43$ in^2 OK

This example demonstrates that common AASHTO type sections can be used for decked girders incorporating details for future deck replacement with adequate horizontal shear transfer between the two casting stages.

Conclusions

The examples presented in this study demonstrate that the proposed details for facilitating future deck replacement are adequate for horizontal shear transfer across the interface between the two casting stages. For the optimized section, reinforcement connecting the sub-flange to the top-flange near the outside tips of the sub-flange can be considered as horizontal shear reinforcement if needed. For AASHTO Type II section with narrow top surface, smaller spacing between the shear keys is required

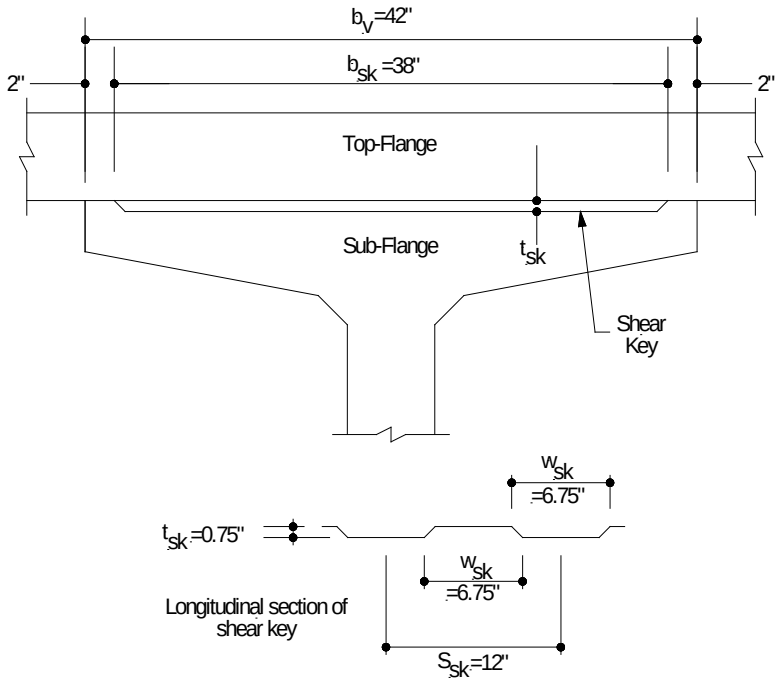

Figure C-1. Shear Key Dimensions for Optimized Section.

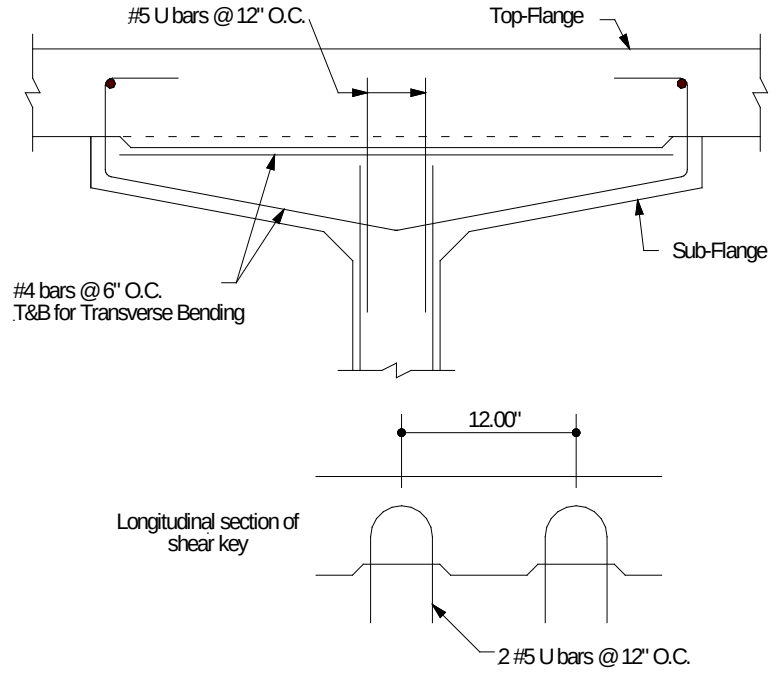

Figure C-2. Horizontal Shear Reinforcement for in Sub-flange of Optimized Section.

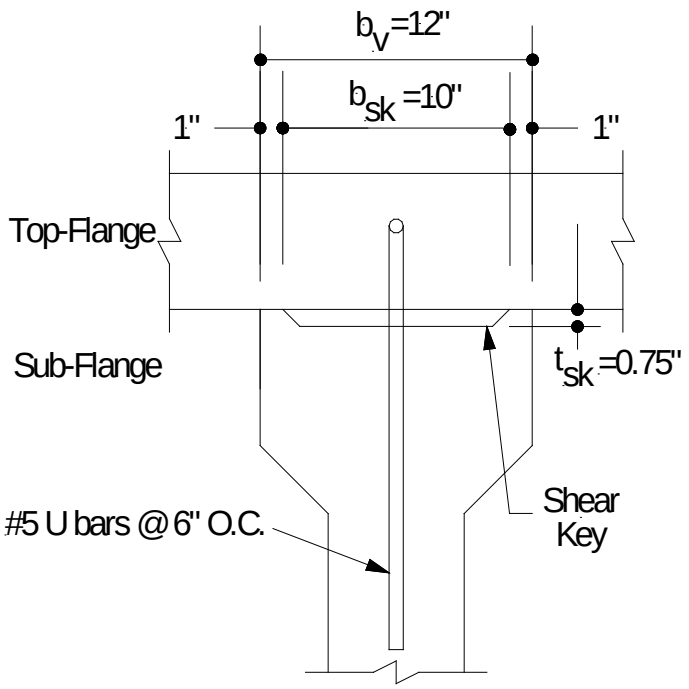

Figure C-3. Shear Key Dimensions for AASHTO Type II Section.

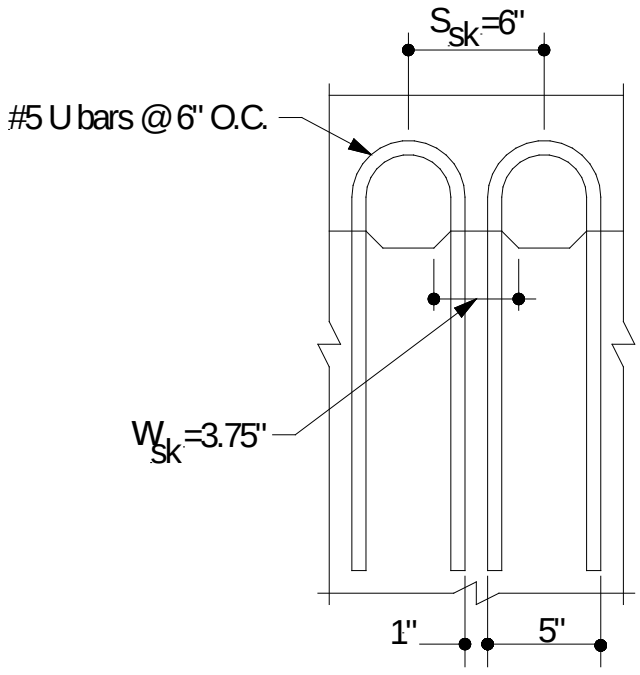

Figure C-4. Horizontal Shear Reinforcement for AASHTO Type II Section.